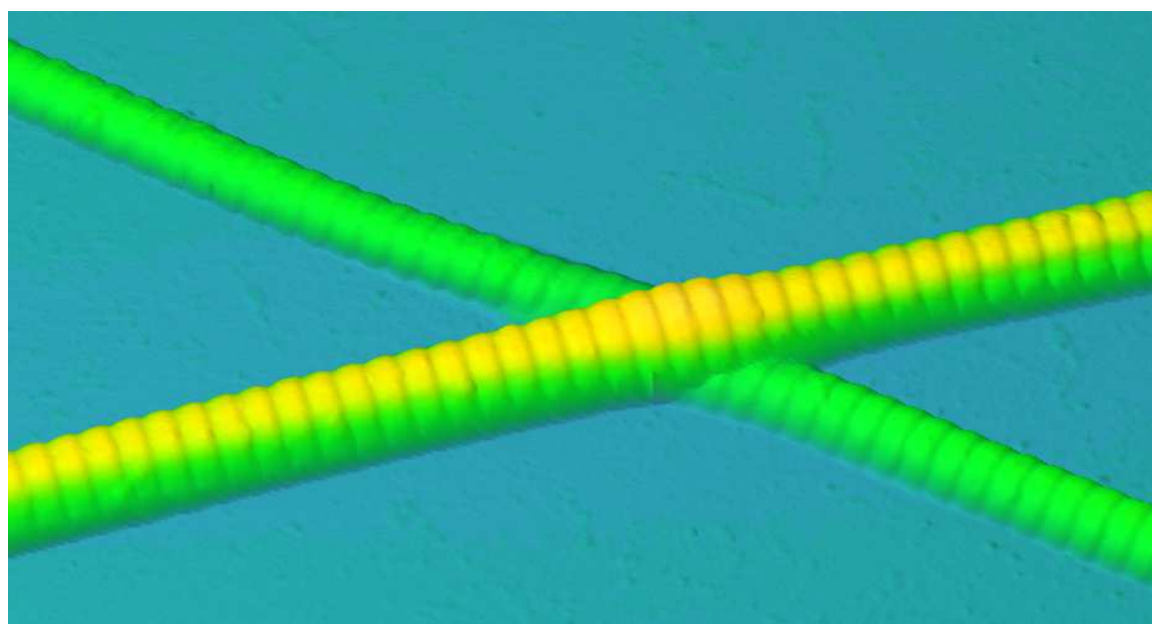# PhD thesis

Rene B. Svensson

Tendon Force Transmission at the Nanoscale

Institute of Sports Medicine Copenhagen

Bispebjerg Hospital & Center for Healthy Aging

Academic advisor: S. Peter Magnusson

Submitted: 30/06/12

1. CONTENTS

1. Contents

2. PREFACE AND ACKNOWLEDGEMENTS

The present Ph.D. thesis is based on work performed over the past three years during my scholarship at the University of Copenhagen. The work has primarily revolved around measuring and understanding the mechanical behavior of collagen fibrils, especially in relation to force transmission through tendons.

The work was performed at the Institute of Sports Medicine Copenhagen (ISMC), Bispebjerg Hospital and in addition a significant part of the laboratory work was performed on the atomic force microscopes at the Nano-Science Center, University of Copenhagen.

I owe special gratitude to Peter Magnusson for inviting me to undertake this Ph.D. study and supporting me in building the project and getting the necessary funding. Throughout the study Peter has been an amazing supervisor, always showing great interest in my work and providing invaluable scientific discussion. I am also particularly thankful to Philip Hansen who provided my initial contact to the institute and was a great inspiration, colleague and collaborator throughout. I also thank the rest of the Biomechanics group, Christian Couppé, Bjarki Haraldsson and Mads Kongsgaard who have all participated in shaping my research questions and providing inspiration for my work.

A special thank goes to Michael Kjaer, head of the ISMC, for providing great research facilities and an inspiring research environment. I thank the rest of my colleagues at the ISMC, fellow Ph.D. students, lab technicians and secretaries for their help along the way. And a particularly warm thanks Monika Bayer for being a great colleague and for her great help in collecting tissue from surgery. On the subject of surgery I will also express my gratitude to the orthopedic surgeons at the Bispebjerg Hospital lead by Michael Krogsgaard without whom I would have had no material to work with.

I want to thank Tue Hassenkam at the Nano-Science Center for teaching me the use of atomic force microscopy, getting me into this project, guiding and supporting me. Without Tue, this project would never have happened.

Finally I also want to thank the funding bodies, primarily the Faculty of Health Sciences who provided the 3-year grant for my Ph.D., but also funding of the ISMC, providing the facilities for doing the project: The Nordea Foundation (CEHA), the Novo Nordisk Foundation, the Lundbeck Foundation and the Danish Medical Research Council (FSS).

3. LIST OF PAPERS

Study 1

Svensson RB, Hassenkam T, Hansen P, Magnusson SP. Viscoelastic behavior of discrete human collagen fibrils. J Mech Behav Biomed Mater 2010;3(1):112-5.

Study 2

Svensson RB, Hassenkam T, Grant CA, Magnusson SP. Tensile properties of human collagen fibrils and fascicles are insensitive to environmental salts. Biophys J 2010;99(12):4020-7.

Study 3

Svensson RB, Hansen P, Hassenkam T, Haraldsson BT, Aagaard P, Kovanen V, et al. Mechanical properties of human patellar tendon at the hierarchical levels of tendon and fibril. J Appl Physiol 2012;112(3):419-26.

Study 4

Svensson RB, Hassenkam T, Hansen P, Kjaer M, Magnusson SP. Tensile force transmission in human patellar tendon fascicles is not mediated by glycosaminoglycans. Connect Tissue Res 2011;52(5):415-21.

Study 5

Svensson RB, Mulder H, Magnusson SP. Fracture mechanics of collagen fibrils: Influence of natural cross-links. (In preparation) 2012.

4. ABBREVIATIONS

ACL: Anterior Cruciate Ligament

AFM: Atomic Force Microscopy

AGE: Advanced Glycation End-product

Ch-ABC: Chondroitinase ABC

CS: Chondroitin Sulfate

CSA: Cross-sectional Area

DMBA: 4-Dimethylaminobenzaldehyde

DS: Dermatan Sulfate

EMG: Electromyography

GAG: Glycosaminoglycan

HEPES: 4-(2-hydroxyethyl)-1-piperazineethanesulfonic acid

HP: Hydroxylysyl-Pyridinoline

HPLC: High Performance Liquid Chromatography

LOX: Lysyl Oxidase

LP: Lysyl-Pyridinoline

PBS: Phosphate Buffered Saline

PG: Proteoglycan

RTT: Rat-tail Tendon

SLRP: Small Leucine Rich Proteoglycan

TEM: Transmission Electron Microscopy

ZDF rat: Zucker Diabetic Fat rat

5. DANSK RESUMÉ

I dette studie undersøgtes bindevævs mekaniske egenskaber med fokus på sener. Bindevæv består af en ekstracellulær matrix af proteinet kollagen som er ansvarlig for vævets mekaniske integritet. Selvom bindevæv kan virke simple i opbygning, er der stadig mange aspekter af bindevævs funktion, som ikke er fuldt belyste. Et af disse aspekter er de mikroskopiske mekanismer som ligger til grund for kraftoverførsel gennem en sene over makroskopiske afstande. Da kraftoverførsel er kernen i senens funktion, er dette spørgsmål af væsentlig betydning, men det store skalaspænd i senens hierarkiske opbygning har gjort det vanskeligt at undersøge. Senens hierarki spænder fra molekyler (2 nm) over fibriller (200 nm), fibre (2 µm) og fascicler (200 µm) til sener (10 mm) og for at forstå hvordan kraft overføres imellem disse niveauer, er det nødvendigt at kende de mekaniske egenskaber på hvert niveau.

Målet med projektet var at undersøge mekanismerne bag kraftoverførsel i sener, primært ved at undersøge de mekaniske egenskaber på fibril niveau. Vi har udviklet en metode baseret på atomic force mikroskopi (AFM) til mekaniske målinger på individuelle kollagenfibriller. Afhandlingen indeholder fem artikler, de første to fokuserer på kollagenfibrillers grundlæggende mekaniske egenskaber, da eksisterende viden er sparsom. Den første artikel med titlen *"Viscoelastic behavior of discrete human collagen fibrils"* undersøgte kollagenfibriller under dynamisk belastning og fandt, at fibriller opfører sig viskoelastisk, det vil sige at deres stivhed øges med øget belastningshastighed. Den anden artikel *"Tensile properties of human collagen fibrils and fascicles are insensitive to environmental salts"* belyste betydningen af salte i testmediet og fandt ingen effekt af saltkoncentration og sammensætning, i modsætning til hvad der tidligere er rapporteret.

De næste to arbejder beskæftigede sig mere direkte med kraftoverførsel i sener. I artiklen *"Mechanical properties of human patellar tendon at the hierarchical levels of tendon and fibril"* undersøgte vi forholdet mellem mekaniske egenskaber på fibril og sene niveau. Resultatet indikerer at fibriller ikke i udpræget grad glider i forhold til hinanden inde i senen. Den anden artikel, *"Tensile force transmission in human patellar tendon fascicles is not mediated by glycosaminoglycans"* undersøgte om glycosaminoglycaner medvirker til seners kraftoverførsel og kunne ikke påvise en sådan rolle.

I den sidste artikel (endnu ikke publiceret) undersøgtes sammenhængen mellem biokemiske forskelle i krydsbindinger og fibrillernes mekaniske egenskaber. Vi fandt, at humant collagen som indeholder 'modne' krydsbindinger, opfører sig fundamentalt forskelligt fra rottehale collagen som indeholder 'umodne' tværbindinger.

6. ENGLISH SUMMARY

The subject of this study is connective tissues, in particular tendon. Connective tissues consist of an extracellular matrix made of the protein collagen, which is responsible for the mechanical integrity of the body. While connective tissues may appear simple, there are still many aspects of connective tissue function that are poorly understood. One such aspect is the microscopic mechanisms of force transmission through tendons over macroscopic distances. Force transmission is at the heart of tendon function, but the large range of scales in the hierarchical structure of tendons has made it difficult to tackle. The tendon hierarchy ranges from molecules (2 nm) over fibrils (200 nm), fibers (2 µm) and fascicles (200 µm) to tendons (10 mm), and to derive the mechanisms of force transmission it is necessary to know the mechanical behavior at each hierarchical level.

The aim of the present work was to elucidate the mechanisms of force transmission in tendons primarily by investigating the mechanical behavior at the hierarchical level of collagen fibrils. To do so we have developed an atomic force microscopy (AFM) method for tensile testing of native collagen fibrils. The thesis contains five papers; the first two deal with the basic mechanical behavior and properties of collagen fibrils since existing knowledge is scarce and provide varying results. The first report "*Viscoelastic behavior of discrete human collagen fibrils*" investigated the behavior of collagen fibrils under dynamic loading and found that fibrils behave viscoelastically, which means that the stiffness depends on the rate of loading. The second paper "*Tensile properties of human collagen fibrils and fascicles are insensitive to environmental salts*" looked at differences in saline environment, and found no effect on the mechanical properties, in contrast to a previous report.

The next two papers deal more directly with tendon force transmission. The one called "*Mechanical properties of human patellar tendon at the hierarchical levels of tendon and fibril*" investigated the relation between mechanical properties at the fibril and tendon hierarchical levels. The results suggested that there is little fibril slippage within a tendon. The other "*Tensile force transmission in human patellar tendon fascicles is not mediated by glycosaminoglycans*" looked at the involvement of glycosaminoglycans in tendon force transmission, finding no evidence for such a role.

In the final (unpublished) paper, the failure mechanics of collagen fibrils were related to differences in cross-linking and found that human collagen, containing mature cross-links, behaves fundamentally different from rat-tail collagen, containing only immature cross-links.

7. INTRODUCTION

Tendons are important connective tissues in the body, which are commonly injured during sports. In spite of several decades of research, the microscopic mechanisms that underlie tendon function are still poorly understood. The aim of the present thesis was to utilize relatively new methods for assessing tendon mechanical function at the nano- to microscale, in order to provide novel insights into tendon properties at this level. It was our hope that these insights would help unravel the mechanisms behind tendon mechanical function, especially in relation to force transmission.

7.1. Tendons

The primary subject of the present studies was human tendon. Tendon is a tissue with a distinct white color, which is found in connection to muscles and bones. The archetypical tendon is an elongated band, separate from surrounding tissue along its length and connected at one end to a muscle and at the other to a bone (Figure 1). Tendon functions as a connector, much like a rope, transmitting muscle force to the bone thereby creating joint movement [2]. The reason why muscles connect to bone through tendons rather than direct attachment is likely to reduce the muscle mass that needs to be moved by keeping the muscle further away
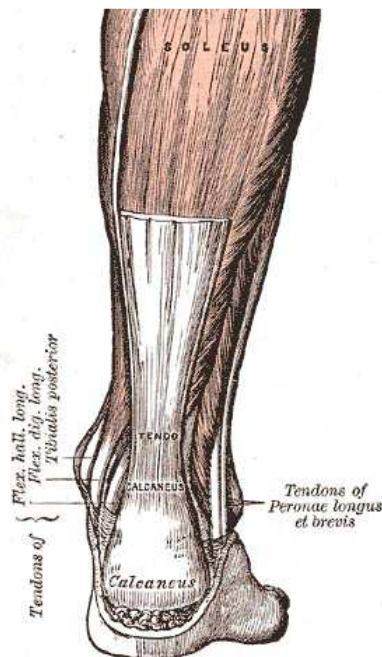
Figure 1: Schematic drawing of an Achilles tendon connecting the soleus muscle at the top to the calcaneus bone at the bottom thereby enabling foot flexion. From Gray's Anatomy (1918) [1].

from the joint. In addition muscle is cellular and relatively soft and would be at risk of damage on contact with hard bone. In contrast tendon has intermediate stiffness and is less cellular making it more resistant to damage at the bone insertion [3]. Finally, some tendons like the Achilles can store elastic energy thereby reducing the energy required for movement over longer distances [4].

7.2. Tendon Structure

Just like tendons function as ropes they are also structurally similar to a rope [6]. Zooming in on a tendon, the first level of structural hierarchy is cylindrical strands ~0.3 mm in diameter called fascicles (Figure 2 c). Zooming further in, the fascicles are found to consist of fibers on the ~10 µm scale and at even greater magnification the fibers are seen to be bundles of even smaller threads (~100 nm in diameter) which are called fibrils (Figure 2 d,e,f). The fibrils are made from a protein called collagen, which is the primary component of tendons. Collagen is found as elongated molecules, 300 nm long and 1.5 nm in diameter, which are formed by the
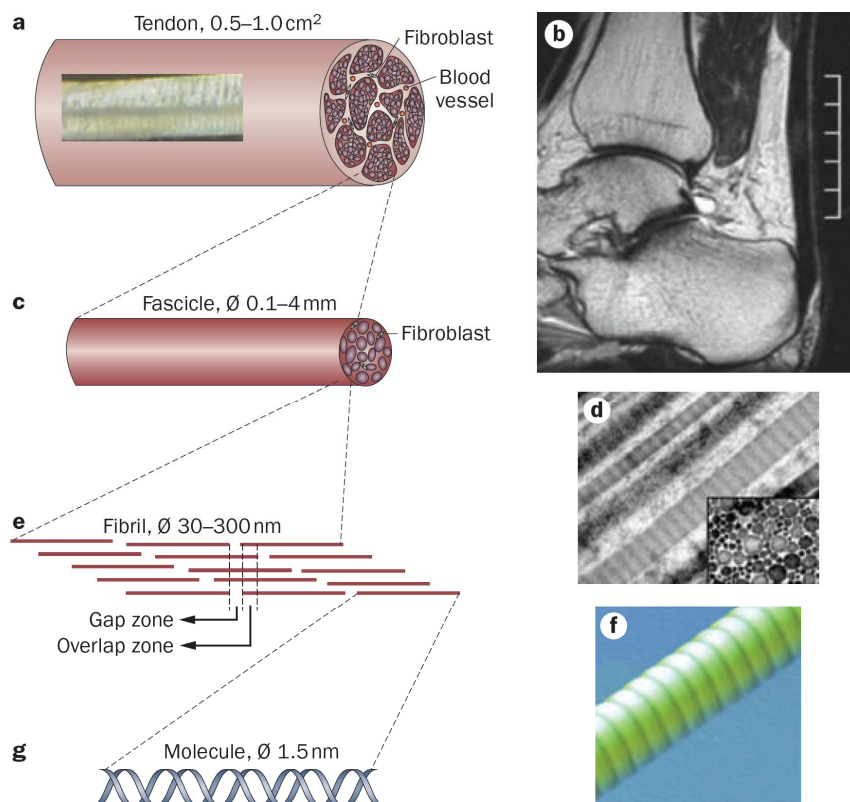
Figure 2: Schematic of tendon structure. Tendon (a,b) is made up of smaller substructures called fascicles (c). The fascicles consist of bundles of fibrils (d,e,f) that are made of collagen molecules (g), which is a triple helix of peptide strands. From Magnusson et al. (2010) [5].

aggregation of three peptide strands into a triple helix (Figure 2 g) [7-10]. Collagen is secreted by cells found between the fibers, and because it is present outside the cells it is referred to as an extracellular matrix. When the tendon is slack the fibrils lie in a wavy pattern referred to as crimps [11-12] and when the tendon is loaded the crimps are stretched out. This structural feature has implications for the mechanical properties (see section 7.10).

7.3. Tendon Composition

Collagen makes up the primary load-bearing fibers of tendons and account for ~60-90% of the dry material [13-15]. Another important tendon component is proteoglycans (PGs) that make up ~0.5-3% of the dry mass depending on location [15-16]. Proteoglycans are proteins bound to long negatively charged sugar chains called glycosaminoglycans (GAGs), which are able to bind large amounts of water [17]. The PGs decorin, biglycan and fibromodulin belong to the group of small leucine rich proteoglycans (SLRPs) and are commonly found in tendon [17-18]. They have been shown to bind to the surface of collagen fibrils [19-21] and affect collagen fibril formation [22-24]. Another component with potential mechanical function is elastin, which is present in low concentration <2% [25]. The role of elastin is not fully understood but it may be involved in contracting the tendon following mechanical load [2].

7.4. Collagen

Connective tissues including tendons are made primarily from proteins of the collagen family [26]. There are many different collagens with varying structure and function but the common feature defining collagens is the formation of a triple helix with the tri-peptide repeat Gly-X-Y where X and Y are non-glycine amino acids (see for example UniProt registry P02452 (type I) and Q8IZC6 (type XXVII)). The Gly-X-Y repeat is essential for triple helix formation because only glycine is sufficiently small to be packed into the core of the helix [27]. The primary collagen in tendon is type I, which belongs to the fibril forming collagens together with type II, III, V and XI [28]. The peptide strands that go into the triple-helix are called α-chains, and some of the collagen types form heterogeneous molecules with two or three different α-chains.
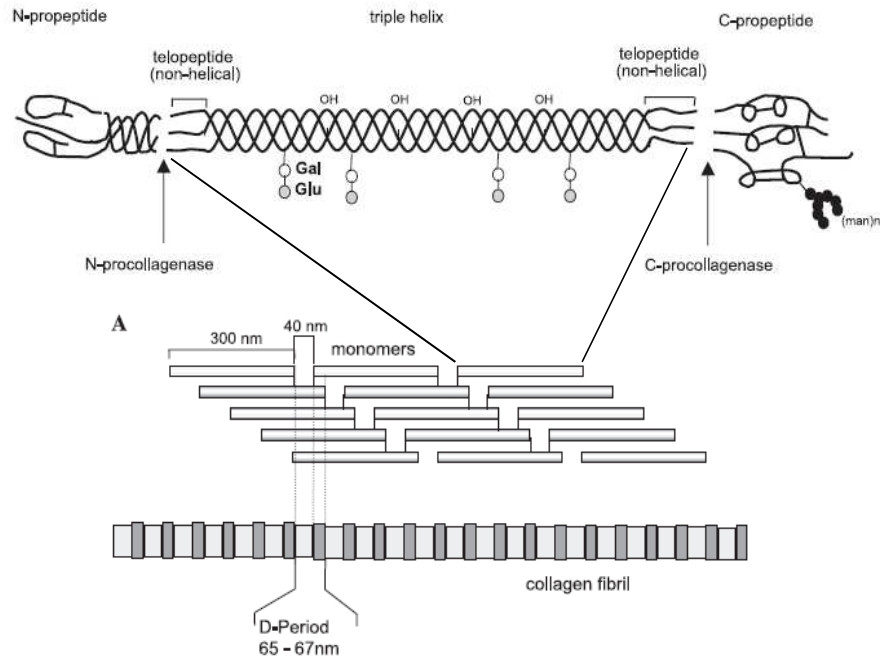
Figure 3: Schematic of collagen production and fibrillogenesis. Two α1 and one α2 chains are synthesized and come together to form the triple helical procollagen molecule. Propeptides at either end are removed by procollagenases, and then the molecules are excreted and aggregate into fibrils. Aggregation occurs in a highly ordered stagger, producing a periodic pattern on the fibril. Adapted from Gelse et al. (2003) [26].

7.5. Collagen Synthesis

The formation of type I collagen is shown schematically in Figure 3. Initially the procollagen α-chains ~1000 amino acids in length are synthesized [28]. The procollagen has regions at the N and C terminal ends (propeptides) hindering random aggregation. The C-propeptide contains a chain-recognition site that controls which three α-chains come together in the triple helix [29]. In the case of type I collagen two α1 and one α2 chains are involved. Several post-translational modifications of collagen take place within the cell. An important modification is the enzymatic hydroxylation of specific prolines and lysines. 4-Hydroxylation of prolines is associated with greater thermal stability of collagen [30] and lysine hydroxylation is important for the cross-link formation described in section 0. In addition to extensive proline 4-hydroxylation, there are also a few specific prolines that are 3-hydroxylated and appear to influence collagen properties although the mechanisms are not understood [31-32]. Following helix formation, procollagenases cleave off the N- and C-propeptides. The resulting collagen molecule contains a central triple helical part approximately 338 Gly-X-Y repeats long [28], while short regions at the N- and C-terminal ends lack the triplet repeat and are non-helical. The non-helical regions are called telopeptides and are involved in cross-link formation between molecules.

7.6. Collagen Fibrillogenesis

Following their production, collagen molecules aggregate into fibrils. While the initial processes to produce procollagen molecules take place intracellularly, it is not entirely clear if small fibrils are formed (or partially formed) within cells following propeptide cleavage. Recent evidence suggests that fibrils form intracellularly during embryonic development and extracellularly after maturation [33-34]. In the embryonic case intracellular fibrils are excreted through large cell membrane invaginations called fibripositors, which may play a role in fibril alignment [33]. Fibripositors are absent in mature tissue, suggesting a change in collagen synthesis mechanism from production of new fibrils to growth of existing ones [34]. Type I collagen molecules can easily self-assemble into fibrils in vitro, but in vivo fibril formation is a controlled process involving numerous other molecules such as type V and XI collagen, fibronectin and proteoglycans to control nucleation, growth and diameter [22-23, 35-36]. To form a fibril, collagen molecules aggregate laterally by non-covalent interactions in a highly organized staggered fashion where each molecule is shifted by 67 nm (known as the D-period) (Figure 3). The staggered arrangement is possibly achieved by periodicity in hydrophobic regions along the molecule [37] although hydrophilic interactions have been reported to be stronger [38]. After initial aggregation the molecules are only held together by non-covalent interactions.

Following nucleation and initial fibril formation there is an increase in fibril diameter and length as the organism matures, but the mechanisms are unknown. In early embryonic tissue most fibrils are generally uniform in size ~40nm in diameter and <40µm long [39-40], however, in maturity fibrils have a broad diameter distribution up to ~500 nm with lengths of at least several hundred µm and probably reaching into the cm range [10, 41-42]. Basically two mechanisms have been proposed. One is molecular accretion by which individual molecules are added to existing short fibrils formed in the nucleation phase [43-44], much like crystal growth. The other involves lateral and longitudinal fusion of the initial small fibrils [45-46]. Molecular accretion appears to be the assembly mechanism in vitro [47] and accretion also fits well with the observation of highly uniform circular fibril diameters in vivo. On the other hand fibril fusion has an advantage in explaining how fibrils are aligned, since it only requires that the initial short fibril segments are aligned. In contrast growth of individual fibrils by accretion would be similar to pushing a piece of string forward and would require some form of straightening mechanism to avoid curling.
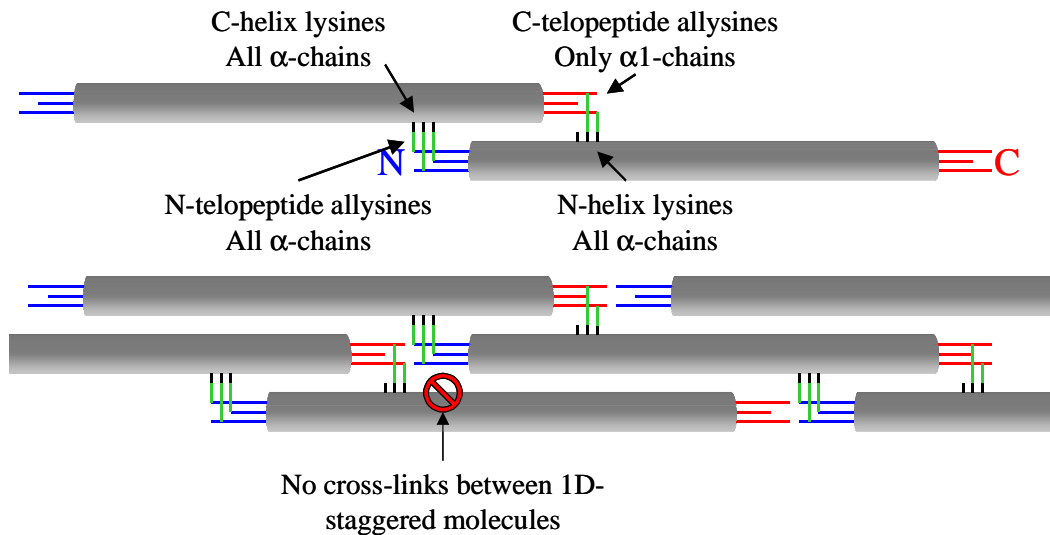
Figure 4: Schematic of covalent cross-link formation between 4D-staggered collagen molecules. Cross-links are not formed between 1D-staggered molecules.

7.7. Collagen Cross-links

Improved molecular bonding within the fibril is achieved by the formation of covalent cross-links. Cross-link formation is initiated by the enzyme lysyl oxidase (LOX) which is present in the extracellular matrix and catalyses the oxidative deamination of specific lysines on collagen to form allysines (replacing the amino group with an aldehyde) [48]. LOX acts on lysines in the telopeptide region but is recruited by a site on the helical region of a neighboring molecule, ensuring that the modification only takes place after molecules have aggregated, possibly to avoid spurious cross-linking [48]. In type I collagen this modification can take place at both ends of the α1-chains but only at the N-telopeptide of the α2-chain [49]. The precise stagger in the collagen aggregation ensures that two molecules staggered by 4 D-periods will have their telopeptide allysines situated next to lysine residues in the helical region of each other (Figure 4). This allows the amino group on the lysine to react with the aldehyde on the telopeptide allysine to form a covalent bond [50]. In total this gives each collagen molecule 11 possible sites of cross-linking, 3 N-telopeptide, 3 N-helix, 3 C-helix and 2 C-telopeptide sites.

As previously mentioned some of the lysines are post-translationally hydroxylated, and this gives rise to different types of cross-links depending on the combination of hydroxylated and non-hydroxylated lysines and allysines (Table 1). Non-hydroxylated allysines form acid labile imine cross-links that are easily hydrolysed [51],

Table 1: Overview of enzymatic cross-links.

Telopeptide	Helix	Immature cross-link	2nd Telopeptide	Mature cross-link
Allysine	Lysine	**Lysino-norleucine (LNL)**	Allysine	**Unknown**
			Hydroxyallysine	**Unknown**
	Hydroxylysine	**Hydroxylysino-norleucine (HLNL)**	Allysine	**Unknown**
			Hydroxyallysine	**Lysyl-pyrrole (L-pyrrole)**
Hydroxyallysine	Lysine	**Hydroxylysino-ketonorleucine (HLKNL)**	Allysine	**Hydroxylysyl-pyrrole (H-pyrrole)**
			Hydroxyallysine	**Hydroxylysyl-pyridinoline (HP)**
	Hydroxylysine	**Lysino-ketonorleucine (LKNL)**	Allysine	**Lysyl-pyrrole (L-pyrrole)**
			Hydroxyallysine	**Lysyl-pyridinoline (LP)**

while cross-links formed from hydroxylated allysines are more stable because they can undergo amadori rearrangement to produce a non-labile secondary keto-imine [48].

The initially formed divalent cross-links are called immature and over time they can react further to form mature trivalent cross-links. The mechanism for this reaction is debated but the result is the addition of another telopeptide allysine or hydroxyallysine to one of the existing immature cross-links, forming either a pyrrole or pyridinoline compound (Table 1). The type of cross-links formed is therefore essentially controlled by the extent of hydroxylation of the lysine residues and significant variations exist between tissues [52]. Even within one tissue type, there can be variations with the magnitude of load on the specific component and it has been reported that there is a tendency for more hydroxyallysine-derived cross-links in tissues under load compared to 'loose' tissue [53].

It is known that connective tissue from young organisms contain mostly immature cross-links and during early development the amount of these go down as they are replaced by mature cross-links [54]. The mature cross-links are trivalent but whether they connect three α-chains on three different molecules or just two in the same molecule with one in another is unclear. In order to connect three molecules, two of them need to be in register, which appears to be possible in one of the more recent packing model described by Orgel et al. (2006) [55]. Connecting three molecules would be expected to strengthen the fibril more than connecting only two.

In addition to the enzymatic cross-links there is also another type called advanced glycation end-products (AGEs). They are formed by reaction of protein with

reducing sugars such as glucose [56]. The cross-links form spontaneously over time, and therefore proteins with a low turnover such as collagen can accumulate significant amounts [57]. In diabetes the accumulation can be further increased due to higher levels of blood sugar [58]. While the enzymatic cross-links are required for proper tissue function, AGEs are detrimental to the function of different tissues possibly due to stiffening and embrittlement [59-61].

7.8. Microfibrils

Several studies have found that collagen fibrils themselves contain a filamentous substructure called micro-fibrils [62-64]. The D-periodic stagger in collagen molecule packing produces a repeated structure for every five molecules (Figure 5) and it was proposed that micro-fibrils would consist of such pentads. The observed filaments have diameters of ~4 nm in fair agreement with this model. Basically two micro-fibril arrangements have been observed; in cornea, blood vessels dermis and tendon sheets, micro-fibrils have been found to arrange in a right-handed helix with a constant angle of ~15º, while in tendons and cartilage micro-fibrils are straight along the fibril [65-66], we are not aware of any reports of left-handed helix
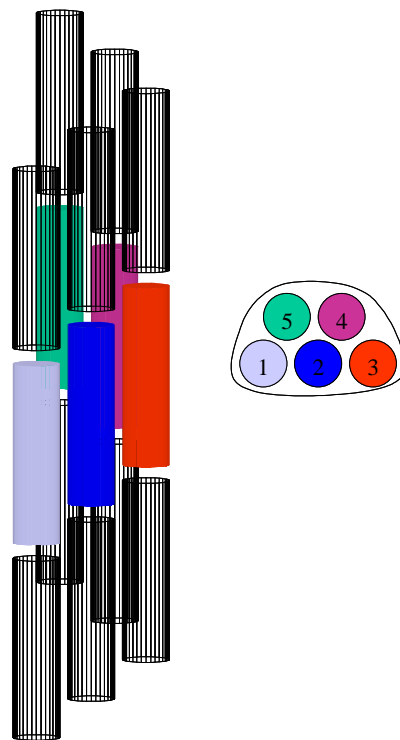
Figure 5: Simplified micro-fibril schematic. The left shows three repeats of the molecule pentad, the central pentad is colored for improved visibility. The right shows a cross-section of the pentad to outline the micro-fibril. More recent packing models (Orgel et al. (2006) [55]) modify this simplified view, and find that molecules are interwoven between microfibrils, which means that microfibrils are not separable units.

formation. Helical arrangement would be expected to produce more compliant fibrils by directing some of the strain into alignment of micro-fibrils rather than backbone stretching, and in addition helical fibrils are less prone to buckling when bent [67]. From these considerations it seems reasonable that flexible tissues like blood vessels, dermis and tendon sheets have helical micro-fibrils and that stiff tissues like tendons have straight micro-fibrils. However, the finding that corneal fibrils have helical micro-fibrils and cartilage has straight micro-fibrils somewhat contradicts this hypothesis.

In man-made ropes it is common to use opposite winding at different levels of hierarchy to avoid gross unwinding and the same principle might underlie the conserved winding direction of micro-fibrils. The Gly-X-Y α-chain has a left-handed twist and the three chains come together in a right-handed triple helix when forming a molecule. The handedness of individual micro-fibrils is not entirely clear, but Wess et al. [68] reported a left-handed twist. Based on that model an alternating handedness all the way from α-chains to collagen fibril would exist, explaining the right-handed arrangement of micro-fibrils.

7.9. Mechanics

The primary results of the present work are mechanical measurements and this section will give a brief introduction to the basic concepts in mechanics.

A mechanical test involves placing a material under load and determining how much it deforms in response to that load. The relationship between force and deformation define the mechanical properties of that object. The load may be applied along any direction, but in the present work we use tendons and collagen fibrils that are cylindrical structures with a natural
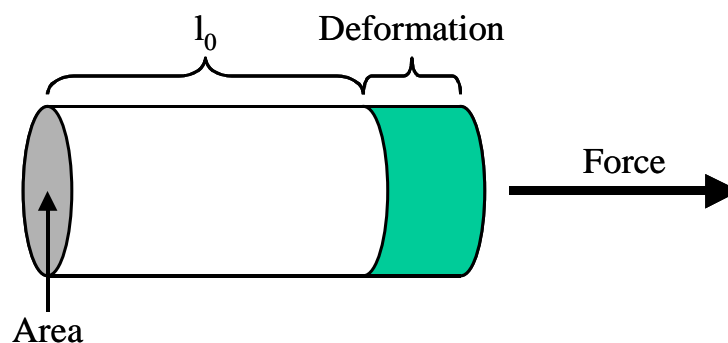
Figure 6: Schematic of a cylindrical material loaded along its axis. The cross-sectional area used for converting force to stress is shown and so is the starting length used for converting deformation to strain.

loading direction along their length. Often it is not the properties of one specific object but rather of its constituent material that is of interest. To determine material properties the force and deformation has to be normalized to the size of the tested object. The normalized force is the stress (σ) defined as force divided by area (A) [69]. For tensile testing of a cylindrical object like a tendon or fibril the area in question is the cross-sectional area (CSA) of the cylinder (Figure 6). The normalized deformation is the strain (ε) defined as deformation divided by the undeformed length (l_0) of the specimen. In the case of a cylindrical material under tension this length is simply the length of the cylinder. The SI unit of stress is N/m^2 or Pascal (Pa) and the strain is unitless but often reported in percent.

The typical features of an idealized stress vs. strain curve can be seen in Figure 7. From such a curve several important physical characteristics of the material can be deduced. First, there is a linear region, which has a slope that defines the modulus (E) (material stiffness). A small slope corresponds to an extensible material and a steep to a rigid one. In the linear region the material constituents can deform while remaining intact and correctly ordered making deformation in this region reversible. Reversibility is a property of an elastic material and the region is therefore also called the elastic region. At the end of the linear region is the yield point where the slope decreases, which marks the beginning of the plastic region Figure 7. Unlike the elastic region, deformation beyond this point is not reversible [70]. This irreversibility can be due to damaging the material constituents or disrupting their order in a way that is not readily recovered. Finally the stress drops abruptly to zero, as the material is broken apart at the failure point.
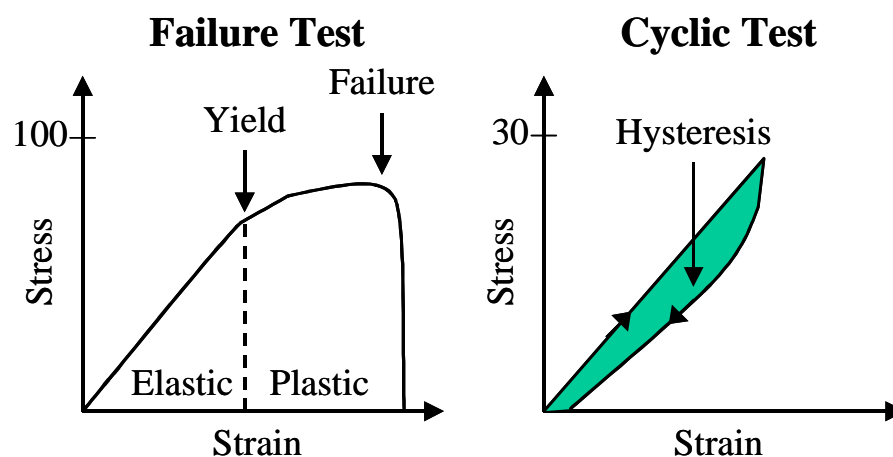
Figure 7: Left, schematic of an idealized failure test showing the linear elastic region leading up to yield, followed by the plastic region up to final failure. Right, schematic of a cyclic test in the linear region. The sample is loaded (top part of curve) then unloaded (bottom part), due to viscoelastic behavior the two curves do not coincide (hysteresis) and energy is dissipated (area inside curve).

In a plot of stress vs. strain the area under the curve has units of energy per volume and signifies the mechanical energy put into the material. In a mechanical test to failure as shown in Figure 7, the area under the curve is the energy required to break the material. To avoid damaging the material, mechanical testing is commonly performed in the elastic range. Such tests are often cyclic with the material being loaded and then unloaded (Figure 7). Here the area under the loading curve defines the energy put into the system, and the area under the unloading curve is the energy that was returned. The difference between the two defines the energy that was dissipated during the cycle, which is also called the hysteresis.

The stress-strain behavior may depend on the rate at which the material is loaded, a phenomenon called viscoelasticity. Viscoelasticity is caused by rearrangement of molecules to reduce the load often by slippage or unwinding. Rapid loading will allow less time for rearrangement than slow loading thereby resulting in greater forces. Viscoelasticity gives rise to a number of mechanical effects. When a constant strain is applied the stress that is reached will decay over time (Figure 8), this is called stress relaxation [69, 71]. A similar effect is observed when a constant stress is applied causing the strain to increases over time, an effect called creep, which will eventually lead to rupture (Figure 8) [72]. Finally, it is observed that with increasing strain-rates several mechanical properties increase, including increased modulus, increased maximum stress and increased strain at maximum stress [69, 73].
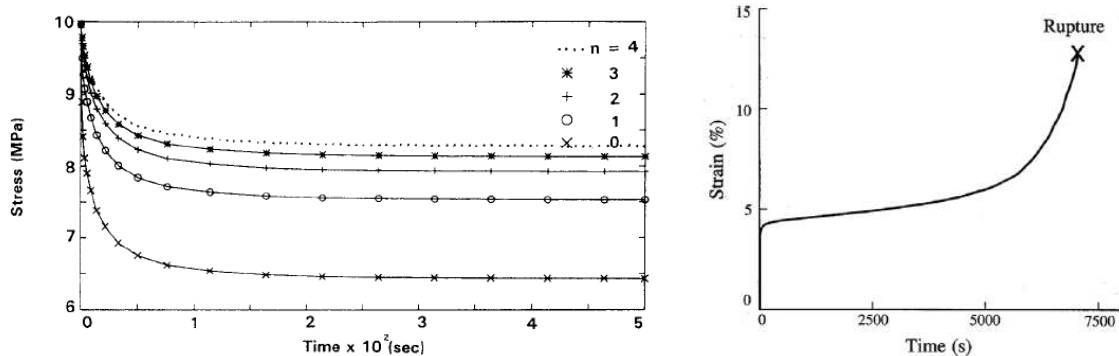
Figure 8: Left: An example of stress relaxation. The different curves represent tests performed after different numbers of loading cycles before the stress relaxation. Reprint from [71]. Right: Creep experiment on wallaby tail tendon. Stress was held constant at 30MPa. Reprint from [72].
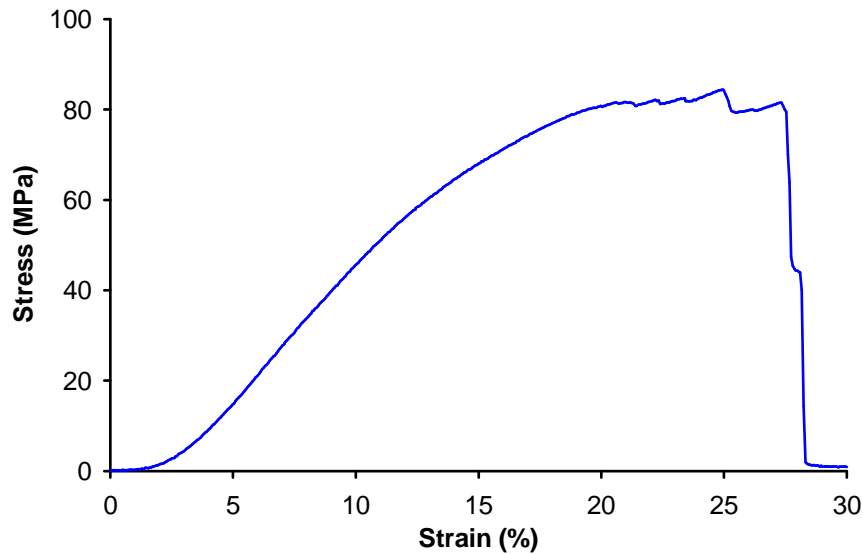
Figure 9: Stress-strain relation for a human tendon fascicle. Notice that below 5% strain there is a slow rise in the stress (toe-region). The toe-region is followed by a relatively linear response (elastic region), before the curve starts breaking off (plastic region) up to final failure.

7.10. Tendon Mechanics

Tendon function is primarily mechanical and tendon mechanical properties have therefore been a natural area of research. Tendon is a relatively simple tissue in both composition (consisting almost entirely of collagen) and structure (almost all fibrils aligned in parallel). In spite of this the mechanical properties and underlying mechanisms are poorly understood with large variations in the range of reported mechanical properties (Table 2) and opposing views on fundamental mechanisms behind force transmission [10, 74].

A special feature of tendon mechanics is a region observed at low strain where the curve has a slowly increasing slope before reaching the linear part (Figure 9). This so-called toe-region is related to straightening out the fibrils, which in the slack position lie in a wavy pattern (crimps), thereby gradually increasing the number of load-bearing fibrils [75-76]. The length of the toe region is rarely quantified and relies significantly on how the zero-point in deformation is defined, making it difficult to compare between studies.

Beyond the toe-region there is a fairly linear region, which is related to the loading of the now straight fibrils. There are very large variations in the reported magnitude of the slope (modulus) in this region. Some studies report values in the few hundred MPa while others report values of GPa (Table 2). Part of the variation may be due to real natural variations between tendons but this cannot explain the entire range. A number of studies have shown that the mechanical properties depend greatly on the length of the tested specimen, with longer specimens having larger modulus [77-79], and increased modulus with smaller

7. Introduction

Table 2: Overview of tendon mechanical properties

Tissue	Modulus (GPa)	Failure Stress (MPa)	Failure Strain	Reference
Tendon in vivo				
Human Patellar	1.9±0.6	-	-	[13]
Human Patellar	1.0±0.1	-	-	[81]
Human Achilles	1.7±0.3	-	-	[82]
Tendon in vitro				
Human flexor and extensor	1.0-1.4	75-92	~8%	[83]
Various animals	1.0-2.0	62-107	-	[77]
Human semitendinosus and gracilis	0.36-0.61	89-112	27-33%	[84]
Fascicle/Subunit				
Human Patellar	0.15-0.40	11-40	10-18%	[85]
Human Patellar	0.70±0.30	65±15	14±6%	[86]
Rat tail	1.6±0.3	~75	8.1±0.3%	[78]
Fibrils				
Sea cucumber	0.47±0.41	230±160	80±44%	[87]
Bovine Achilles	0.6±0.2	60±10	13±2%	[88]
Human patellar[#]	1.25±0.1	190±50	20±1%	Study 5

[#] Corrected for hydration and tendon fibril content for better comparability (see study 5 for details).

specimen cross-sectional area (CSA) has also been reported [79-80]. The cause is not entirely clear but a likely explanation is so-called end-effects caused by sample gripping and stress concentration at the grips. These findings point out that using short specimens may overestimate strains resulting in reduced modulus values. In other words the lower range of reported modulus values are most likely an artifact of the testing method and the greater modulus values in the GPa range would appear more credible.

Regarding failure properties, the reported values of ultimate stress and strain also differ significantly between studies (Table 2). Similar issues as mentioned for the modulus also apply here. The stress may be underestimated due to stress concentrations leading to premature failure, and stress values in the higher range are therefore more credible. The strain may be overestimated due to gripping issues, which would make the lower strain values the more credible, however, since failure may occur prematurely due to stress concentrations this conclusion is less clear.

The underlying mechanisms at the fibril and molecular level that give rise to the mechanical properties of tendon are not entirely agreed upon. Fundamentally there are two possibilities, either fibrils are continuous or they are discontinuous. The question may appear simple to answer by measuring the fibril length but no one has succeeded in doing so. It is known that newly formed fibrils during embryogenesis are short (~30μm), but fibrils grow with maturation and beyond a certain point it becomes impossible to extract intact fibrils of full length [45]. It is possible to extract intact fibrils from mature tissue following injury, but these are short and most likely newly formed fibrils [89]. Other approaches have been used to estimate fibril length such as counting the number of ends visible within electron micrographs

and comparing with the total fibril length in the images [10], which found no ends across ~2 mm of fibril. Preliminary work in our lab using a similar approach have found one end across ~45 mm of fibril. Others have used geometric considerations based on cell distribution resulting in a fibril length of ~10 mm [42], and yet others have used a viscoelastic model to estimate fibril lengths of ~1 mm [90]. Some of these estimates are sufficiently large to support a model of continuous fibrils, but others are short enough that a model of long yet discontinuous fibrils cannot be ruled out.

X-ray diffraction has been used to study the strain of collagen fibrils within tendon under load and have found that fibril strain is generally less than half of the externally applied tissue strain, and that fibrils do not extend during creep [74, 91-93]. These findings strongly suggest that fibrils are discontinuous and that the remainder of the strain takes place by fibril sliding. However, end-effects may have caused an overestimate in external strains, and some of the external strain may be accounted for by alignment of fibril crimps. The latter effect can be seen in an X-ray study by Sasaki and Odajima [94] where the fibril strain at a given stress is significantly less than the tissue strain due to the toe-region in the tissue. In contrast, the fibril modulus is very similar to the tissue modulus indicating that fibril and tissue strain are almost identical in the linear region [94]. The continuity of fibrils and the extent of sliding are therefore still unclear and consequently whether the failure mechanism is fibril breakage or slippage is equally unknown.

Recently mechanical properties of individual collagen fibrils have been reported and just as for tendons the values vary significantly (Table 2). With such large variations it can be difficult determine which values are most credible, but it is worth noting that no material can be stiffer than the stiffest of its components. It is reasonable to assume that the stiffest component of a tendon is the collagen and therefore one should be critical of fibril modulus values that are significantly lower than the expected tendon modulus.

7.11. Tendon Injury and Disease

Because tendons function by transmitting load, the most severe injury a tendon can sustain is a complete rupture resulting in the loss of force transmission. While acute rupture occurs by loading the tendon beyond its ultimate strength, it is generally believed that some form of degeneration takes place to reduce the strength of the tendon prior to the rupture event [95-96]. The cause of degeneration is not known but accumulation of damage over numerous sub-failure loading cycles is known to cause fatigue and eventual failure in vitro and may be a

possible mechanism [97-98]. Another form of tendon injury is the tendinopathy, which is a state of chronic pain with tendon swelling and changes in the expression of different matrix components [5, 99]. The cause of tendinopathy is poorly understood but may also be related to micro ruptures at sub-failure loads. It has been proposed that micro ruptures could lead to a local loss of mechanical cell-stimulus and consequent changes in cellular behavior [100].

Another type of tendon dysfunction comes from rare genetic disorders in genes coding for various matrix proteins. An example of such a disorder is Ehlers-Danlos Syndrome (EDS). EDS covers a range of genetic defects and symptoms generally presenting with a combination of joint laxity, skin hyperelasticity and vascular fragility of varying severity [101]. Genetic defects leading to EDS are most commonly found in type V collagen, but also in type I and III as well as non-collagen proteins such as tenascin-X and lysyl hydroxylase [102-103]. The genetic defect results in reduced quality or quantity of type I collagen fibrils, underlining the importance of type V collagen in type I fibrillogenesis. The tissue affected and the severity of the disease can vary greatly amongst patients even if the affected gene is the same, showing that although many connective tissues are based on the same type I collagen protein, the underlying mechanisms of development differ markedly [102].

7.12. Atomic Force Microscopy

Atomic Force Microscopy (AFM) is the primary methodology utilized in the present study [104]. AFM is a microscopy technique that can produce high magnification images like other microscopy methods, but it also enables nanoscale mechanical measurements, which was the main use of the technique in the present works (for an extensive review see [105]). In relation to connective tissue, AFM has been used for a wide range of investigations including imaging of subfibrils [106], proteoglycans [20, 107], fibroblast cells [108] and in vitro collagen self-assembly [47]. In terms of mechanics, individual collagen fibrils [109], sclera [110] and bone [111] are amongst the materials tested.

7.12.1.AFM imaging

AFM is a scanning probe technique, meaning that it involves a probe in physical contact with the sample, and images are produced by scanning the probe across an area. The purpose is to generate a topographical image of the sample. In practice the probe consists of a tip at the end of a cantilever (Figure 10 A). The operating principle is similar to that of a record player. The tip is brought into contact with the sample and scanned across a small area (can range from a
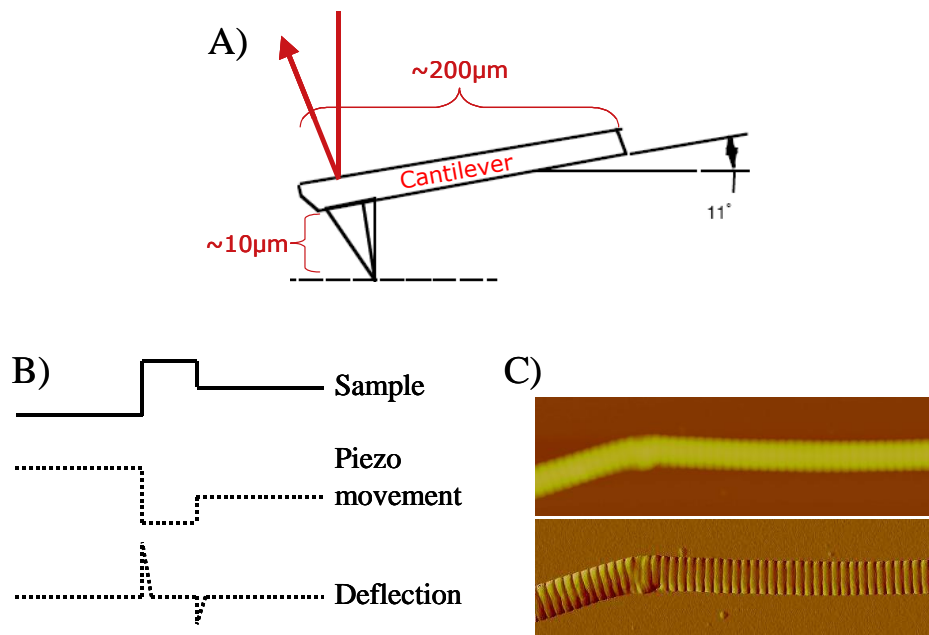
Figure 10: A) Schematic of an AFM probe consisting of a tipped cantilever with a laser reflected on the back. B) Operating principle in AFM imaging. When the tip encounters a change in height (top), the feedback loop counteracts by moving the sample with the piezo scanner (mid). At the edges some deflection occurs due to the finite response time of the feedback (bottom). C) Height image of collagen fibril generated from the piezo movement (top) and deflection image (bottom).

few nm to more than a hundred µm). In order to scan the area with sufficient resolution, either the cantilever or the sample is attached to a piezoelectric scanner capable of moving in 3D with nm precision. Topographical differences cause the tip to move up and down thereby deflecting the cantilever, which is measured by a laser reflected from the back of the cantilever onto a photodiode (Figure 10 A). A feedback loop keeps the deflection at a constant value by controlling the tip-sample distance and this distance becomes the measure of height (Figure 10 B+C). Due to delay in the feedback loop the cantilever will unavoidably bend a little when a steep edge is encountered, this deflection signal is used to generate an image with strong edge contrast (Figure 10 B+C). On soft or loose samples a more gentle contact can be achieved by using tapping mode AFM in which the cantilever vibrates in order to only tap lightly on the surface. In tapping mode it is the amplitude of vibration rather than absolute cantilever bending that is used in the feedback loop, but the imaging process is otherwise identical.

7.12.2. AFM mechanical measurements

Due to the physical interactions taking place between tip and sample, the AFM is not only useful for imaging but can also be used for probing mechanical properties. The piezoelectric scanner can control tip-sample distance to produce a deformation and the cantilever behaves as a linear spring making cantilever deflection a measure of force. Thereby AFM provides the two parameters, deformation and force, required for mechanical testing.

Two basic testing methods are possible with the AFM; either compressive tests using the AFM tip to indent the material, or tensile pulling tests where the tip is attached to the material (could be a single molecule), which is then stretched between a substrate and the tip. To perform the tensile test it is necessary to grip the material. For single molecules, passive adhesion or binding with antibodies or avidin/biotin can be used, but larger structures like collagen fibrils require stronger adhesion using for example epoxy [112-115].

8. HYPOTHESES

8.1. Tendon Force Transmission

The ultimate goal of the present work was to elucidate the mechanisms of force transmission through tendons, and in connection to this also failure mechanisms. This would point out the weak links of the structure, which should be the focus when assessing tendon mechanical function.

Tendons are often viewed as fiber reinforced composites with collagen fibrils as the fiber reinforcement and the proteoglycan gel acting as the interfibrillar matrix. One of the primary factors influencing force transmission is the length of the fibers, if they are discontinuous load has to be transmitted between them, and the structures responsible for this force transmission can become a weak link. Several studies have found implications that fibrils in tendons are indeed discontinuous [74, 91, 116-118] but a source of lateral linkage between fibrils has not been found. A strong candidate was the fibril-associated proteoglycan decorin. Decorin is attached to the surface of collagen fibrils with their glycosaminoglycan (GAG) side chains sticking out [19-21] and our hypothesis was that they would transmit force between fibrils either by direct contact of the GAG chain to a neighboring collagen fibril or by entanglement with the GAG chain from a decorin on a neighboring fibril. Study 4 was performed to investigate this.

8.2. Hierarchical Relations

Another approach to understanding force transmission through the tendon is to compare the properties observed at different organizational levels. Knowledge of the mechanical properties of individual collagen fibrils and of the tendons they form makes it possible to infer basic information on the force transmission. In particular the softer the tendon is compared to the fibril the greater the involvement of interfibrillar components in the behavior of tendons. Our hypothesis was that tendon mechanical behavior is dominated by the fibrils with little involvement of other components, and that the two levels of hierarchy would therefore have closely similar mechanical properties. Primarily study 3 investigated this hypothesis, but the findings in study 5 are also related.

8.3. Intrafibrillar Force Transmission

Besides the mechanisms governing force transmission through the tendon, we also have an interest in understanding the mechanisms governing force transmission through individual collagen fibrils. A fundamental aspect of this are the cross-links involved in interconnecting collagen molecules throughout the length of a fibril. The importance of cross-links for connecting otherwise disconnected molecules in a fibril is conceptually obvious and has been shown in terms of increased collagen thermal stability, decreased solubility and resistance to proteolysis as well as increased mechanical properties at the macroscopic level [119-124]. However, the effect of cross-links occur fundamentally at the fibril level and determining their influence on mechanical function at this level is important to appreciate the ways in which the macroscopic level is affected. We hypothesized that fibrils containing mostly immature cross-links would be softer and weaker than those containing mature cross-links due to breakage of labile bonds in the immature fibrils. This was investigated in Study 5.

Collagen fibrils are initially formed by non-covalent interactions between collagen molecules and these interactions could also play a major role in the force transmission through a fibril [38]. These interactions may be affected by the ionic environment surrounding the fibril [125]. Previous studies have found a significant influence of ionic concentration on compressive properties of collagen fibrils formed in vitro [126], and of Ca^{2+} ions on the adhesive properties of bone collagen [111, 127]. Our hypothesis was that tensile mechanical properties of mature human collagen would not be greatly affected by the ionic environment due to the presence of natural cross-links. We addressed this issue in Study 2.

9. METHODS

In the following, a brief description will be given of the methods used in the studies including a discussion of the particular concerns regarding the use of that method. For methods related to mechanical testing special focus is placed on the key elements of sample gripping, measurement of dimensions, force measurement and deformation measurement.

9.1. Materials

All of the studies presented in this thesis used native tendon tissue samples, mostly from human patellar tendons but also from rat-tails. Human patellar tendon tissues were acquired from anterior cruciate ligament (ACL) reconstruction surgery in which the central part of the patellar tendon is taken out and used for making an autograft to replace the ACL. During these procedures some excess material often remains after forming the graft and it was this material that we obtained. The tissue had clear fascicular structure with crimps. All procedures had received ethical approval and all patients gave their informed consent prior to surgery. Rat-tails were obtained from other studies where the tail was not used.

Rat and human tendon samples were stored at –20ºC. Human tissue was wrapped in gauze soaked with phosphate buffered saline (PBS) before freezing, while rat-tails were frozen whole. Later the tissues were unfrozen to dissect out fascicles and the fascicles were wrapped in PBS soaked gauze and stored at –20ºC. Storage at –20ºC has been shown to have minimal impact on mechanical properties [128-130].

9.2. Single Fibril Mechanical Testing

Due to the relative novelty of the atomic force microscopy (AFM) based mechanical test of single collagen fibrils, a detailed description of the steps involved is given here.

9.2.1. AFM sample preparation

Samples were prepared under a dissecting microscope by placing a small piece (<0.3mm) of tendon on a silicon substrate covered by a droplet of mQ water and gently shearing it apart with a pair of tweezers. Between the two tissue-ends that are pulled apart thin filaments can be seen, and these filaments are then dragged across the center of the substrate causing fibrils to be deposited. After collagen deposition the sample was gently rinsed with mQ water and

dried under nitrogen flux. The dry sample was inspected in a higher resolution optical microscope (5-50x objective) to locate 5-8 suitable fibril segments.

9.2.2. Depositing epoxy on fibrils:

A two-component epoxy glue was mixed and allowed to pre-cure for an hour to keep it from running along the fibril (Figure 11). A small droplet of the epoxy (~15µm in diameter) was picked up with a triangular AFM cantilever (OMCL-TR800PSA). The cantilever was gently set down on each fibril to place two droplets interspaced by the desired testing length (Figure 11). More epoxy was picked up on the cantilever as necessary, 2-3 droplets could be placed with each pickup. Placing glue droplets on the chosen fibril segments took around 30min at which point the epoxy had cured too much to be used any further, and the sample was allowed to fully cure overnight.

9.2.3. Fibril characterization:

The following day optical images were captured using a 50x objective to measure fibril lengths between the droplets (DPX ViewPro, DeltaPix, Måløv, Denmark). AFM tapping mode images were acquired to ensure that fibrils were not structurally damaged during sample preparation, and to check that glue had not run along the fibril (Figure 11). Images (3µm, 512 pixels) were also used for measuring cross-sectional area (CSA) of the fibrils at the middle and at both ends (two measurements at each site).
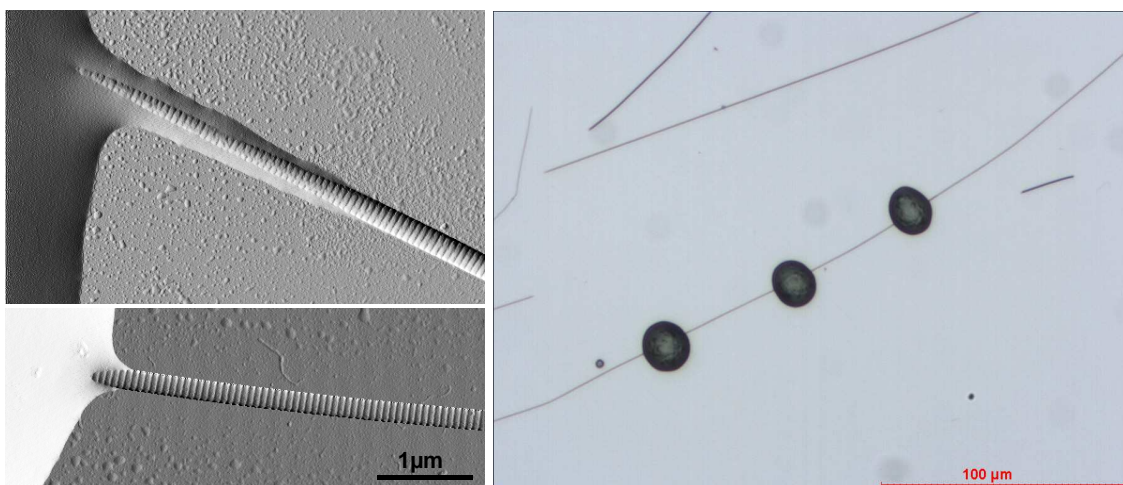
Figure 11: Collagen fibrils. Top left, AFM deflection image of epoxy having run along the collagen fibril. Bottom left, similar image of a fibril where the epoxy has not run along. Right, Bright field optical microscope image of a collagen fibril with epoxy droplets deposited for testing ~40µm long segments.

9.2.4. Fibril attachment to cantilever:

A stiff cantilever was used to detach one glue droplet from the surface by scraping it gently from the sides and it was ensured that the detached droplet was flipped over (Figure 12). This detached droplet was to be used as a grip for the mechanical test. To ensure that the fibril had not been inadvertently stretched during these manipulations, optical microscopy was used to check that the part of the fibril closest to the anchor point had not detached from the surface. Epoxy was mixed and pre-cured for one hour, then a small droplet was picked up on the cantilever used for mechanical testing. In the AFM the cantilever was then gently set down on the detached patch of glue with the tip slightly (~2μm) ahead of the edge where the fibril attached (Figure 12). The epoxy was allowed to cure overnight.

9.2.5. Mechanical testing:

Following the overnight cure, a testing medium (usually phosphate buffered saline (PBS)) was introduced for at least 30 min before starting to lift the cantilever. We did not observe changes in mechanical properties over time indicating that 30 min was sufficient to fully hydrate the fibril. The cantilever was moved to a position vertically above the surface anchor point by maintaining a low tension on the fibril and locating the horizontal position with minimum tension. From this position various mechanical tests were performed by cyclically ramping the tip-sample distance (see detailed test procedures in studies 1, 2, 3 and 5).
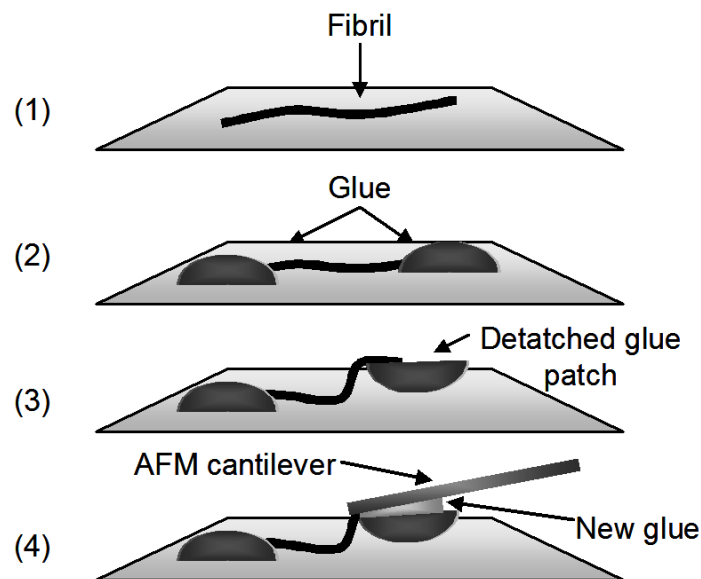
Figure 12: Schematic of AFM sample preparation for mechanical testing. 1) Fibrils are spread on substrate. 2) Epoxy droplets are deposited. 3) After curing an AFM cantilever is used to detach one droplet and flipping it over for use as a 'grip'. 4) The mechanical testing cantilever is attached with epoxy to the 'grip' droplet.

9.3. AFM Methodological Considerations:

9.3.1. Sample Preparation:

In study 5 we observed that using mQ water during sample preparation of acid labile rat-tail collagen caused some of the fibrils to have disordered regions (Figure 13), presumably due to low pH in the mQ water. This issue was alleviated by using PBS during sample preparation and only rinsing the samples in mQ water to remove the salts that would otherwise precipitate. In the earlier studies on human fibrils (study 1, 2 and 3) mQ water had been used, however, we do not believe that this has affected our results in these studies because the human fibrils are stable to acid (see study 5) and never displayed disordered regions. In addition the mechanical behavior was similar to that measured on human fibrils after the improved method.

Another issue is the dry period that is required for the glue to cure. We are not aware of any studies that have managed to test tensile properties of fibrils without drying them at some point, so the effect is uncertain. At the tissue level there is evidence for increased strength and stiffness as a result of long-term dry storage [90], and we may therefore expect some overestimate of fibril mechanical properties. Based on the findings at the tissue level we assume that the effect of two days of dry storage on the modulus is relatively small [90].
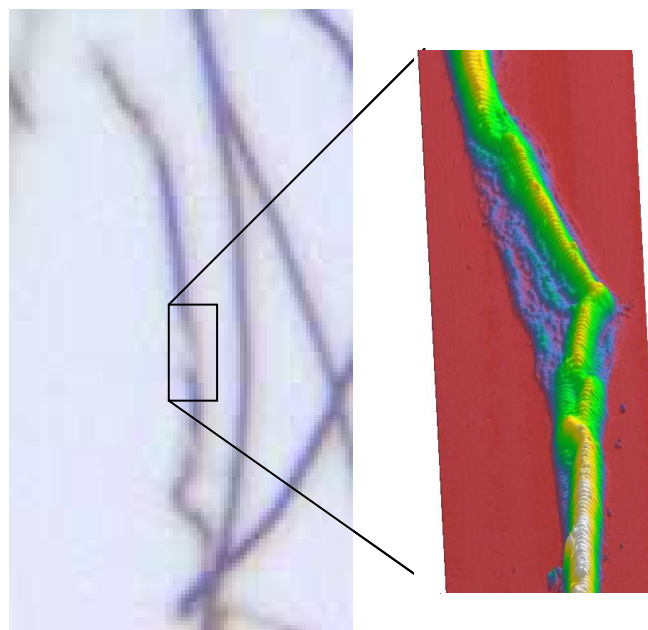
Figure 13: Distorted regions on rat-tail collagen fibrils. Left, bright field optical microscope image of rat-tail collagen fibrils, distorted regions appear faint. Right, 3D AFM image of a distorted region of a rat-tail collagen fibril.

9. Methods

9.3.2. Fibril Gripping:

The described method where one droplet of glue was detached from the surface and used as a grip for cantilever attachment was chosen because we had previously experienced that the fibril could pull out from the lower surface of the glue if it was not 'sandwiched' by the epoxy (Figure 12). Study 1 and 3 made use of a somewhat flexible epoxy (Dana Blå epoxy) that fails at ~10% strain. To ensure the best possible gripping we changed to a hard and brittle epoxy (Araldite 2014) that fails at <1% strain. A harder more brittle epoxy is advantageous in avoiding deformation in the grips; however, we saw no changes in the fibril measurements. This shows that significant deformation did not take place even with the flexible epoxy, in agreement with theoretical calculations (see study 1).

9.3.3. Fibril Deformation:

In study 5 we saw evidence of end-effects similar to those described for macroscopic specimens (section 7.10). We believe this is in part because the fibrils lie horizontally on the sample when the epoxy droplets are applied, which forces them to bend at the glue interface when they are brought into a vertical position for mechanical testing. When testing long specimens the relative contribution of the end-deformation to the total strain is small, but for short specimens it may increase the measured strains significantly. The overestimate in strains for study 1, 2 and 3 (200 µm fibrils) is estimated to be ~20%, while for study 5 (40 µm fibrils) it is ~45% (see study 5 for details).

9.3.4. Fibril Force Measurement:

The range of force that can be measured depends on the stiffness of the cantilever and the range of measurable deflection. In the first studies (study 1, 2 and 3) we had only succeeded in using a soft cantilever (k_{spring} ~0.5 N/m), making it necessary to measure deflections that were outside the range of the photodetector. Mechanical data was therefore acquired in multiple pieces by moving the detector to increase the measurable range (Figure 14). The pieces were then stitched together afterwards. The testing procedure involved continuous cyclic stretching, which yielded a stable response after a number of cycles, and then acquiring each piece of the curve in separate cycles. To ensure linearity of the recorded laser deflection across detector positions, the same type of measurement was performed on a cantilever bending against a hard substrate (Figure 14).
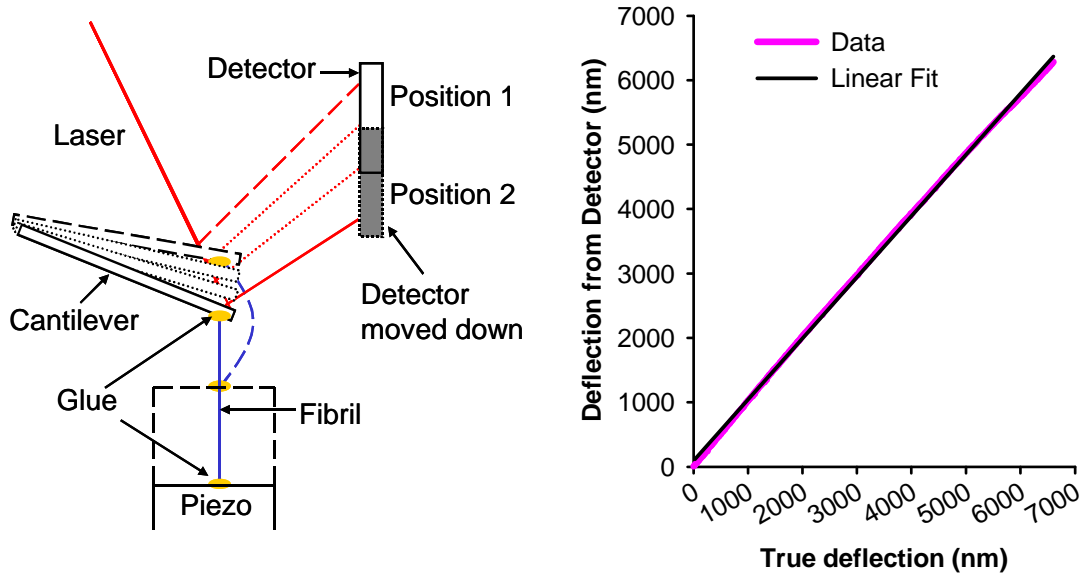
Figure 14: Left, schematic of a fibril mechanical test showing how the detector was moved to cover a wider deflection range. Right, linearity of measured deflection signal over several detector positions. Measured by deflecting the cantilever against a hard Si substrate, the movement of which was considered the 'true deflection'.

The method described above cannot be used for failure testing, so in study 5 we improved the method to use a stiff cantilever (OMCL-AC160TS, k_{spring} ~30 N/m). This required removal of the tip because it was so long that the cantilever could not get in contact with the fibril. The tip was removed by mechanically breaking it against a hard Si substrate. Using a stiffer cantilever eliminated the need to move the photodetector and stitching together data.

To quantify mechanical properties the spring constant of the cantilever has to be determined. The method that we have used is called thermal tuning and is based on the thermal vibration spectrum of the cantilever [131]. Thermal energy (Equation 1) causes the cantilever to vibrate at its resonance frequency, and in such a vibration half the mean energy is in the form of potential energy (the other half is kinetic energy). The spring constant is related to the potential energy through the mean square deflection (Equation 2), which can be measured as the area under the curve in a vibration power spectrum (Figure 15). This allows the spring constant to be determined (Equation 3) [131].

(1) $\langle E_{Therm} \rangle = K_B \cdot T$

(2) $\langle E_{Pot} \rangle = \frac{1}{2} \cdot k_{spring} \cdot \langle x^2 \rangle, \quad x = deflection$

(3) $\langle E_{Pot} \rangle = \frac{1}{2} \langle E_{Therm} \rangle \Rightarrow k_{spring} = \dfrac{K_B \cdot T}{\langle x^2 \rangle}$

9. Methods
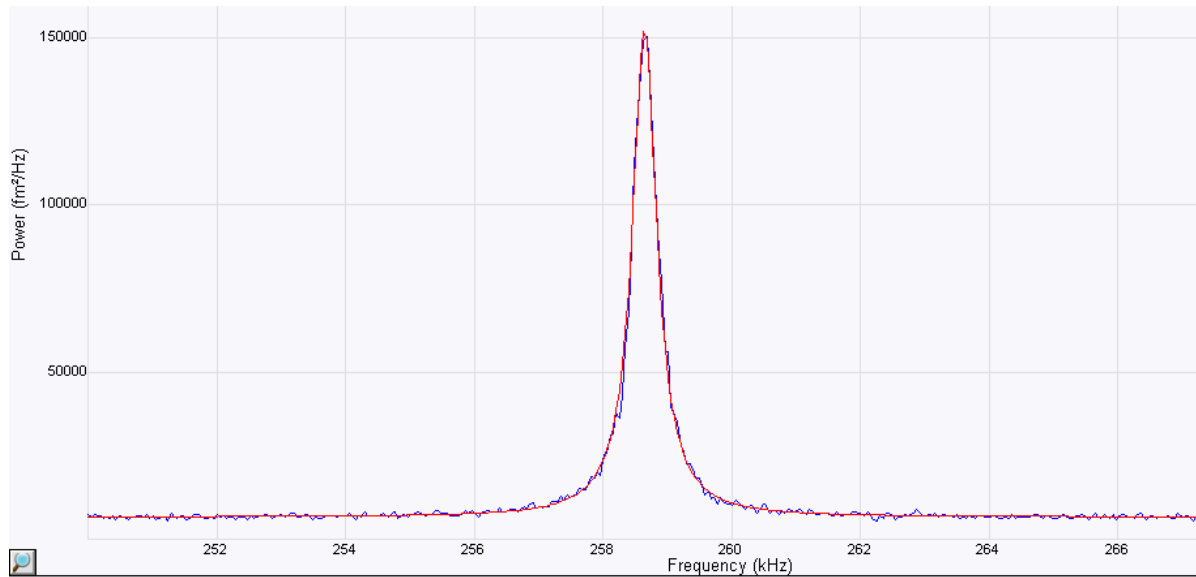
Figure 15: Thermal power spectrum in air of a cantilever with spring constant ~30 N/m. A Lorentzian fit (red) is applied to the data (blue).

The force is given by multiplying the cantilever spring constant with the deflection. The laser system used for determining cantilever deflection has to be calibrated for each experiment. This calibration results in a deflection sensitivity that describes how many nm the cantilever has to bend in order to produce a change in photodetector signal of one volt. Deflection sensitivity depends on the environment (dry or liquid), the type of cantilever used, the shape of the laser spot and the position of the laser spot on the back of the cantilever. We wanted to avoid determining the deflection sensitivity of every cantilever in liquid because the cantilever would then need to be dried before applying the epoxy, and doing so is time consuming and risks altering the laser position on the cantilever. In studies 1, 2 and 3 a triangular cantilever was used for sub-failure testing. We found that the deflection sensitivity in liquid only varied by ~3% with laser position and therefore we used the mean value of six different cantilevers (29.0 ±0.6 nm/V) as the deflection sensitivity in all experiments. In study 5 a rectangular cantilever was used for failure-testing and here the deflection sensitivity varied more with laser position, however, we found a good linear correlation between dry and wet deflection sensitivity which we used to determine the wet value based on measurements in the dry state.

It is worth noting that when using thermal tune to determine the spring constant, then errors in the deflection sensitivity will partially cancel when calculating the force. This is because the force is the deflection multiplied with the spring constant, which from the thermal tune has an inverse dependence on the squared deflection (Equation 3).

34
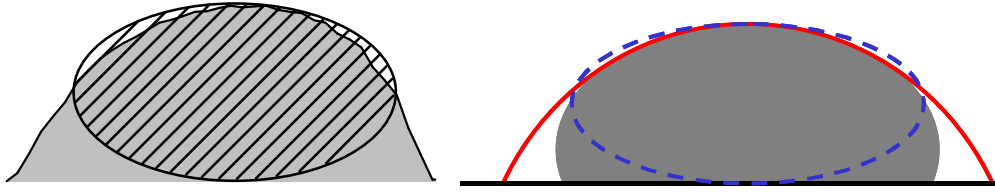
Figure 16: Collagen fibril cross-section. Left, the gray area is the total integrated area under the section. The dashed area is the de-convoluted elliptical fit. Right, schematic of the situation when the fibril adheres to the substrate. Grey is the fibril, the full red line represents the convoluted area, and the dashed blue line is the de-convoluted area. It can be seen that the true area is in between the convoluted and de-convoluted measures.

9.3.5. Fibril Dimension:

Fibril CSA was measured by AFM and in AFM the lateral imaging resolution is limited by the size and shape of the tip. This may result in tip convolution and an overestimate of CSA. We estimated a de-convoluted CSA based on an ellipse with one axis equal to the measured height, and the other equal to the width at half the height (Figure 16). However, fibrils adhere to the substrate, which will likely increase their surface contact area and thereby reduces the convolution effect. We have therefore used the mean of the de-convoluted CSA and the directly measured CSA by integration (Figure 16). The difference between the two methods is approximately 20%.

9.4. Micromechanical Fascicle Testing

Tendons consist of distinct cylindrical substructures called fascicles, and these structures have been shown to be mechanically independent [132]. Their mechanical independence enables the separation of fascicles and makes them suitable for mechanical testing as a sort of small-scale tendon. Mechanical measurements have been conducted on fascicles on both human and animal tissue [133-136]. How the mechanical response changes when going to smaller subunits is not fully understood, both reduced and increased mechanical properties have been reported [80, 137], however, there are great differences in absolute values reported at all levels and much of the effect may be related to gripping issues [79]. In the present studies, force and deformation on individual fascicles was measured using a micromechanical rig (200-N tensile stage, Petri dish version, Deben, Suffolk, UK) (Figure 17). This system can apply deformations up to 10 mm at deformation rates of 0.5-6 mm/min and measures force up to 20N with a resolution of 0.01 N. The system is equipped with a Petri dish to allow a liquid environment for the fascicles during testing or other treatment. The rig was associated with a dissecting microscope allowing images to be captured to determine sample dimensions.
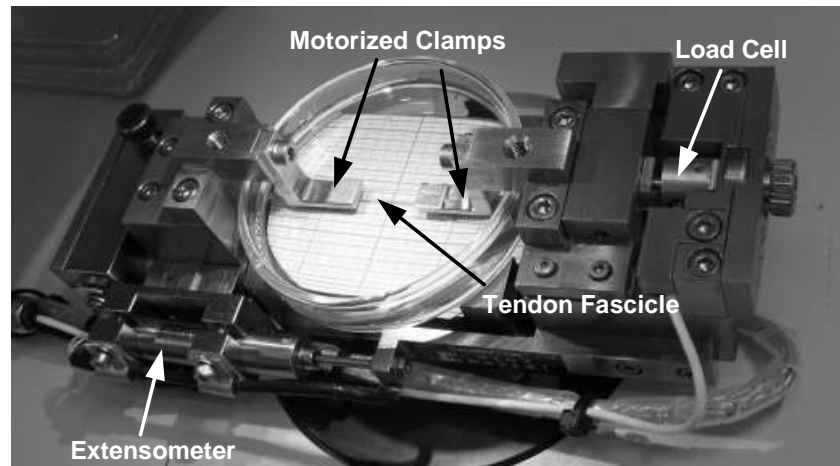
Figure 17: Photograph of the micromechanical rig used for fascicle testing.

9.5. Micromechanical Methodological Considerations:

In the following, a number of methodological issues are listed. However, it should be pointed out that all the issues listed below are greatly alleviated by our experimental design, which makes use of repeated measures on the same specimen such that any errors in clamping, straining or CSA are equal when comparing treatment effects.

9.5.1. Fascicle Gripping:

Obtaining a firm grip on the sample is one of the major concerns in any mechanical test. With our system we decided to use a combination of cyanoacrylate glue and drying of the clamped ends for gripping. Glue has a number of advantages because it offers an evenly distributed attachment of the specimen, which should diminish stress concentration at the grip, and in addition it does not produce compressive loads that could damage the sample. The primary drawbacks of glue is that it only attaches to the specimen surface (Figure 18) and binds poorly to wet materials. The issue of surface attachment increases with increasing specimen size and is therefore alleviated somewhat by the use of small samples like fascicles with diameters of ~300µm (see study 2 and 4). Allowing the ends of the specimens to dry reduces the surface
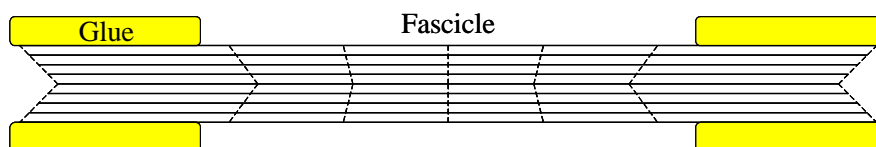
Figure 18: Schematic illustration of the issues related to only gripping a fascicle at the surface. As can be seen the core of the fascicle is free to partially slip while the surface is held by the glue. The extent of slippage depends on internal shear resistance.

attachment issue because it increases the shear resistance thereby improving force transmission between the surface and center of the specimen. In addition drying causes a short gradient region between the completely dry and fully hydrated part of the specimen, which we speculate would help alleviate stress concentration.

In spite of these advantages there was a tendency for failure to occur closer to the ends than the center, however, the broken ends had fibers of varying length, indicating failure over a larger volume. In a previous study of gripping methods it was found that even the best grips had a high occurrence (70%) of failures near the grip, but that failure site did not appear to affect the mechanical properties [138].

9.5.2. Fascicle Deformation:

Another important issue is how to measure strain. There are two common options, either measuring clamp-clamp distances or having surface markers on the central part of the specimen. The use of surface markers is based on the idea that stress concentration cause increased tissue deformation at the clamps, which is not representative of the deformation in the central part. Using surface markers results in lower strains and consequently higher modulus and stiffness values [133]. One argument against surface markers is that they only represent the strain of the surface layer, which may be more of a sheet than proper tendon. We used clamp-clamp distance because in our opinion this is more representative of the overall tissue strain, but in hindsight having both measures would have been a preferable.

9.5.3. Fascicle Dimensions:

With the present equipment the fascicle was not easily accessible from the sides while immersed in the Petri dish and the diameter was therefore measured from the top by optical microscopy, and CSA was calculated assuming a circular cross-section. Recently we have used a 45°-inclined mirror to also measure fascicle thickness and found that it was on average ~15% lower than the width. This suggests a 15% underestimate in stress and modulus values in study 2 and 4.
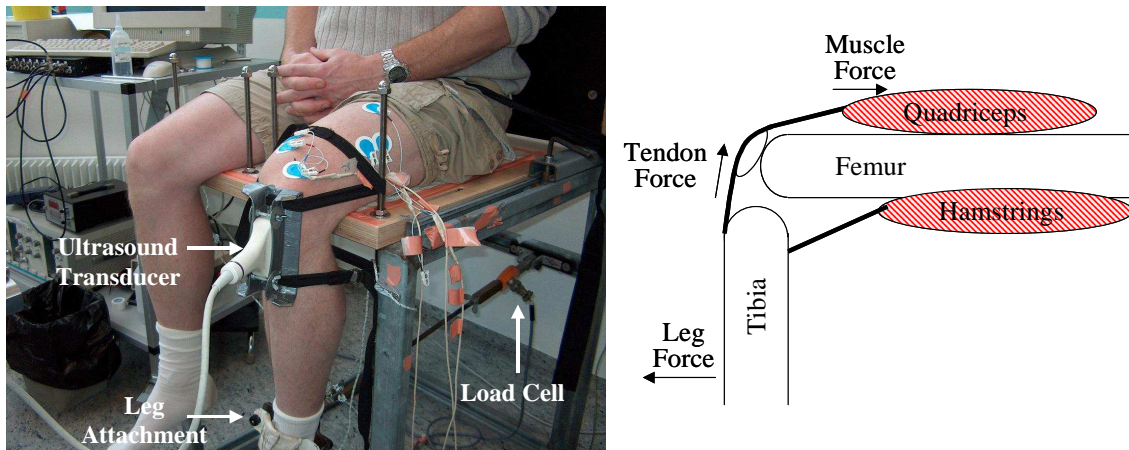
Figure 19: Left, photograph of the setup for in vivo mechanical testing of patellar tendons. Right, schematic of a knee indicating the muscles and forces involved.

9.6. Ultrasound in vivo Tendon Testing

Recently the use of ultrasound to image deformation of tendons under load has been applied to study mechanical properties in vivo [81, 139-141]. Being able to measure in vivo is clearly an advantage since it provides the most physiologically relevant results and overcomes any gripping and hydration issues. A limitation with in vivo testing is that the subjects own muscle force is used to load the tendon, which limits the mechanical range of measurements and in particular failure properties cannot be assessed. Since the tendon in vivo is less accessible, measurements of force, deformation and tendon dimensions also become more difficult.

The method used in our lab to measure patellar tendon mechanical properties in vivo has been described in details and validated by Hansen et al. [142]. In brief the subject was placed in a rigid chair and had their ankle attached to a load cell through an inflexible rod with their knee at 90º (Figure 19). An ultrasound transducer long enough to image both the patella and tibia was attached to the knee (Figure 20) and the subject was asked to produce an isometric contraction of the quadriceps (Figure 19) by 'kicking' forward over a 10s ramp up to their maximum voluntary effort. The dimensions of the patellar tendon were measured by magnetic resonance imaging (MRI) (Figure 20).
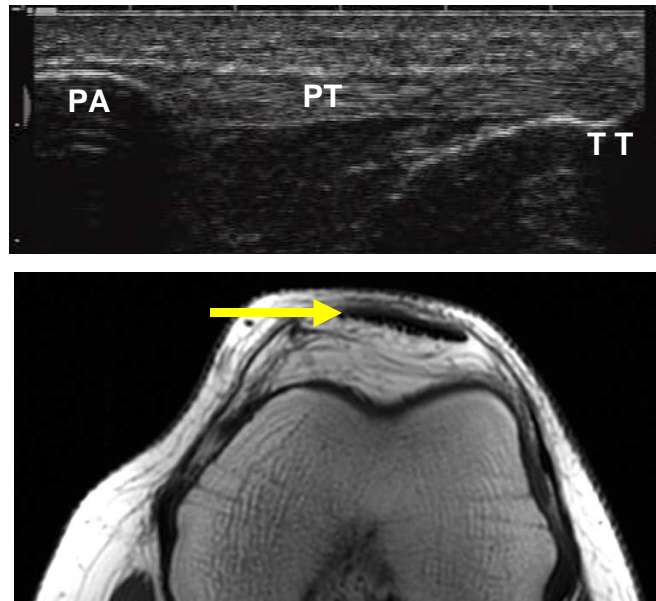
Figure 20: Top, ultrasound image of a human patellar tendon (PT) including the patella apex (PA) and tibial tuberosity (TT). Bottom, MRI cross-section of a human knee displaying the patellar tendon as a dark area (arrow).

9.7. Ultrasound Methodological Considerations:

9.7.1. In vivo tendon deformation

With the ultrasound imaging we defined tendon deformation as the change in distance between the bones at the patella apex and the tibial tuberosity, which seems appropriate since the bones are too stiff to deform appreciably. It is worth noting that this method is unable to distinguish differences in mechanical properties along the tendon and therefore represents an average. On excised tissue it has been found that greater deformation takes place at the bone insertions [143], meaning that the deformation in the central part would be less than the measured average. The movement of the patella and tibia was measured using an automatic tracking algorithm [144], however, the tracking quality depends on manual selection of the optimal image features for tracking. Poor tracking always resulted in an underestimate of the deformation because the tracking markers were unable to follow the movement of the feature. For this reason each ultrasound video was tracked multiple times to ensure reproducibly high deformation values while traces resulting in low deformation were discarded.

9.7.2. In vivo Tendon Force

Because force was measured by a load cell attached to the leg and not directly to the tendon, determining the tendon force requires the moment arms to be measured (Figure 19). The moment arms of interest here are the distance from the center of rotation in the knee to the

load cell on the leg and to the tendon respectively. The leg moment arm can be measured with good precision using measuring tape, but the tendon moment arm is more difficult. Some studies have measure the distance from the axis of rotation to the tendon, but it is difficult to precisely define the position of the rotational axis [140]. Another approach is to look at the movement of the unloaded muscle-tendon unit as a function of joint angle, which provides very nicely the moment arm experienced by the tendon [145], however, it cannot be used in vivo since the muscle must be dissected to move freely. We chose to measure the femur length and infer the moment arm using the correlation reported by Visser et al. [145] at a joint angle of 90º. The mean moment arm of rectus femoris, vastus intermedialis, the lateral part of vastus medialis and the medial part of vastus lateralis was used, yielding a tendon moment arm that that is 0.065 times the femur length.

When performing the quadriceps ramp some co-activation of the hamstrings is expected (Figure 19), which would cause an underestimate of tendon force. It was our intention to account for this by measuring hamstring co-activation with electromyography (EMG), but unfortunately faulty equipment caused high levels of noise in the EMG signal making this correction impossible. Other studies suggest that an underestimate in tendon force of ~10% could be expected [146-147].

9.7.3. In vivo Tendon Dimensions

MRI was used to measure the length and CSA of the patellar tendon. The length was measured from the apex of the patella to the insertion at the tibial tuberosity, which is the length of the free tendon. The CSA was measured at the middle and the ends of the free tendon. The tendon CSA increases from the proximal to the distal end [148] and the mean CSA was used. Using the mean CSA means that the stress is underestimated at the proximal end and overestimated at the distal end but is probably fairly correct for the central part.

9.8. Hydroxyproline Assay

Quantifying collagen content in connective tissues is important both to determine the absolute content of these load-bearing structures and also to be able to normalize collagen modifications such as cross-links to the number of molecules thereby allowing a stoichiometry to be established. The most common method of quantification is based on the high content of hydroxylated proline residues in collagen and the rarity of this compound in other proteins. In the assay that we utilized, detection of the hydroxyproline is based on

oxidation with Chloramine-T resulting in the transformation of hydroxyproline to pyrrole [149-150]. Pyrrole content is then determined by reaction with 4-dimethylaminobenzaldehyde (DMBA) also known as Ehrlich's reagent. On reaction with pyrroles DMBA produces a blue color with an absorbance peak around 560nm [151] and the absorbance is measured spectrophotometrically. Pyrroles are also one of the mature enzymatic cross-links found in collagen (see section 0), which may in principle contribute to the measurement, however, there are approximately 300 hydroxyprolines per collagen molecule and generally less than 1 pyrrole cross-link [152] making this contribution insignificant.

When used for determining absolute collagen amounts the method suffers from uncertainty in the hydroxyproline content of collagen molecules. The content varies significantly between species [30, 153] and possibly also between tissues. We have used 300 moles per collagen molecule, which is about 14% by weight.

9.9. HPLC Cross-link Analysis

In study 3, the content of the mature hydroxylysyl-pyridinoline (HP) and lysyl-pyridinoline (LP) cross-links as well as the advanced glycation end-product (AGE) cross-link pentosidine were measured by our collaborator Vuokko Kovanen at the University of Jyväskylä Finland. The analysis was based on the high performance liquid chromatography (HPLC) method by Bank et al. [154] and has previously been reported [13]. In brief, tissue was freeze dried, weighed and hydrolyzed in 6 M HCl at 110ºC for 24 hours and then evaporated to dryness. The dry hydrolysate was dissolved in water and the cross-linked peptides were separated on a reverse phase HPLC column using an acetonitrile/water gradient with heptafluorobutyric acid (HFBA) as an ion-pairing reagent. Cross-links were detected by their natural fluorescence: HP and LP at 400/295 nm (emission/excitation) and pentosidine at 378/328 nm. Quantification was based on pure HP, LP and pentosidine standards included in each run. Cross-link concentrations were expressed relative to collagen content based on a colorimetric hydroxyproline assay (section 9.8).

9.10. Glycosaminoglycan Quantification

In study 4 the primary glycosaminoglycans (GAGs) of tendon, dermatan sulfate (DS) and chondroitin sulfate (CS) were digested with chondroitinase ABC enzyme (0.1 U/mL in Tris buffered saline containing 5mM $CaCl_2$). Following enzyme treatment the specimens were placed in a stop-buffer containing EDTA to block the Ca^{2+} dependent activity of the enzyme.

At the time we were unfortunately unaware that only the activity towards DS is calcium dependent while activity towards CS is not, but can be blocked by Zn^{2+} [155]. In hindsight a Zn^{2+} containing stop-buffer should therefore have been included, however, since samples were dried immediately after the stop-buffer, we do not believe that significant CS digestion would have had time to occur.

The GAG content of treated and control samples was measured by the dimethylmethylene blue (DMMB) assay. The assay involves enzymatic digestion of the tissue using papain followed by reaction of sulfated GAGs with DMMB producing a shift in the DMMB absorbance with a peak difference at 525 nm [156]. In study 4 we found that the papain treatment caused a reduction in the GAG content of DS standards and this loss was taken into account when determining the sample GAG contents. An attempt to reduce papain concentration to half made no improvement, but we later became aware that the specific activity of our papain was probably more than ten fold greater than in the published method that we had used, which could explain the loss of GAGs (see study 4 for details).

10. STUDIES

10.1. Study 1 - Viscoelastic behavior of discrete human collagen fibrils

The first study was a short communication based on our very first fibril measurements. We observed that the mechanical response of collagen fibrils was dependent on the applied deformation rate and that stress relaxation was also present, both features of viscoelasticity. Because mechanical models of connective tissue rely on descriptions of the properties at each level we found it important to report these findings relatively rapidly, possibly allowing other researchers to include it in their models.

When it comes to analyzing viscoelastic properties, there are several possible approaches including creep, stress-relaxation, and cyclic testing [97, 157-159]. It was not readily possible to setup our equipment for creep testing, which was therefore omitted. Stress-
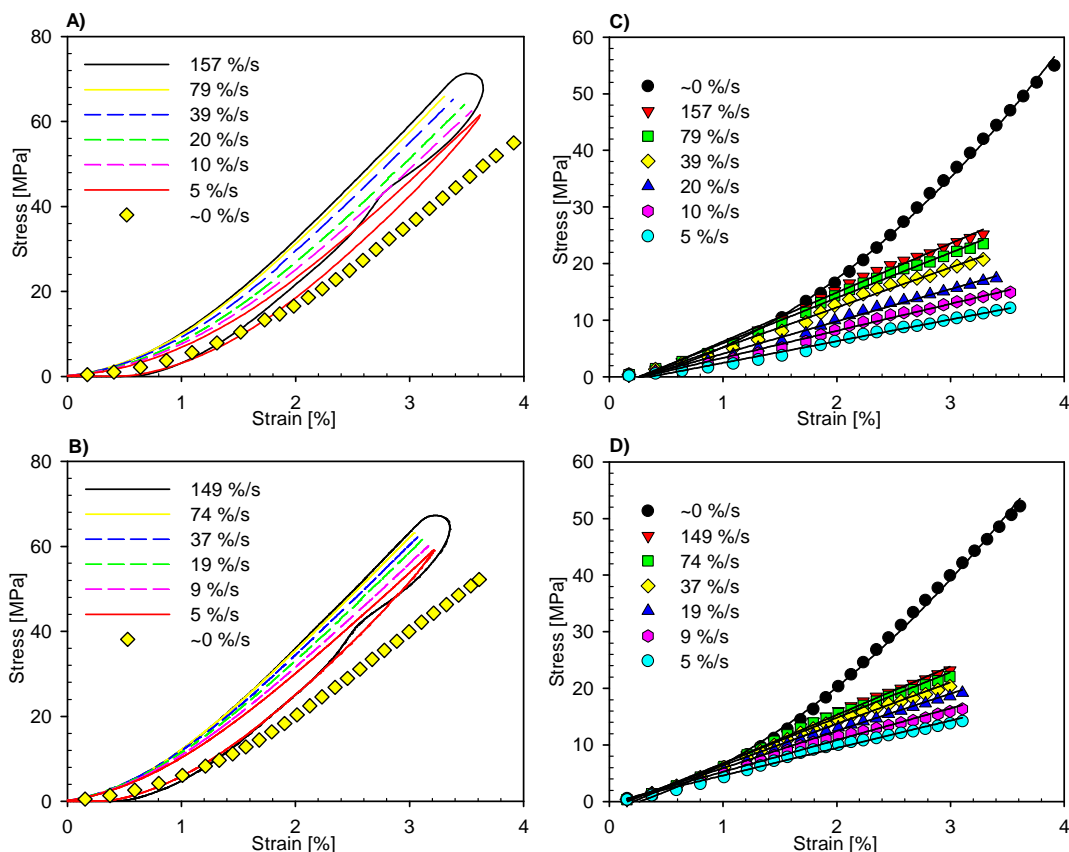
Figure 21: A+B) Cyclic stress-strain response of two collagen fibrils at different strain rates. The 0-rate data points were obtained by step-wise stress-relaxation. C+D) Division of the stress-strain response into elastic (0-rate) and viscous components. The viscous component was obtained by subtracting the 0-rate stress-strain response from the curves at the other rates. A second order polynomial is fit to the elastic component and linear fits are applied to the viscous components.

relaxation was possible, but drift in the deflection signal over longer time periods and poor equipment control of the loading rate made it impossible to analyze the stress vs. time properly. Instead we performed cyclic tests in the elastic region (~4% strain) yielding non-linear stress-strain curves and then used a stepwise stress-relaxation test as an effectively 0-rate measurement to isolate the elastic response, an approach that has also been reported on collagen fibers (Figure 21) [158, 160]. For comparison to other studies, low amplitude cyclic testing to determine loss and storage modulus may in hindsight have been a good addition [161]. We initially did not utilize this method because the noise at small deformations was high, but this issue could probably have been overcome by averaging over several cycles.

We found that the elastic stress was well described by a 2nd order polynomial function of the strain, and that the remaining viscous stress component had a linear strain dependence with a slope that depended on strain rate according to a power function (Equation 4) with power ~0.2 (Figure 21).

(4) $\eta = A \cdot v^B$

Here η is the slope of the viscous component and v is the strain rate. A and B are parameters of the power function fit. Since the results in this study were based on only two fibrils, we repeated the measurements as part of study 3, and found the same behavior. From this larger dataset we determined the power of the strain rate dependence to be 0.22-0.24 (95% confidence interval). Purely Newtonian viscosity has a linear dependence on strain rate, in other words a power of 1, and the lower power observed in our experiments is an example of non-Newtonian behavior known as shear thinning. In study 1 I used the term thixotropic to describe this behavior, which is strictly not correct since it refers to time dependence rather than the dependence. However, the two phenomena are strongly related and can be difficult to separate [162]. Similar shear thinning has previously been reported on collagen fibers; where it was proposed to occur by hydroplaning of subfibrillar structures at high rate [158]. Our results corroborate this view. Looking at the relative magnitudes of the viscous and elastic components it can be seen from Figure 21 that the elastic fraction increases with strain, starting at approximately 50% below 1% strain. This is similar to what has been reported on fibers from rat-tail [90].

Viscoelasticity at the fibril level has also recently been reported by others [88, 163-164], and while viscoelasticity at the tissue level has generally been thought to originate in interfibrillar mechanisms such as fibril slippage, these findings suggest that at least part of the viscoelastic response may originates in the fibrils them selves.

10.2. Study 2 - Tensile properties of human collagen fibrils and fascicles are insensitive to environmental salts

During our collagen fibril mechanical tests we observed that some evaporation of the buffer took place and we were concerned that resulting changes in buffer concentration could affect our results. At this time a paper was published which showed very significant effects of salt concentration on fibril mechanical properties measured by AFM indentation [126], and we therefore decided to investigate if this was also the case for the tensile properties of our fibrils. If buffer concentration and composition indeed had such significant effects it would necessitate great care in designing a buffer that correctly imitates physiological conditions.

Human patellar tendon fascicles and collagen fibrils were mechanically tested in the elastic region (~4% strain) and the modulus and energy dissipation was determined in five different buffer solutions for each specimen. In addition AFM was also used to image fibrils in the same buffers to determine any effect on swelling. The tested buffers were a hypotonic 20 mM PBS solution, an isotonic 150 mM PBS, a hypertonic 1000 mM PBS, an isotonic HEPES buffered NaCl solution and an isotonic HEPES solution with calcium, all at physiological pH = 7.4. The three PBS solutions were tested first in a randomized order, followed by the HEPES and then finally the calcium containing buffer. This design was necessary because calcium precipitates in the presence of PBS so the HEPES has to be introduced in between to wash out the phosphate.

We found that fibril swelling was unaffected by the buffer composition, which is in agreement with previous AFM findings [126]. Others have reported that small ions (NaCl)
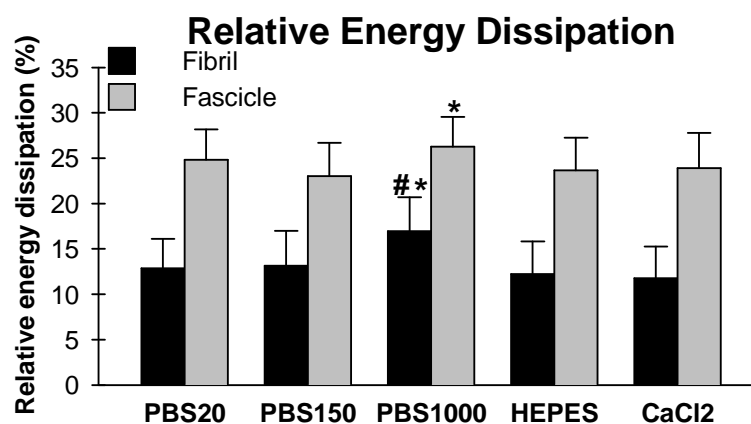
Figure 22: Results for the energy dissipation during cyclic testing of collagen fibrils and fascicles from human patellar tendon in various buffers. * Significantly different from 150 mM PBS, # significantly different from 20 mM PBS.

45

do have an osmotic effect on collagen [165], causing the molecular spacing to reduce with increased concentration, however, the effect was only ~6% at 1 M NaCl. This may be too little for the AFM technique to detect, especially considering that the absolute swelling is larger when measured by AFM than by other methods (see study 3).

At the mechanical level the only consistent finding was a statistically significant increase of energy dissipation in the 1000 mM PBS, both at the fibril and fascicle level (Figure 22). The magnitude of the difference however was less than 5%. We propose that the high salt concentration may have stabilized the deformed state of the fibrils by screening electrostatic charges on the collagen molecules, which have become exposed due to mechanical strain. This stabilization would reduce the energy returned during relaxation and thus increase the total energy dissipation.

Overall there were no relevant effects of environmental composition on mechanical properties, particularly in the range that could be considered physiological. We wanted to elucidate why our findings contradicted those of the previous report [126], and to do so we performed additional measurements in collaboration with the main author of that paper, Dr. Colin Grant. The results are included in the supplement for study 2 and showed that the sensitivity to saline was increased at low pH. In addition it was found that our samples were not sensitive to saline in indentation measurements. Together, these results suggest that the insensitivity to saline environment in our study is due to the more stable cross-linked collagen fibrils from mature human patellar tendon compared to the reconstituted fibrils used in the indentation study [126]. The choice of buffer for mechanical testing of mature tendon is therefore not critical but when testing reconstituted or possibly immature collagen the potential influence of test medium should be considered.

10.3. Study 3 - Mechanical properties of human patellar tendon at the hierarchical levels of tendon and fibril

This was chronologically the second study of the thesis although it was published later than some of the others. The purpose was to determine the mechanical properties of collagen fibrils and of their parent tendons in order to elucidate the mechanism of load transmission by investigating the differences between the two levels.

Our hypothesis was that collagen fibrils are mechanically continuous throughout a mature tendon and that consequently the tendon mechanical properties would be governed primarily by the fibril properties. Even in that case, fibril arrangement for example in the form of crimps would affect the tendon behavior e.g. introducing a toe-in region, but we expect the majority of fibrils to be engaged in the linear region thus yielding comparable peak modulus values. Based on these considerations we expected that fibril toe-region strain would be lower than that of tendon while the elastic modulus would be comparable between the two levels when taking fibril content of the tendon into account. If the hypothesis was incorrect and fibrils are not mechanically continuous, tendon modulus would be expected to be lower than fibril modulus due to fibril slippage.

Individual collagen fibril segments 200µm long were tested in PBS using the AFM method previously described, and tendon properties were measured using the in vivo ultrasound method. Toe-region strain was determined by extrapolating the linear region down to the strain axis and determining the intersect.

Measuring at each hierarchical level separately yielded a fibril modulus of 2.8 ±0.3 GPa with a toe-region strain of 0.86 ±0.08% and a tendon modulus of 2.0 ±0.5 GPa with a toe-region strain of 3.3 ±1.9%. The greater toe region at the tendon level agrees with the presence of macroscopic crimps but says nothing about the mechanical continuity of fibrils. In order to compare the modulus values it is essential to assess the fibril content of the tendon. According to the so called rule of mixtures commonly used in composite materials science [166], the modulus the components are weighed by their volume fraction. In this rule it is assumed that all components experience the entire externally applied strain, if this is not the case (e.g. due to slippage) some components experience less strain and the composite modulus becomes lower than predicted by the rule of mixtures.
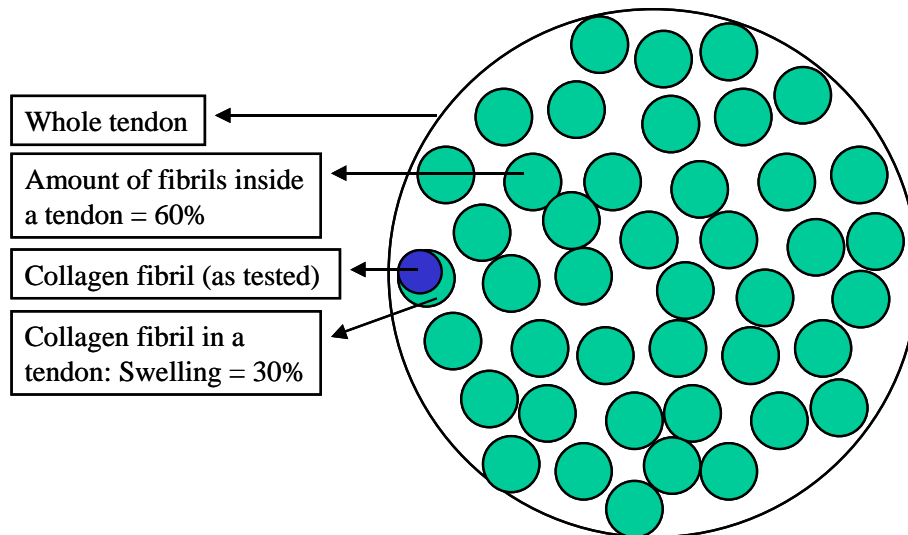
Figure 23: Schematic of a tendon and the conversion factors involved in relating fibril cross-sectional area (CSA) to tendon CSA. Notice that the fibrils were tested in buffer and 'Collagen fibril (as tested)' refers only to the use of dry CSA in stress calculations.

As a composite we consider the tendon to contain only two components (Figure 23), collagen fibrils and an interfibrillar gel of mainly proteoglycans and water (see section 7.3), furthermore we assume that the modulus of the gel is negligible compared to that of the collagen fibrils. The volume fraction of the collagen can be determined from transmission electron microscopy (TEM) cross-sectional images by quantifying the relative area occupied by fibrils. The TEM preparation procedures involve dehydration, however, since water is lost in both the intra- and interfibrillar space the effect on the volume fraction will be reduced. X-ray results suggest that interfibrillar water may be lost more rapidly than intrafibrillar water [167-168], which could cause an overestimate of fibril volume fraction, but the measured values do not appear excessive so we believe this is not a major issue. Reported values of fibril volume fraction in human patellar tendon are fairly consistent around 60% [152, 169].

In the AFM measurements we determine fibril CSA in the dry state because this is the simplest and most reliable method, but in order to compare with native hydrated tendon, the hydrated CSA has to be used. We have measured swelling upon hydration with AFM finding ~100% increase in diameter (study 2) which is in agreement with other single fibril AFM studies [170-172], however, it does not agree well with X-ray studies on whole tendon [167, 173]. The value obtained on single fibrils also appears excessive considering the total water content in tendon. Swelling of 100% would equal a four fold increase in CSA and thus ~75% of the hydrated fibril volume would be water. In addition the tendon also contains water in the interfibrillar space so a water content exceeding 75% would be expected, yet the

reported content in native tendon is ~65% [174-175]. The native water content is in better agreement with X-ray measurements that find an ~30% increase in fibril diameter [167].

When recalculating the fibril stress with the hydrated CSA using 30% swelling and applying the rule of mixtures with a volume fraction of 60% (Figure 23), the 2.8 GPa fibril modulus predicts a tendon modulus of only 1 GPa as opposed to the 2 GPa that we measured. This result agrees neither with our hypothesis of continuous fibrils, which would predict an equal modulus, nor with the alternative hypothesis of discontinuous fibrils, according to which the tendon modulus should be lower than predicted from the fibril modulus. More recent results (study 5) have shown us that the presence of end-effects may lead to underestimates in the fibril modulus which for 200µm long fibrils would amount to ~20%, but even with this correction the fibril modulus remains significantly lower than that of the tendon in vivo.

From the literature, it is not the ~1.2 GPa modulus predicted from fibril measurements that stand out, but rather the high 2 GPa modulus values obtained on the tendon in vivo. Other in vivo studies have also found similarly high modulus values while reports on excised tissue, either whole tendon or fascicles, usually fall in the range of 0.5-1.5 GPa (see Table 2 in section 7.10). As described in section 7.10, the higher values are likely more credible but the in vitro values still appear to be lower than from the in vivo tests. It would therefore appear that removing the tendon from its natural environment causes a reduction in modulus. We believe that the effect occurs at the fibril level, but is not related to
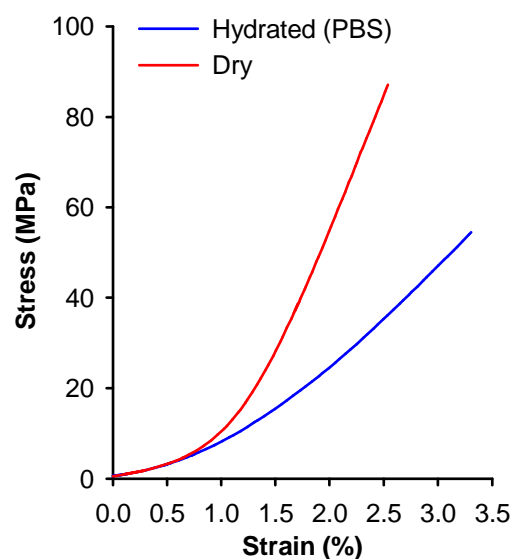
Figure 24: Example of mechanical test on a collagen fibril before and after hydration with PBS. A clear increase in stiffness is observed for the dry fibril.

fibril degradation since we have observed no structural damage on our tested fibrils. We propose as an explanation that collagen fibrils are mildly dehydrated within the native tendon, and that external hydration during in vitro experiments cause increased fibril hydration resulting in a lower modulus. External hydration is necessary for in vitro testing since tendon and especially the thin fascicles dry out rapidly. Others have reported increased modulus with complete dehydration [171-172] and we have found the same (Figure 24). That in vitro fibril modulus corresponds well with in vitro tendon modulus strongly supports the hypothesis of mechanically continuous fibrils, although the apparent reduction in modulus in vitro compared to in vivo makes the conclusion less clear.

10.4. Study 4 - Tensile force transmission in human patellar tendon fascicles is not mediated by glycosaminoglycans

The hypothesis of mechanically discontinuous fibrils necessitates the presence of some mechanical linkage to transmit forces between discrete fibrils. This could take place simply through friction between fibrils but molecular linkers are also a possibility. One of the major contestants is the fibril-associated proteoglycan decorin, which has a horseshoe shaped core protein that binds to collagen fibrils [176], and a single glycosaminoglycan (GAG) chain protruding in a straight fashion [177-178]. This structure could in principle allow force transmission by binding collagen fibrils together through interactions of the GAG chain, either with GAG chains on a neighboring fibril or directly with the fibril.

At the time we began the study, there were to our knowledge only two studies of proteoglycan mediated force transmission in tendons or ligaments, one showing increased mechanical properties after removal of the GAG chain [179], the other showing no change following a similar treatment [180]. We had a few preliminary measurements that suggested reduced mechanical properties and the influence of GAGs on tendon mechanics was therefore unclear.

The experimental protocol involved cyclic testing of fascicles from human patellar tendon into the elastic region (4% strain) before and after treatment with chondroitinase ABC (Ch-ABC), an enzyme that digests the two different types of GAG present on decorin (dermatan sulfate and chondroitin sulfate). Along with the fascicles that were mechanically tested, an additional piece of tissue from the same sample went through the same treatments and part of it was used for determining the efficacy of the enzyme treatment by measuring the content of sulfated GAGs. We planned to use another part of the tissue for transmission electron microscopy (TEM) and X-ray diffraction measurements to investigate possible changes in fibril spacing. Unfortunately the TEM samples for unknown reasons provided poor quality images that could not be used for analyzing fibril spacing. The X-ray measurements also turned out to be impossible due to the wide diameter distribution of fibrils in tendon as opposed to cornea where fibril spacing has previously been estimated by this method [167].

We considered preparing new samples to get better TEM images, however, in the meantime two other papers were published with similar design and with the same conclusions at the mechanical level as our work, and one of them found no effect on fibril
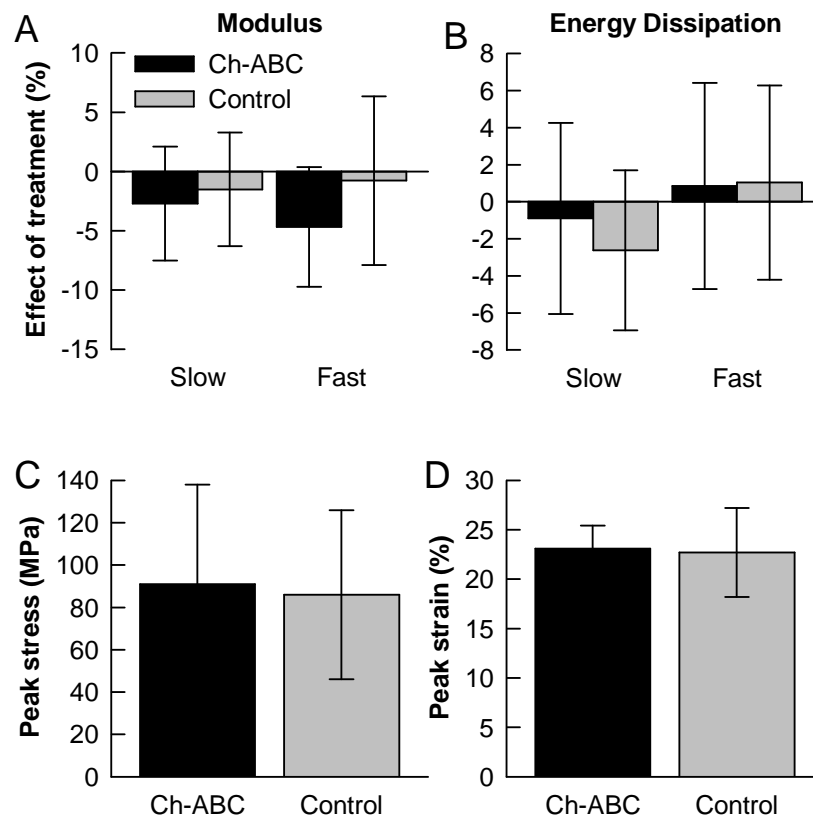
Figure 25: Mechanical effects of glycosaminoglycan removal by chondroitinase ABC (Ch-ABC). A) Effect of the Ch-ABC and control treatment on modulus at two strain rates. B) Same effects on the energy dissipation. C+D) Stress and strain at failure in the Ch-ABC treated and control group following the sub-failure tests. None of the differences were significant.

packing with TEM [16, 159]. We therefore decided to publish the mechanical results alone in support of the two studies.

We found that the Ch-ABC treatment was efficient in removing the sulfated GAGs, although a technical issue related to our papain digestion reduced the precision of the GAG assay and only allowed us to determine that at least 79% of the GAG was removed. GAG removal had no effect on the mechanical properties for modulus, energy dissipation (hysteresis), failure stress and failure strain (Figure 25). Due to the paired design for measuring modulus and energy dissipation, the confidence of the measurement is relatively high allowing us to say with 95% confidence that any treatment effect was less than 10%. For the un-paired failure measurements the confidence was much lower only allowing 95% confidence in saying that the difference was less than 50% in failure stress and 15% in failure strain.

Our findings in combination with those of others clearly show that GAGs are not required to transmit force between fibrils in the sub-failure regime. A recent modeling study reported that in the extreme situation of covalent GAG bonding, an 80% reduction in GAGs would reduce the modulus by 14% [181]. The authors conclude that under more

realistic bonding conditions the effect of GAG removal would be greater and thus the absence of an effect greater than 10% supports that GAGs are not involved in force transmission. The conclusion is less certain for the failure properties but it appears unlikely that non-covalent bonds between GAGs and collagen fibrils would be able to resist the high stresses up to failure [182].

10.5. Study 5 - Fracture mechanics of collagen fibrils: Influence of natural cross-links

In the final study we investigated the mechanical behavior of collagen fibrils from tissues with different natural cross-linking, more specifically mature human patellar tendon and rat-tail tendon (RTT) collagen. Other studies have looked at the effect of synthetically induced cross-links on collagen fibrils [88, 183] and also at the macroscopic level [120, 134], but we were interested in the naturally occurring cross-links. In relation to this study we had succeeded in extending our fibril testing method to allow determination of failure properties, which is particularly important in relation to cross-links because cross-links are expected to be mostly involved under high load [184-185]. This study is in manuscript form, as it has not yet been published.

Mature load-bearing human tendon contains significant amounts of mature enzymatic cross-links [52, 152], which are trivalent and stable against acids. In contrast young rat-tail tendon contains almost only immature cross-links that are divalent and labile in acid [186]. These two tissues were therefore chosen for the study of differences in enzymatic cross-linking. We performed mechanical failure tests on collagen fibrils from the patellar tendon of three different human subjects 33-39 years of age, the tail tendon of three different
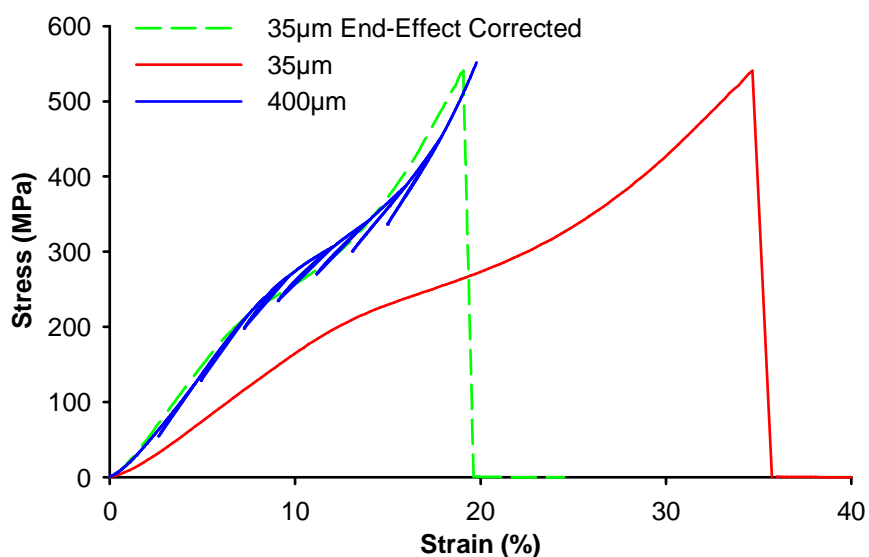
**Figure 26:** Presence of end-effects in fibril failure testes. The stress strain response of a 35µm long collagen fibril segment before and after correction for end-effects (45% reduced strain) is compared to the response of a 400µm long segment. The response of the long segment is pieced together from multiple stepwise strain increments. The overall curve-shape is identical for both the long and the short fibril.

12-week old wistar rats and the tail tendon of two different 16-week old Zucker Diabetic Fat (ZDF) rats.

To perform the failure tests we were technically limited to fibril segments of <40µm length and from our results we became aware that fibril length correlated with modulus suggesting the presence of so-called end-effects [77, 79]. Using a simple model, the magnitude of this effect was assessed, and a general correction was applied to the data in the form of a 45% reduction in the strain values (see study 5 for details). This correction and the resulting 45% increase in the modulus were included in all reported values. This simple correction assumes that the end-effects are equal throughout the strain range, which may not be true, however, from testing a 400µm long fibril it appears to be the case (Figure 26). To measure on the long fibril it was necessary to stitch together the curve from multiple cyclic pulls, each starting at a higher strain. Once the cycles enter the region of plastic deformation, permanent damage accumulate between cycles and failure may occur prematurely. The method is therefore not reliable for the actual tests but provides an idea of the response when end-effects are negligible.

We observed that the human collagen fibrils displayed a stress-strain curve with three distinct regions (Figure 27). The first region (region I) covered the range of ~0-7% strain and had increasing stress and modulus with increasing strain. In the middle region (region II) covering ~7-15% strain, the modulus decreased causing a plateau in the stress-strain response. The final region (region III) from ~15% strain up to failure (~20% strain) had
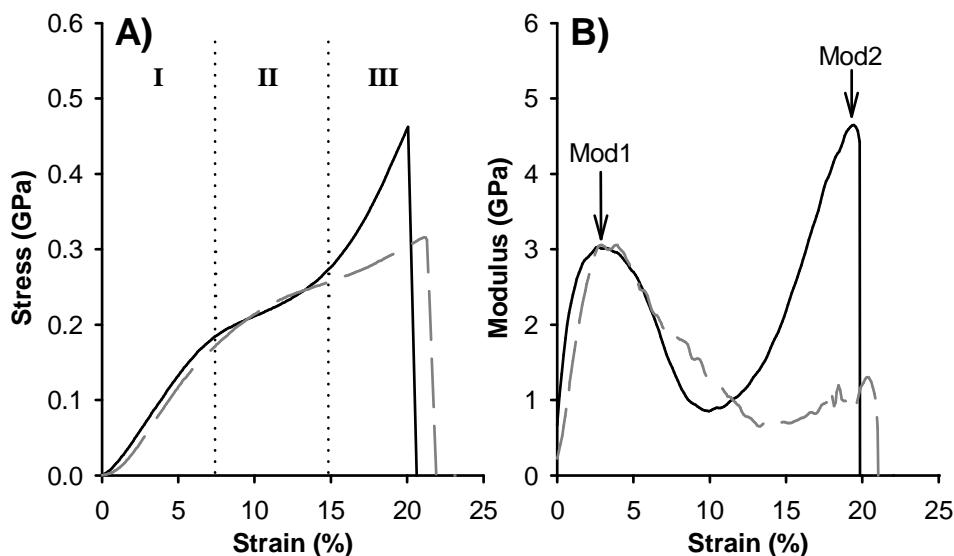
Figure 27: Example of failure tests on collagen fibrils (full line = human patellar, dashed = rat-tail). A) Three distinct regions are observed in the stress-strain response of human fibrils. B) Clear changes in the modulus within the three regions can be identified.
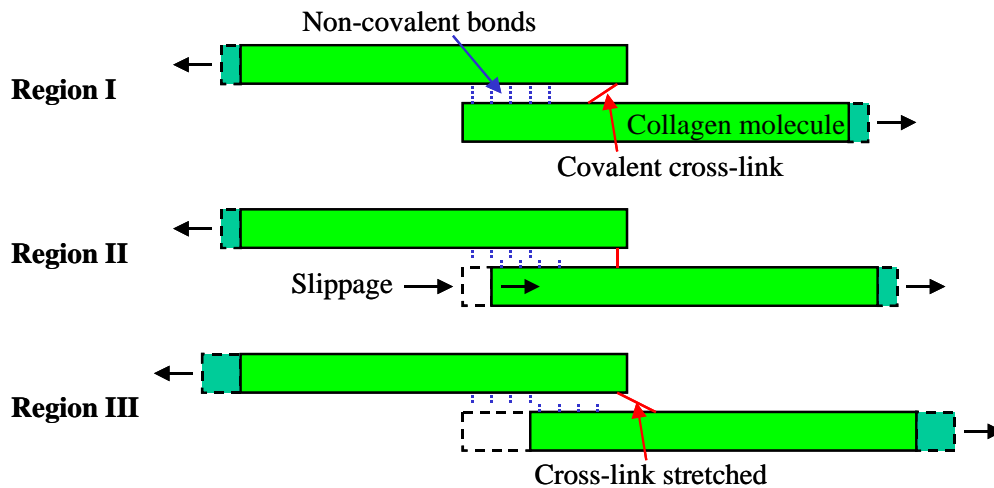
Figure 28: Schematic showing the proposed elongation mechanism in the three regions seen in Figure 27. In region I, non-covalent interactions restrain the collagen molecules from slipping. In region II, non-covalent interactions break and allow molecular slippage. In region III, molecular slippage is stopped by covalent cross-links.

increasing modulus usually reaching a peak value that was greater than the peak in region I (Figure 27). Failure properties of individual human collagen fibrils have not been studied before and the described mechanical behavior has not previously been reported in other tissues [87-88], but it was highly consistent in all of our measurements.

With inspiration from modeling studies on cross-linking [184-185] we propose that the three regions correspond to three different situations at the molecular level (Figure 28). In region I, non-covalent interactions at the molecular interfaces are able to withstand the applied force without slipping and the modulus and stress rises as the molecules are stretched (Figure 28). In region II, the non-covalent interactions are no longer strong enough and the molecules start slipping relative to each other thus producing a plateau in the mechanical response. In region III, the slippage is stopped by covalent cross-links and the molecular backbone is stretched causing the modulus and stress to increase again until final failure.

The behavior of native RTT fibrils was different from that of human patellar tendon fibrils (Figure 27). Region I for RTT fibrils was similar to that of the human fibrils, although the modulus was lower on average. In region II the reduction in modulus continued over a longer strain range and only rose little or not at all towards the failure point, thereby making region III much less distinct than for the human fibrils. These differences resulted in significantly lower ultimate stress and modulus in region III for the native rat-tail fibrils compared to the human patellar tendon fibrils.

That the immaturely cross-linked RTT and maturely cross-linked human fibrils differed most markedly in region III is consistent with this region being governed by cross-

links. We hypothesized that the difference was due to breakage of the labile immature cross-links and we therefore treated fascicles from the same rats with $NaBH_4$, a reducing agent that can stabilize the immature cross-link. The efficacy of the treatment was verified by a complete loss of solubility in dilute acetic acid. Fibrils tested following this treatment behaved similar to the untreated fibrils and still had significantly lower ultimate stress and modulus in region III compared to the human fibrils. This result disproved our hypothesis that the labile nature of the immature cross-link was the cause of the weaker RTT fibrils. Instead we proposed that the cause of the mechanical difference was the number of bonds formed; with the mature cross-link connecting three α-chains and the immature only connecting two. A potential mechanism could be that immature cross-links only produce linear filaments that lack connectivity to their surroundings and are therefore able to slide. In contrast if mature cross-links connect three molecules, they would cause filaments to be interconnected and be less able to slide (Figure 29). We have not been able to test this hypothesis as we lack the means to directly manipulate cross-link valence.

We also wanted to look at possible differences caused by advanced glycation (AGE) cross-links and we therefore included a group of ZDF rats with greatly increased blood glucose, which should induce increased glycation. Due to equipment breakdown we only have four measurements on these rats, but based on those there was no apparent difference to the other rat-tail fibrils. Cross-link analysis on the rat-tail tissues is planned but has not yet been
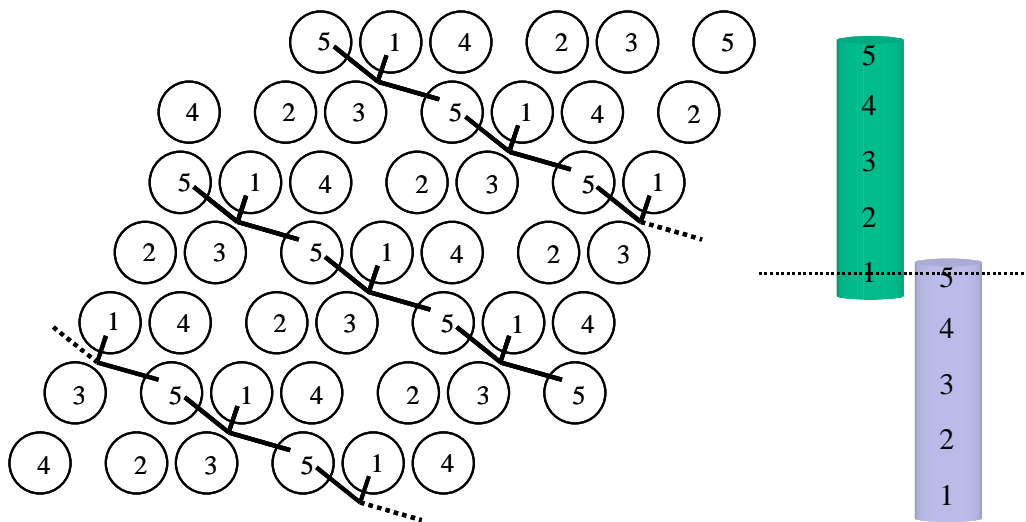
Figure 29: Schematic of possible mature cross-link formation between three molecules. The figure shows a cross-section through collagen molecules in a fibril such that it cuts through the telopeptide of molecules marked with 5 and the equivalent helix cross-link site on 4D-staggered molecules marked as 1. The two '5' molecules closest to the '1' molecule are in register and could provide the two telopeptide allysines required for trivalent cross-linking. Molecular packing based on Orgel et al. (2006) [55].

performed and we are therefore unable to say how the level of AGE cross-links in the ZDF rats compares to that of the other tissues.

Comparing the failure properties at the fibril level with those observed for macroscopic specimens, there appears to be a reasonably good correspondence for the rat-tail fibrils in terms of ultimate stress and strain, which suggests that tissue failure involves failure of individual fibrils in agreement with a continuous fibril model. For the human tissue however, the fibrils appear to be significantly stronger than tendons, which would indicate that tissue failure involves fibril slippage thus supporting discontinuous fibrils. While the failure mechanisms could be different between rat-tail and human patellar tendons, it should be noted that particularly failure properties are sensitive to stress-concentrations and should therefore generally be regarded as minimal values [77]. It is also possible that full-length fibrils are weaker than the 40 µm segments tested here due to local defect along the fibril.

In addition to the mechanical findings, differences were also observed in the fibril structure following failure. Two basic structures were seen; a relatively clean break where the rest of the fibril remained intact, or a more global disruption of the entire fibril. Fibrils that broke at the end all showed the intact structure, suggesting that failure occurred at a stress concentration. Fibrils that broke in the middle showed both structures, but predominantly the disrupted one. There was a tendency for human fibrils to have the intact structure and RTT fibrils having the disrupted. This may relate to the potentially greater molecular slippage in the RTT fibrils.

11. CONCLUSIONS

The ultimate goal of the study was to determine the mechanisms that underlie mechanical force transmission in human tendons. Although there are still aspects of tendon force transmission that are unclear, we believe that the present work has elucidated several important aspects. While the presence of viscoelasticity at the tissue level was well known, it has usually been attributed to slippage of fibrils. We showed that collagen fibrils them selves also behave viscoelastically, which allows for at least part of the tissue viscoelasticity to be explained at this level rather than by fibrils slipping. This finding would help to accommodate a model of continuous fibrils, which would otherwise be difficult. Pointing in the same direction was our results on the elastic modulus of fibrils, which was found to be in the same range as that of tissues, and not significantly stiffer as would have been expected if there was a high degree of fibril slippage.

We also found that glycosaminoglycans do not influence sub-failure tendon mechanical properties, corroborating the findings of others. A positive finding would have firmly supported discontinuous fibrils whereas the present negative result does not provide a clear conclusion, since other molecules may still provide interfibrillar linkages.

Our study on the failure properties of collagen fibrils suggests that divalent immature cross-links are less capable of blocking molecular slippage than trivalent mature cross-links, which in turn support that trivalent cross-links are formed between three molecules and not just three α-chains in two molecules. Rat-tail collagen fibrils with immature cross-links had a more pronounced plateau in the stress-strain response, which is also seen in immature tissue at the macroscopic level. In addition the strength of the rat-tail fibrils was similar to that reported for rat-tails at the macroscopic level and these findings together would support that fibrils are continuous. In contrast the mature human collagen fibrils were stronger and had a different stress-strain behavior than is seen at the tissue level, this discrepancy would support that fibrils are discontinuous. It appears unlikely that a property as fundamental as fibril continuity would differ between the two tissues, and the conclusion is therefore somewhat unclear.

Based on the findings in all of our studies there is significant support for the presence of mechanically continuous collagen fibrils throughout tendons such that the tendon properties rely primarily on the molecular assembly of collagen in the fibrils with little to no influence of intermediate levels.

12. PERSPECTIVE

The conclusions made in the previous section point at the collagen fibril as the key player in determining tissue mechanical function and thereby make fibrils a primary focus for future efforts. We are currently working on a study that looks at fibril length and structure over longer distances in tendon, and preliminary results suggest that collagen fibrils form a continuous branched network, in agreement with the overall conclusion of the present work.

While it is ultimately the macroscopic tissue function that is important, we believe that a multi-level approach looking also at the lower levels of hierarchy, such as fibrils, will be beneficial to understanding tissue function and pathology. A subject that could be of great importance is the cross-links formed by advanced glycation end-products (AGEs), which were briefly touched upon in study 5. These cross-links accumulate with age and at increased rate in diabetics, and it has been speculated that they lead to stiffening and brittleness of collagen. The results in study 5 suggests a possible mechanism of embrittlement in which the exogenous AGEs block the slippage in the plateau region thereby causing a reduction in failure strain and energy. We have material from elderly men and plan to study this in the future.

A related topic is that of AGE-breaking pharmaceuticals. If AGEs indeed affect collagen brittleness then drugs capable of breaking them would be of great interest. Several such drugs have been proposed but so far with limited success. Their efficacy is generally assessed at the tissue level, however, cross-linking takes place at the fibril level, and measurements on fibrils should therefore provide greater insight into the function of such drugs.

A different issue that we are also keen to look into is that of genetic disease in connective tissues, in particular Ehlers-Danlos syndrome (EDS). EDS can cause changes to the fibril structure but the mechanical implications of these changes are largely unknown. At the tissue level EDS is related to increased extensibility but it is unknown if this is caused by fibrillar or interfibrillar mechanisms.

13. REFERENCES

[1]   Gray H. Anatomy of the human body. Philadelphia: Lea & Febiger, 1918. Online: Bartleby.com (2000). URL: http://www.bartleby.com/107/

[2]   Kannus P. Structure of the tendon connective tissue. Scand J Med Sci Sports 2000;10(6):312-20.

[3]   Paxton JZ, Baar K. Tendon mechanics: The argument heats up. J Appl Physiol 2007;103(2):423-4.

[4]   Farley CT, Glasheen J, Mcmahon TA. Running springs: Speed and animal size. J Exp Biol 1993;185:71-86.

[5]   Magnusson SP, Langberg H, Kjaer M. The pathogenesis of tendinopathy: Balancing the response to loading. Nat Rev Rheumatol 2010;6(5):262-8.

[6]   Danylchuk KD, Finlay JB, Krcek JP. Microstructural organization of human and bovine cruciate ligaments. Clin Orthop Relat Res 1978(131):294-8.

[7]   Parry DAD, Craig AS. Quantitative electron microscope observations of collagen fibrils in rat-tail tendon. Biopolymers 1977;16(5):1015-31.

[8]   Hodge AJ, Petruska JA. Recent studies with the electronmicroscope on ordered aggregates of the tropocollagen macromolecule. In: Ramachandran GN, editor. Aspects of protein structure. New York: Academic Press, 1963. p. 299-300.

[9]   Kadler KE, Holmes DF, Trotter JA, Chapman JA. Collagen fibril formation. Biochem J 1996;316:1-11.

[10]   Provenzano PP, Vanderby R. Collagen fibril morphology and organization: Implications for force transmission in ligament and tendon. Matrix Biol 2006;25(2):71-84.

[11]   Raspanti M, Manelli A, Franchi M, Ruggeri A. The 3D structure of crimps in the rat achilles tendon. Matrix Biol 2005;24(7):503-7.

[12]   Franchi M, Ottani V, Stagni R, Ruggeri A. Tendon and ligament fibrillar crimps give rise to left-handed helices of collagen fibrils in both planar and helical crimps. J Anat 2010;216(3):301-9.

[13]   Kongsgaard M, Kovanen V, Aagaard P, Doessing S, Hansen P, Laursen AH, et al. Corticosteroid injections, eccentric decline squat training and heavy slow resistance training in patellar tendinopathy. Scand J Med Sci Sports 2009.

[14]   Suzuki D, Takahashi M, Abe M, Nagano A. Biochemical study of collagen and its crosslinks in the anterior cruciate ligament and the tissues used as a graft for reconstruction of the anterior cruciate ligament. Connect Tissue Res 2008;49(1):42-7.

[15]   Koob TJ, Vogel KG. Site-related variations in glycosaminoglycan content and swelling properties of bovine flexor tendon. J Orthop Res 1987;5(3):414-24.

[16]   Fessel G, Snedeker JG. Evidence against proteoglycan mediated collagen fibril load transmission and dynamic viscoelasticity in tendon. Matrix Biol 2009;28(8):503-10.

[17]   Yoon JH, Halper J. Tendon proteoglycans: Biochemistry and function. J Musculoskelet Neuron Interact 2005;5(1):22-34.

[18]   Iozzo RV. Matrix proteoglycans: From molecular design to cellular function. Annu Rev Biochem 1998;67:609-52.

[19]   Cribb AM, Scott JE. Tendon response to tensile-stress - an ultrastructural investigation of collagen - proteoglycan interactions in stressed tendon. 1995: Cambridge Univ Press; 1995. p. 423-8.

13.   References

[20]   Raspanti M, Congiu T, Alessandrini A, Gobbi P, Ruggeri A. Different patterns of collagen-proteoglycan interaction: A scanning electron microscopy and atomic force microscopy study. Eur J Histochem 2000;44(4):335-43.

[21]   Scott JE. Supramolecular organization of extracellular matrix glycosaminoglycans, in vitro and in the tissues. FASEB J 1992;6(9):2639-45.

[22]   Vogel KG, Trotter JA. The effect of proteoglycans on the morphology of collagen fibrils formed in vitro. Coll Relat Res 1987;7(2):105-14.

[23]   Raspanti M, Viola M, Sonaggere M, Tira ME, Tenni R. Collagen fibril structure is affected by collagen concentration and decorin. Biomacromolecules 2007;8(7):2087-91.

[24]   Corsi A, Xu T, Chen XD, Boyde A, Liang J, Mankani M, et al. Phenotypic effects of biglycan deficiency are linked to collagen fibril abnormalities, are synergized by decorin deficiency, and mimic Ehlers-Danlos-like changes in bone and other connective tissues. J Bone Miner Res 2002;17(7):1180-9.

[25]   Kirkendall DT, Garrett WE. Function and biomechanics of tendons. Scand J Med Sci Sports 1997;7(2):62-6.

[26]   Gelse K, Poschl E, Aigner T. Collagens - structure, function, and biosynthesis. Adv Drug Deliv Rev 2003;55(12):1531-46.

[27]   van der Rest M, Garrone R. Collagen family of proteins. FASEB J 1991;5(13):2814-23.

[28]   Exposito JY, Valcourt U, Cluzel C, Lethias C. The fibrillar collagen family. Int J Mol Sci 2010;11(2):407-26.

[29]   Khoshnoodi J, Cartailler JP, Alvares K, Veis A, Hudson BG. Molecular recognition in the assembly of collagens: Terminal noncollagenous domains are key recognition modules in the formation of triple helical protomers. J Biol Chem 2006;281(50):38117-21.

[30]   Burjanadze TV. New analysis of the phylogenetic change of collagen thermostability. Biopolymers 2000;53(6):523-8.

[31]   Morello R, Bertin TK, Chen YQ, Hicks J, Tonachini L, Monticone M, et al. CRTAP is required for prolyl 3-hydroxylation and mutations cause recessive osteogenesis imperfecta. Cell 2006;127(2):291-304.

[32]   Eyre DR, Weis M, Hudson DM, Wu JJ, Kim L. A novel 3-hydroxyproline (3hyp)-rich motif marks the triple-helical C terminus of tendon type I collagen. J Biol Chem 2011;286(10):7732-6.

[33]   Canty EG, Lu YH, Meadows RS, Shaw MK, Holmes DF, Kadler KE. Coalignment of plasma membrane channels and protrusions (fibripositors) specifies the parallelism of tendon. J Cell Biol 2004;165(4):553-63.

[34]   Humphries SM, Lu YH, Canty EG, Kadler KE. Active negative control of collagen fibrillogenesis in vivo - intracellular cleavage of the type I procollagen propeptides in tendon fibroblasts without intracellular fibrils. J Biol Chem 2008;283(18):12129-35.

[35]   Kadler KE, Hill A, Canty-Laird EG. Collagen fibrillogenesis: Fibronectin, integrins, and minor collagens as organizers and nucleators. Curr Opin Cell Biol 2008;20(5):495-501.

[36]   Wenstrup RJ, Smith SM, Florer JB, Zhang GY, Beason DP, Seegmiller RE, et al. Regulation of collagen fibril nucleation and initial fibril assembly involves coordinate interactions with collagens V and XI in developing tendon. J Biol Chem 2011;286(23):20455-65.

[37]   Hulmes DJS, Miller A, Parry DAD, Piez KA, Woodhead-Galloway J. Analysis of the primary structure of collagen for origins of molecular packing. J Mol Biol 1973;79(1):137-48.

13.   References

[38]   Leikin S, Rau DC, Parsegian VA. Temperature-favored assembly of collagen is driven by hydrophilic not hydrophobic interactions. Nat Struct Biol 1995;2(3):205-10.

[39]   Holmes DF, Graham HK, Trotter JA, Kadler KE. STEM/TEM studies of collagen fibril assembly. Micron 2001;32(3):273-85.

[40]   Birk DE, Nurminskaya MV, Zycband EI. Collagen fibrillogenesis in situ: Fibril segments undergo post-depositional modifications resulting in linear and lateral growth during matrix development. Dev Dyn 1995;202(3):229-43.

[41]   Holmes DF, Kadler KE. The precision of lateral size control in the assembly of corneal collagen fibrils. J Mol Biol 2005;345(4):773-84.

[42]   Craig AS, Birtles MJ, Conway JF, Parry DAD. An estimate of the mean length of collagen fibrils in rat tail-tendon as a function of age. Connect Tissue Res 1989;19(1):51-62.

[43]   Holmes DF, Tait A, Hodson NW, Sherratt MJ, Kadler KE. Growth of collagen fibril seeds from embryonic tendon: Fractured fibril ends nucleate new tip growth. J Mol Biol 2010;399(1):9-16.

[44]   Silver D, Miller J, Harrison R, Prockop DJ. Helical model of nucleation and propagation to account for the growth of type I collagen fibrils from symmetrical pointed tips: A special example of self-assembly of rod-like monomers. Proc Natl Acad Sci USA 1992;89(20):9860-4.

[45]   Birk DE, Zycband EI, Woodruff S, Winkelmann DA, Treilstad RL. Collagen fibrillogenesis in situ: Fibril segments become long fibrils as the developing tendon matures. Dev Dyn 1997;208(3):291-8.

[46]   Graham HK, Holmes DF, Watson RB, Kadler KE. Identification of collagen fibril fusion during vertebrate tendon morphogenesis. The process relies on unipolar fibrils and is regulated by collagen-proteoglycan interaction. J Mol Biol 2000;295(4):891-902.

[47]   Cisneros DA, Hung C, Franz CA, Muller DJ. Observing growth steps of collagen self-assembly by time-lapse high-resolution atomic force microscopy. J Struct Biol 2006;154(3):232-45.

[48]   Bailey AJ, Paul RG, Knott L. Mechanisms of maturation and ageing of collagen. Mech Ageing Dev 1998;106(1-2):1-56.

[49]   Yamauchi M, Katz EP. The post-translational chemistry and molecular packing of mineralizing tendon collagens. Connect Tissue Res 1993;29(2):81-98.

[50]   Hanson DA, Eyre DR. Molecular site specificity of pyridinoline and pyrrole cross-links in type I collagen of human bone. J Biol Chem 1996;271(43):26508-16.

[51]   Clayden J, Greeves N, Warren S, Wothers P. Organic chemistry: Oxford University Press, 2001.

[52]   Eyre DR, Paz MA, Gallop PM. Cross-linking in collagen and elastin. Annu Rev Biochem 1984;53:717-48.

[53]   Eyre DR, Wu JJ. Collagen cross-links. Top Curr Chem 2005;247:207-29.

[54]   Bailey AJ, Shimokomaki MS. Age related changes in reducible cross-links of collagen. FEBS Lett 1971;16(2):86-8.

[55]   Orgel J, Irving TC, Miller A, Wess TJ. Microfibrillar structure of type I collagen in situ. Proc Natl Acad Sci USA 2006;103(24):9001-5.

[56]   Monnier VM, Sell DR. Prevention and repair of protein damage by the maillard reaction in vivo. Rejuv Res 2006;9(2):264-73.

[57]   Verzijl N, DeGroot J, Thorpe SR, Bank RA, Shaw JN, Lyons TJ, et al. Effect of collagen turnover on the accumulation of advanced glycation end products. J Biol Chem 2000;275(50):39027-31.

13. References

[58] Monnier VM, Kohn RR, Cerami A. Accelerated age-related browning of human collagen in diabetes-mellitus. Proc Natl Acad Sci-Biol 1984;81(2):583-7.

[59] Brownlee M. Negative consequences of glycation. Metab Clin Exp 2000;49(2):9-13.

[60] Corman B, Duriez M, Poitevin P, Heudes D, Bruneval P, Tedgui A, et al. Aminoguanidine prevents age-related arterial stiffening and cardiac hypertrophy. Proc Natl Acad Sci USA 1998;95(3):1301-6.

[61] Hammes HP, Martin S, Federlin K, Geisen K, Brownlee M. Aminoguanidine treatment inhibits the development of experimental diabetic-retinopathy. Proc Natl Acad Sci USA 1991;88(24):11555-8.

[62] Silver FH. Type I collagen fibrillogenesis in vitro - additional evidence for the assembly mechanism. J Biol Chem 1981;256(10):4973-7.

[63] Holmes DF, Kadler KE. The 10+4 microfibril structure of thin cartilage fibrils. Proc Natl Acad Sci USA 2006;103(46):17249-54.

[64] Raspanti M, Ottani V, Ruggeri A. Different architectures of the collagen fibril: Morphological aspects and functional implications. Int J Biol Macromol 1989;11(6):367-71.

[65] Ruggeri A, Benazzo F, Reale E. Collagen fibrils with straight and helicoidal microfibrils: A freeze-fracture and thin-section study. J Ultrastruct Res 1979;68(1):101-8.

[66] Holmes DF, Gilpin CJ, Baldock C, Ziese U, Koster AJ, Kadler KE. Corneal collagen fibril structure in three dimensions: Structural insights into fibril assembly, mechanical properties, and tissue organization. Proc Natl Acad Sci USA 2001;98(13):7307-12.

[67] Franchi M, Raspanti M, Dell'Orbo C, Quaranta M, De Pasquale V, Ottani V, et al. Different crimp patterns in collagen fibrils relate to the subfibrillar arrangement. Connect Tissue Res 2008;49(2):85-91.

[68] Wess TJ, Hammersley AP, Wess L, Miller A. A consensus model for molecular packing of type I collagen. J Struct Biol 1998;122(1-2):92-100.

[69] Butler DL, Grood ES, Noyes FR, Zernicke RF. Biomechanics of ligaments and tendons. Exerc Sport Sci Rev 1978;6:125-81.

[70] Estermann I, editor. Classical methods. New York and London: Academic Press, 1959.

[71] Wang JL, Parnianpour M, ShiraziAdl A, Engin AE. Failure criterion of collagen fiber: Viscoelastic behavior simulated by using load control data. Theor Appl Fract Mech 1997;27(1):1-12.

[72] Ker RF. Mechanics of tendon, from an engineering perspective. Int J Fatigue 2007;29(6):1001-9.

[73] Haut RC. Age-dependent influence of strain rate on the tensile failure of rat-tail tendon. J Biomech Eng 1983;105(3):296-9.

[74] Fratzl P, Misof K, Zizak I, Rapp G, Amenitsch H, Bernstorff S. Fibrillar structure and mechanical properties of collagen. J Struct Biol 1998;122(1-2):119-22.

[75] Hansen KA, Weiss JA, Barton JK. Recruitment of tendon crimp with applied tensile strain. J Biomech Eng 2002;124(1):72-7.

[76] Franchi M, Fini M, Quaranta M, De Pasquale V, Raspanti M, Giavaresi G, et al. Crimp morphology in relaxed and stretched rat achilles tendon. J Anat 2007;210(1):1-7.

[77] Bennett MB, Ker RF, Dimery NJ, Alexander RM. Mechanical properties of various mammalian tendons. J Zool 1986;209:537-48.

[78] Haut RC. The influence of specimen length on the tensile failure properties of tendon collagen. J Biomech 1986;19(11):951-5.

13. References

[79] Legerlotz K, Riley GP, Screen HRC. Specimen dimensions influence the measurement of material properties in tendon fascicles. J Biomech 2010;43(12):2274-80.

[80] Atkinson TS, Ewers BJ, Haut RC. The tensile and stress relaxation responses of human patellar tendon varies with specimen cross-sectional area. J Biomech 1999;32(9):907-14.

[81] Carroll CC, Dickinson JM, Haus JM, Lee GA, Hollon CJ, Aagaard P, et al. Influence of aging on the in vivo properties of human patellar tendon. J Appl Physiol 2008;105(6):1907-15.

[82] Arya S, Kulig K. Tendinopathy alters mechanical and material properties of the achilles tendon. J Appl Physiol 2010;108(3):670-5.

[83] Benedict JV, Walker LB, Harris EH. Stress-strain characteristics and tensile strength of unembalmed human tendon. J Biomech 1968;1(1):53-63.

[84] Butler DL, Grood ES, Noyes FR, Zernicke RF, Brackett K. Effects of structure and strain measurement technique on the material properties of young human tendons and fascia. J Biomech 1984;17(8):579-96.

[85] Chun KJ, Butler DL. Spatial variation in material properties in fascicle-bone units from human patellar tendon. In: Lee S, Kim Y, editors. Experimental mechanics in nano and biotechnology. Stafa-Zurich: Trans Tech Publications Ltd, 2006. p. 797-802.

[86] Johnson GA, Tramaglini DM, Levine RE, Ohno K, Choi NY, Woo SLY. Tensile and viscoelastic properties of human patellar tendon. J Orthop Res 1994;12(6):796-803.

[87] Shen ZL, Dodge MR, Kahn H, Ballarini R, Eppell SJ. In vitro fracture testing of submicron diameter collagen fibril specimens. Biophys J 2010;99(6):1986-95.

[88] Yang L, van der Werf KO, Dijkstra PJ, Feijen J, Bennink ML. Micromechanical analysis of native and cross-linked collagen type I fibrils supports the existence of microfibrils. J Mech Behav Biomed Mater 2012;6:148-58.

[89] deVente JE, Lester GE, Trotter JA, Dahners LE. Isolation of intact collagen fibrils from healing ligament. J Electron Microsc (Tokyo) 1997;46(4):353-6.

[90] Silver FH, Christiansen DL, Snowhill PB, Chen Y. Role of storage on changes in the mechanical properties of tendon and self-assembled collagen fibers. Connect Tissue Res 2000;41(2):155-64.

[91] Folkhard W, Geercken W, Knorzer E, Mosler E, Nemetschekgansler H, Nemetschek T, et al. Structural dynamic of native tendon collagen. J Mol Biol 1987;193(2):405-7.

[92] Mosler E, Folkhard W, Knorzer E, Nemetschekgansler H, Nemetschek T, Koch MHJ. Stress-induced molecular rearrangement in tendon collagen. J Mol Biol 1985;182(4):589-96.

[93] Puxkandl R, Zizak I, Paris O, Keckes J, Tesch W, Bernstorff S, et al. Viscoelastic properties of collagen: Synchrotron radiation investigations and structural model. Philos Trans R Soc Lond, B, Biol Sci 2002;357(1418):191-7.

[94] Sasaki N, Odajima S. Elongation mechanism of collagen fibrils and force-strain relations of tendon at each level of structural hierarchy. J Biomech 1996;29(9):1131-6.

[95] Maffulli N. Rupture of the achilles tendon. J Bone Joint Surg Am 1999;81A(7):1019-36.

[96] Kannus P, Jozsa L. Histopathological changes preceding spontaneous rupture of a tendon - a controlled study of 891 patients. J Bone Joint Surg Am 1991;73A(10):1507-25.

[97] Thornton GM, Schwab TD, Oxland TR. Cyclic loading causes faster rupture and strain rate than static loading in medial collateral ligament at high stress. Clin Biomech 2007;22(8):932-40.

13. References

[98] Ker RF. The implications of the adaptable fatigue quality of tendons for their construction, repair and function. Comp Biochem Phys A 2002;133(4):987-1000.

[99] Samiric T, Parkinson J, Ilic MZ, Cook J, Feller JA, Handley CJ. Changes in the composition of the extracellular matrix in patellar tendinopathy. Matrix Biol 2009;28(4):230-6.

[100] Arnoczky SP, Lavagnino M, Egerbacher M. The mechanobiological aetiopathogenesis of tendinopathy: Is it the over-stimulation or the under-stimulation of tendon cells? Int J Exp Pathol 2007;88(4):217-26.

[101] De Paepe A, Malfait F. Bleeding and bruising in patients with Ehlers-Danlos syndrome and other collagen vascular disorders. Br J Haematol 2004;127(5):491-500.

[102] Eyre D, Shao P, Weis MA, Steinmann B. The kyphoscoliotic type of Ehlers-Danlos syndrome (type VI): Differential effects on the hydroxylation of lysine in collagens I and II revealed by analysis of cross-linked telopeptides from urine. Mol Genet Metab 2002;76(3):211-6.

[103] Pope FM, Burrows NP. Ehlers-Danlos syndrome has varied molecular mechanisms. J Med Genet 1997;34(5):400-10.

[104] Binnig G, Quate CF, Gerber C. Atomic force microscope. Phys Rev Lett 1986;56(9):930-3.

[105] Butt HJ, Cappella B, Kappl M. Force measurements with the atomic force microscope: Technique, interpretation and applications. Surf Sci Rep 2005;59(1-6):1-152.

[106] Yamamoto S, Hashizume H, Hitomi J, Shigeno M, Sawaguchi S, Abe H, et al. The subfibrillar arrangement of corneal and scleral collagen fibrils as revealed by scanning electron and atomic force microscopy. Arch Histol Cytol 2000;63(2):127-35.

[107] Ng L, Grodzinsky AJ, Patwari P, Sandy J, Plaas A, Ortiz C. Individual cartilage aggrecan macromolecules and their constituent glycosaminoglycans visualized via atomic force microscopy. J Struct Biol 2003;143(3):242-57.

[108] Friedrichs J, Taubenberger A, Franz CM, Muller DJ. Cellular remodelling of individual collagen fibrils visualized by time-lapse AFM. J Mol Biol 2007;372(3):594-607.

[109] Wenger MPE, Bozec L, Horton MA, Mesquida P. Mechanical properties of collagen fibrils. Biophys J 2007;93(4):1255-63.

[110] Grant CA, Thomson NH, Savage MD, Woon HW, Greig D. Surface characterisation and biomechanical analysis of the sclera by atomic force microscopy. J Mech Behav Biomed Mater 2011;4(4):535-40.

[111] Thompson JB, Kindt JH, Drake B, Hansma HG, Morse DE, Hansma PK. Bone indentation recovery time correlates with bond reforming time. Nature 2001;414(6865):773-6.

[112] Rief M, Gautel M, Oesterhelt F, Fernandez JM, Gaub HE. Reversible unfolding of individual titin immunoglobulin domains by AFM. Science 1997;276(5315):1109-12.

[113] Lehenkari PP, Horton MA. Single integrin molecule adhesion forces in intact cells measured by atomic force microscopy. Biochem Biophys Res Commun 1999;259(3):645-50.

[114] Svensson RB, Hassenkam T, Hansen P, Magnusson SP. Viscoelastic behavior of discrete human collagen fibrils. J Mech Behav Biomed Mater 2010;3(1):112-5.

[115] Shen ZL, Dodge MR, Kahn H, Ballarini R, Eppell SJ. Stress-strain experiments on individual collagen fibrils. Biophys J 2008;95(8):3956-63.

[116] Sasaki N, Odajima S. Stress-strain curve and young's modulus of a collagen molecule as determined by the X-ray diffraction technique. J Biomech 1996;29(5):655-8.

13.   References

[117]   Screen HRC. Investigating load relaxation mechanics in tendon. J Mech Behav Biomed Mater 2008;1(1):51-8.

[118]   Screen HRC, Lee DA, Bader DL, Shelton JC. An investigation into the effects of the hierarchical structure of tendon fascicles on micromechanical properties. Proc Inst Mech Eng Part H-J Eng Med 2004;218(H2):109-19.

[119]   Vater CA, Harris ED, Siegel RC. Native cross-links in collagen fibrils induce resistance to human synovial collagenase. Biochem J 1979;181(3):639-45.

[120]   Haroun MA, Khirstova PK, Gasmelseed GA, Covington AD. Influence of oxazolidines and zirconium oxalate crosslinkers on the hydrothermal, enzymatic, and thermo mechanical stability of type 1 collagen fiber. Thermochim Acta 2009;484(1-2):4-10.

[121]   Miles CA, Avery NC, Rodin VV, Bailey AJ. The increase in denaturation temperature following cross-linking of collagen is caused by dehydration of the fibres. J Mol Biol 2005;346(2):551-6.

[122]   Tanzer ML. Intermolecular cross-links in reconstituted collagen fibrils - evidence for nature of covalent bonds. J Biol Chem 1968;243(15):4045-54.

[123]   Reddy GK. Cross-linking in collagen by nonenzymatic glycation increases the matrix stiffness in rabbit achilles tendon. Exp Diabesity Res 2004;5(2):143-53.

[124]   Haut RC. The effect of a lathyritic diet on the sensitivity of tendon to strain rate. J Biomech Eng 1985;107(2):166-74.

[125]   Freudenberg U, Behrens SH, Welzel PB, Muller M, Grimmer M, Salchert K, et al. Electrostatic interactions modulate the conformation of collagen I. Biophys J 2007;92(6):2108-19.

[126]   Grant CA, Brockwell DJ, Radford SE, Thomson NH. Tuning the elastic modulus of hydrated collagen fibrils. Biophys J 2009;97(11):2985-92.

[127]   Fantner GE, Hassenkam T, Kindt JH, Weaver JC, Birkedal H, Pechenik L, et al. Sacrificial bonds and hidden length dissipate energy as mineralized fibrils separate during bone fracture. Nat Mater 2005;4(8):612-6.

[128]   Goh KL, Chen Y, Chou SM, Listrat A, Bechet D, Wess TJ. Effects of frozen storage temperature on the elasticity of tendons from a small murine model. Animal 2010;4(9):1613-7.

[129]   Moon DK, Woo SLY, Takakura Y, Gabriel MT, Abramowitch SD. The effects of refreezing on the viscoelastic and tensile properties of ligaments. J Biomech 2006;39(6):1153-7.

[130]   Giannini S, Buda R, Di Caprio F, Agati P, Bigi A, De Pasquale V, et al. Effects of freezing on the biomechanical and structural properties of human posterior tibial tendons. Int Orthop 2008;32(2):145-51.

[131]   Hutter JL, Bechhoefer J. Calibration of atomic-force microscope tips. Rev Sci Instrum 1993;64(7):1868-73.

[132]   Haraldsson BT, Aagaard P, Qvortrup K, Bojsen-Moller J, Krogsgaard M, Koskinen S, et al. Lateral force transmission between human tendon fascicles. Matrix Biol 2008;27(2):86-95.

[133]   Haraldsson BT, Aagaard P, Krogsgaard M, Alkjaer T, Kjaer M, Magnusson SP. Region-specific mechanical properties of the human patella tendon. J Appl Physiol 2005;98(3):1006-12.

[134]   Hansen P, Hassenkam T, Svensson RB, Aagaard P, Trappe T, Haraldsson BT, et al. Glutaraldehyde cross-linking of tendonmechanical effects at the level of the tendon fascicle and fibril. Connect Tissue Res 2009;50(4):211-22.

13. References

[135] Gentleman E, Lay AN, Dickerson DA, Nauman EA, Livesay GA, Dee KC. Mechanical characterization of collagen fibers and scaffolds for tissue engineering. Biomaterials 2003;24(21):3805-13.

[136] Butler DL, Kay MD, Stouffer DC. Comparison of material properties in fascicle-bone units from human patellar tendon and knee ligaments. J Biomech 1986;19(6):425-32.

[137] Yamamoto E, Hayashi K, Yamamoto N. Mechanical properties of collagen fascicles from the rabbit patellar tendon. J Biomech Eng 1999;121(1):124-31.

[138] Ng BH, Chou SM, Krishna V. The influence of gripping techniques on the tensile properties of tendons. Proc Inst Mech Eng Part H-J Eng Med 2005;219(H5):349-54.

[139] Onambele GNL, Burgess K, Pearson SJ. Gender-specific in vivo measurement of the structural and mechanical properties of the human patellar tendon. J Orthop Res 2007;25(12):1635-42.

[140] Maganaris CN, Paul JP. In vivo human tendon mechanical properties. J Physiol (Lond) 1999;521(1):307-13.

[141] Couppe C, Kongsgaard M, Aagaard P, Hansen P, Bojsen-Moller J, Kjaer M, et al. Habitual loading results in tendon hypertrophy and increased stiffness of the human patellar tendon. J Appl Physiol 2008;105(3):805-10.

[142] Hansen P, Bojsen-Moller J, Aagaard P, Kjaer M, Magnusson SP. Mechanical properties of the human patellar tendon, in vivo. Clin Biomech 2006;21(1):54-8.

[143] Stouffer DC, Butler DL, Hosny D. The relationship between crimp pattern and mechanical response of human patellar tendon-bone units. J Biomech Eng 1985;107(2):158-65.

[144] Magnusson SP, Hansen P, Aagaard P, Brond J, Dyhre-Poulsen P, Bojsen-Moller J, et al. Differential strain patterns of the human gastrocnemius aponeurosis and free tendon, in vivo. Acta Physiol Scand 2003;177(2):185-95.

[145] Visser JJ, Hoogkamer JE, Bobbert MF, Huijing PA. Length and moment arm of human leg muscles as a function of knee and hip-joint angles. Eur J Appl Physiol Occup Physiol 1990;61(5-6):453-60.

[146] Aagaard P, Simonsen EB, Andersen JL, Magnusson SP, Bojsen-Moller F, Dyhre-Poulsen P. Antagonist muscle coactivation during isokinetic knee extension. Scand J Med Sci Sports 2000;10(2):58-67.

[147] Krishnan C, Williams GN. Error associated with antagonist muscle activity in isometric knee strength testing. Eur J Appl Physiol 2010;109(3):527-36.

[148] Kongsgaard M, Reitelseder S, Pedersen TG, Holm L, Aagaard P, Kjaer M, et al. Region specific patellar tendon hypertrophy in humans following resistance training. Acta Physiol 2007;191(2):111-21.

[149] Syk I, Agren MS, Adawi D, Jeppsson B. Inhibition of matrix metalloproteinases enhances breaking strength of colonic anastomoses in an experimental model. Br J Surg 2001;88(2):228-34.

[150] Creemers LB, Jansen DC, van Veen-Reurings A, van den Bos T, Everts V. Microassay for the assessment of low levels of hydroxyproline. Biotechniques 1997;22(4):656-8.

[151] Prockop DJ, Udenfriend S. A specific method for the analysis of hydroxyproline in tissues and urine. Anal Biochem 1960;1(3):228-39.

[152] Hansen P, Haraldsson BT, Aagaard P, Kovanen V, Avery NC, Qvortrup K, et al. Lower strength of the human posterior patellar tendon seems unrelated to mature collagen cross-linking and fibril morphology. J Appl Physiol 2010;108(1):47-52.

[153] Shadwick RE, Rapoport HS, Fenger JM. Structure and function of tuna tail tendons. Comp Biochem Phys A 2002;133(4):1109-25.

13. References

[154] Bank RA, Beekman B, Verzijl N, de Roos JA, Sakkee AN, TeKoppele JM. Sensitive fluorimetric quantitation of pyridinium and pentosidine crosslinks in biological samples in a single high-performance liquid chromatographic run. J Chromatogr B Biomed Sci App 1997;703(1-2):37-44.

[155] Prabhakar V, Capila I, Raman R, Srinivasan A, Bosques CJ, Pojasek K, et al. The catalytic machinery of chondroitinase ABC I utilizes a calcium coordination strategy to optimally process dermatan sulfate. Biochemistry 2006;45(37):11130-9.

[156] Farndale RW, Buttle DJ, Barrett AJ. Improved quantitation and discrimination of sulphated glycosaminoglycans by use of dimethylmethylene blue. Biochim Biophys Acta 1986;883(2):173-7.

[157] Haut RC, Little RW. A constitutive equation for collagen fibers. J Biomech 1972;5(5):423-30.

[158] Silver FH, Ebrahimi A, Snowhill PB. Viscoelastic properties of self-assembled type I collagen fibers: Molecular basis of elastic and viscous behaviors. Connect Tissue Res 2002;43(4):569-80.

[159] Lujan TJ, Underwood CJ, Jacobs NT, Weiss JA. Contribution of glycosaminoglycans to viscoelastic tensile behavior of human ligament. J Appl Physiol 2009;106(2):423-31.

[160] Sanjeevi R, Somanathan N, Ramaswamy D. A viscoelastic model for collagen-fibers. J Biomech 1982;15(3):181-3.

[161] Hoffman AH, Robichaud DR, Duquette JJ, Grigg P. Determining the effect of hydration upon the properties of ligaments using pseudo gaussian stress stimuli. J Biomech 2005;38(8):1636-42.

[162] Barnes HA. Thixotropy - a review. J NonNewton Fluid Mech 1997;70(1-2):1-33.

[163] Gupta HS, Seto J, Krauss S, Boesecke P, Screen HRC. In situ multi-level analysis of viscoelastic deformation mechanisms in tendon collagen. J Struct Biol 2010;169(2):183-91.

[164] Shen ZLL, Kahn H, Ballarin R, Eppell SJ. Viscoelastic properties of isolated collagen fibrils. Biophys J 2011;100(12):3008-15.

[165] Leikin S, Rau DC, Parsegian VA. Direct measurement of forces between self-assembled proteins: Temperature-dependent exponential forces between collagen triple helices. Proc Natl Acad Sci USA 1994;91(1):276-80.

[166] Madsen B, Thygesen A, Lilholt H. Plant fibre composites - porosity and stiffness. Compos Sci Technol 2009;69(7-8):1057-69.

[167] Meek KM, Fullwood NJ, Cooke PH, Elliott GF, Maurice DM, Quantock AJ, et al. Synchrotron X-ray diffraction studies of the cornea, with implications for stromal hydration. Biophys J 1991;60(2):467-74.

[168] Fullwood NJ, Meek KM. A synchrotron X-ray study of the changes occurring in the corneal stroma during processing for electron microscopy. J Microsc 1993;169:53-60.

[169] Kongsgaard M, Qvortrup K, Larsen J, Aagaard P, Doessing S, Hansen P, et al. Fibril morphology and tendon mechanical properties in patellar tendinopathy: Effects of heavy slow resistance training. Am J Sports Med 2010;38(4):749-56.

[170] Heim AJ, Koob TJ, Matthews WG. Low strain nanomechanics of collagen fibrils. Biomacromolecules 2007;8(11):3298-301.

[171] Grant CA, Brockwell DJ, Radford SE, Thomson NH. Effects of hydration on the mechanical response of individual collagen fibrils. Appl Phys Lett 2008;92(23):3902.

[172] van der Rijt JAJ, van der Werf KO, Bennink ML, Dijkstra PJ, Feijen J. Micromechanical testing of individual collagen fibrils. Macromol Biosci 2006;6(9):697-702.

13.   References

[173] Sasaki N, Shiwa S, Yagihara S, Hikichi K. X-ray-diffraction studies on the structure of hydrated collagen. Biopolymers 1983;22(12):2539-47.

[174] Chimich D, Shrive N, Frank C, Marchuk L, Bray R. Water content alters viscoelastic behavior of the normal adolescent rabbit medial collateral ligament. J Biomech 1992;25(8):831-7.

[175] Thornton GM, Shrive NG, Frank CB. Altering ligament water content affects ligament pre-stress and creep behaviour. J Orthop Res 2001;19(5):845-51.

[176] Scott JE. Proteodermatan and proteokeratan sulfate (decorin, lumican/fibromodulin) proteins are horseshoe shaped. Implications for their interactions with collagen. Biochemistry 1996;35(27):8795-9.

[177] Cribb AM, Scott JE. Tendon response to tensile stress: An ultrastructural investigation of collagen:proteoglycan interactions in stressed tendon. J Anat 1995;187:423-8.

[178] Raspanti M, Alessandrini A, Ottani V, Ruggeri A. Direct visualization of collagen-bound proteoglycans by tapping-mode atomic force microscopy. J Struct Biol 1997;119(2):118-22.

[179] Screen HRC, Chhaya VH, Greenwald SE, Bader DL, Lee DA, Shelton JC. The influence of swelling and matrix degradation on the microstructural integrity of tendon. Acta Biomater 2006;2(5):505-13.

[180] Lujan TJ, Underwood CJ, Henninger HB, Thompson BM, Weiss JA. Effect of dermatan sulfate glycosaminoglycans on the quasi-static material properties of the human medial collateral ligament. J Orthop Res 2007;25(7):894-903.

[181] Fessel G, Snedeker JG. Equivalent stiffness after glycosaminoglycan depletion in tendon - an ultra-structural finite element model and corresponding experiments. J Theor Biol 2011;268(1):77-83.

[182] Redaelli A, Vesentini S, Soncini M, Vena P, Mantero S, Montevecchi FM. Possible role of decorin glycosaminoglycans in fibril to fibril force transfer in relative mature tendons - a computational study from molecular to microstructural level. J Biomech 2003;36(10):1555-69.

[183] Yang L, van der Werf KO, Fitié CFC, Bennink ML, Dijkstra PJ, Feijen J. Mechanical properties of native and cross-linked type I collagen fibrils. Biophys J 2008;94(6):2204-11.

[184] Buehler MJ. Nanomechanics of collagen fibrils under varying cross-link densities: Atomistic and continuum studies. J Mech Behav Biomed Mater 2008;1(1):59-67.

[185] Uzel SGM, Buehler MJ. Molecular structure, mechanical behavior and failure mechanism of the C-terminal cross-link domain in type I collagen. J Mech Behav Biomed Mater 2011;4(2):153-61.

[186] Eyre DR, Koob TJ, Vanness KP. Quantitation of hydroxypyridinium crosslinks in collagen by high-performance liquid-chromatography. Anal Biochem 1984;137(2):380-8.

14. PAPERS

Study 1

Short communication

Viscoelastic behavior of discrete human collagen fibrils

René B. Svensson[a], Tue Hassenkam[a], Philip Hansen[b], S. Peter Magnusson[b,*]

[a] Nano-Science Center, University of Copenhagen, Universitetsparken 5, 2100 Copenhagen Ø, Denmark
[b] Institute of Sports Medicine, Bispebjerg Hospital, Faculty of Health Science, University of Copenhagen Copenhagen, Denmark

ARTICLE INFO

ABSTRACT

Whole tendon and fibril bundles display viscoelastic behavior, but to the best of our knowledge this property has not been directly measured in single human tendon fibrils. In the present work an atomic force microscopy (AFM) approach was used for tensile testing of two human patellar tendon fibrils. Fibrils were obtained from intact human fascicles, without any pre-treatment besides frozen storage. In the dry state a single isolated fibril was anchored to a substrate using epoxy glue, and the end of the fibril was glued on to an AFM cantilever for tensile testing. In phosphate buffered saline, cyclic testing was performed in the pre-yield region at different strain rates, and the elastic response was determined by a stepwise stress relaxation test. The elastic stress-strain response corresponded to a second-order polynomial fit, while the viscous response showed a linear dependence on the strain. The slope of the viscous response showed a strain rate dependence corresponding to a power function of powers 0.242 and 0.168 for the two patellar tendon fibrils, respectively. In conclusion, the present work provides direct evidence of viscoelastic behavior at the single fibril level, which has not been previously measured.

© 2009 Elsevier Ltd. All rights reserved.

1. Introduction

Collagenous materials comprise the majority of structural tissues in humans and other mammals, and are therefore of great importance to the biomechanical integrity of the body. A hierarchical order can be distinguished in most of these tissues, and the discrete levels of the hierarchy can have dissimilar mechanical properties (An et al., 2004; Silver and Landis, 2008). A tendon is an example of such a hierarchical collagenous structure with five commonly recognized levels; the whole tendon, the fascicle, the fiber bundle, the collagen fibril and the collagen molecule (Kannus, 2000). The possible differences in mechanical properties between each level originate in the mechanisms of force transfer between the subunits from the lower hierarchical levels, and to understand how this force is transferred it is necessary to first understand the properties at each distinct level.

Mechanical investigations at the topmost hierarchical levels have been performed for decades (Haraldsson et al., 2005; Haut, 1986; Rigby et al., 1959). Direct measurements at the fibril and molecule level, however, have only recently become possible with the advent of nanotechnology, and especially the atomic force microscope (AFM). Although a few mechanical investigations have been made at the fibrillar level none has described the viscoelastic properties (Eppell et al., 2006; van der Rijt et al., 2006; Yang et al., 2007, 2008).

* Corresponding address: Institute of Sports Medicine, Bispebjerg Hospital, Bispebjerg Bakke 23, 2400 Copenhagen NV, Denmark. Tel.: +45 35316087; fax: +45 35312733.
E-mail addresses: P.Magnusson@mfi.ku.dk, renesv@m3.stud.ku.dk (S. Peter Magnusson).

This brief report presents data that for the first time directly demonstrates the strain rate dependence of single human collagen fibrils.

2.   Materials and methods

The experimental procedures partly resemble that reported by van der Rijt et al. (2006). For AFM work, a Veeco MultiMode microscope was used. Imaging was performed using a J-type scanner in tapping mode and force measurements were performed using a Picoforce scanner with a IIIa controller. Two types of cantilevers were used in the present work, both from Olympus. (A) OMCL-AC160-TS ($k_{spring} \sim 42$ N/m) and (B) OMCL-TR800PSA ($k_{spring} \sim 0.57$ N/m). Imaging was executed using cantilever (A), while force measurements were performed using cantilever (B). For force measurements exact cantilever spring constants were determined by a so-called thermal tune involving the analysis of the cantilever's thermal spectrum.

Patellar tendon fascicles were obtained during anterior cruciate ligament reconstruction, and was stored before use at $-18\,^{\circ}$C in PBS soaked gauze. Sample preparation was done in milli-Q water by cutting a small piece of tissue (<1 mm) from a tendon fascicle, transferring it to a silicon substrate and then mechanically spreading the tissue out on the substrate using a pair of tweezers. The sample was then dried under nitrogen flux, which makes the fibrils adhere to the substrate, rinsed with large amounts of flowing deionized water followed by a light rinse with ~ 1 ml of milli-Q water before it was dried again with nitrogen. The dry sample was investigated with optical microscopy to locate a single separate collagen fibril, which was then imaged in the dry state by AFM at four locations along its length to determine the cross-sectional area. Two cross-sectional determinations were made at each location along the fibril. The cross-sectional area was determined in two ways: as the total area under the fibril contour, and as the area of an ellipse with one diameter equal to the fibril height and the other equal to the fibril width at half the height. The average of the two measures was used because the side-angles in some cross-sections were smaller, and in others were equal to, the side-angles of the tip, indicating that tip-convolution effects were present. Along the length of the fibrils the mean diameter derived from the measured area had a standard deviation below the lateral resolution (5.9 nm/pixel) of the images used.

A small drop of epoxy glue (DANA LIM Blå Epoxy 335) was placed on the substrate near the fibril. The glue was picked up using the cantilever (B), and two glue droplets were placed on the substrate; one at the fibril end, and the other $\sim 200\ \mu$m further down the fibril. Then the glue was allowed to cure for at least 42 h. Using the sharp tip of cantilever (A), the glue at the end was cut free from the substrate while still adhering to the fibril, and the length of fibril spanning between the two glue droplets was determined by optical microscopy. Thereafter the force-measuring cantilever (B) was attached with fresh glue to the glue/fibril complex at the fibril end and allowed to cure for at least 18 h. In this way one part of the fibril was anchored to the substrate while the fibril end was glued to the cantilever without direct contact between the fresh glue and the substrate. To ensure that the fibril was attached directly to the cantilever, it was positioned slightly in front of the dry droplet of glue and engaged hard, thereby ensuring that the fresh glue covered the cantilever all the way to the its tip and was in contact with the fibril. After curing, a 150 mM PBS solution was introduced and after 30 min the cantilever was gently lifted away from the surface thus suspending the fibril between the cantilever and the anchoring glue. The suspended fibril was brought into a vertical position by applying a small load and moving the cantilever in the direction reducing that load, until movement in any direction would increase the load. Then the fibril was mechanically tested by extending and retracting the piezo scanner (called ramping) to strain the fibril while measuring the force by the cantilever bending (see Fig. 1). The glue used in the experiment has a shear modulus >0.2 GPa according to the manufacturer. The glue/fibril interface has an area that is $\sim 4\ \mu$m^2, the greatest force reached in the experiment is $\sim 2\ \mu$N and the thickness of the glue is $\sim 3\ \mu$m. This will lead to a deformation of the glue of ~ 7.5 nm which translates to a $<0.01\%$ strain in the experiments; we consider this to be insignificant.

The optical detector used to determine the cantilever deflection has a limited linear range. Therefore, data was acquired in a piecewise manner by physically moving the detector as shown in Fig. 1. By retaining an overlap between the data recorded at two subsequent detector positions, it is possible to stitch together the data. A single curve is from 20–30 pieces stitched together. Data from each detector position has to be acquired on individual ramps and to ensure that the curve does not change between each measured piece, ramping was performed in a continuous cyclic manner until subsequent cycles yielded identical curves (~ 20 cycles). The cycles were then continued while acquiring the data pieces. The linearity of the detected signal during movement of the detector was verified by acquiring an indentation force curve on a hard silicon substrate ($R^2 = 0.9995$). When changing between strain rates, cyclic loading for ~ 1 min at the new rate was performed before acquiring data. Following the dynamic tests, the elastic response was determined by an incremental stress relaxation test where the deformation was increased in discrete steps (0.3–0.5 μm) and the stress was allowed to relax for 5 min at each step.

3.   Results and discussion

Measurements were made on two individual collagen fibrils from freshly harvested human patellar tendon with initial lengths of $200 \pm 5\ \mu$m and $211 \pm 5\ \mu$m, and cross sectional areas of $(17 \pm 1) * 10^3$ nm^2 and $(17.4 \pm 0.5) * 10^3$nm^2 for fibril #1 and #2 respectively. The samples were not intentionally treated to influence cross-linking, but the period of dry storage while
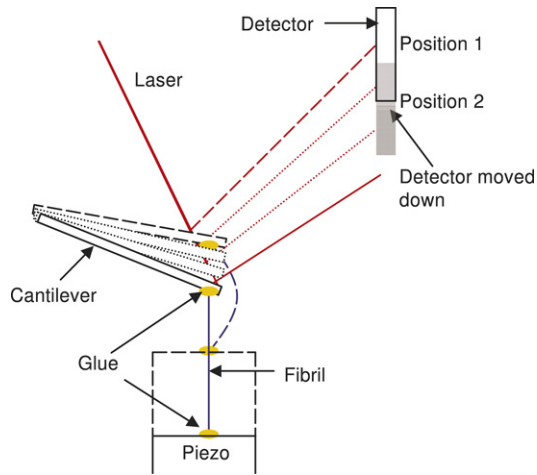
Fig. 1 – Simplified schematic of the AFM setup used for mechanically testing single collagen fibrils. The fibril is suspended between the cantilever and the sample on the piezo by epoxy glue. In the extended position of the piezo, the fibril is relaxed, the cantilever is not bent and the reflected laser hits the top of the detector (dashed lines). In the retracted position of the piezo, the fibril is stretched, the cantilever is bent and the laser hits below the detector (solid lines). In position 1, the detector can record the bending from laser spot 1 to spot 2. By moving the detector to position 2 the bending from laser spot 2 to spot 3 can be determined, thereby the data from detector position 1 and position 2 can be stitched together to provide the full data set from laser spot 1 to spot 3. This can be continued as long as an overlap between detector positions is retained.

the glue cures may have caused an increase in cross-linking and thus stiffness of the fibrils (Silver et al., 2000).

The effect of strain rate on the mechanical behavior was investigated by performing experiments at six different dynamic strain rates besides the elastic measurements at zero strain rate (stress relaxation) (Fig. 2). The strain value at the onset of stress (defined as stress exceeding 200 kPa) decreased with the introduction of a 5 sec delay between each loading cycle. Since this shift is reversible, we believe it is caused by viscous mechanisms. A shift in onset towards higher strains was also observed in curves obtained late in the experiment compared to curves obtained earlier at the same strain rate. This effect was particularly clear for curves obtained after the stress relaxation experiment, compared to those before. The reversibility of this shift was not investigated exhaustively, but leaving the fibril slack for 15 min following the stress relaxation experiment leads to a ~20% recovery of the shift compared to a curve obtained right before the stress relaxation, showing that the shift is at least partly reversible. For better comparison, the curves presented in Fig. 2 have all been shifted such that their onset lies at zero strain; this is the reason why they end at different strains even though the target strain was the same at all strain rates.

For both fibrils, an increase in strain rate resulted in increased stress for a given strain, or likewise decreased strain at a given stress. To analyze this effect, the stress-strain
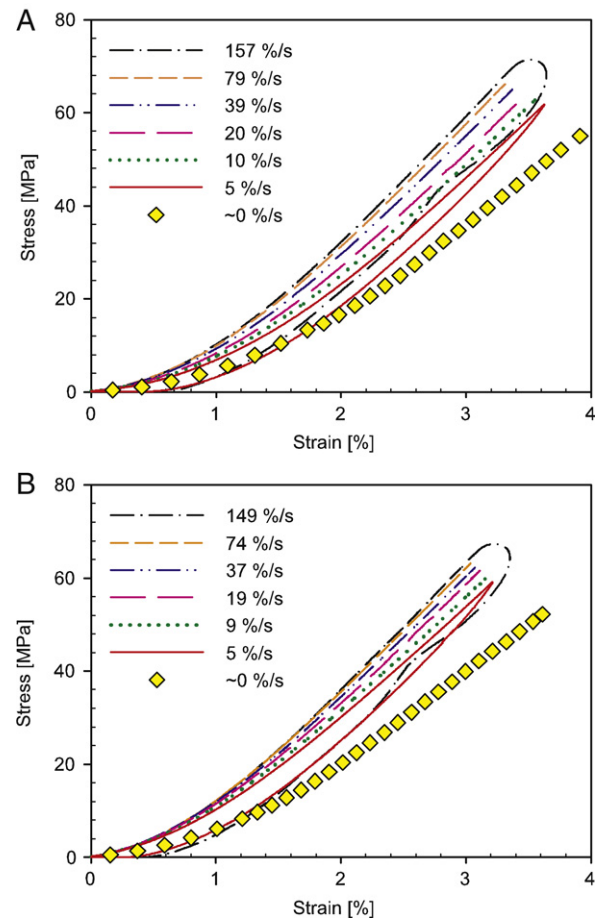
Fig. 2 – Stress–strain relationship of single collagen fibrils. Hysteresis loops are presented for the highest and lowest dynamic strain rates. For clarity only the loading part of the loop is shown for the intermediate strain rates. The results of the incremental stress-relaxation are shown as discrete points. Zero strain for each curve was defined as the point where the stress first exceeded 200 kPa. (A) and (B) are results on fibril #1 and #2 respectively.

data was separated into an elastic and a viscous component. The viscous component was obtained by subtracting the elastic (stress relaxation) stress-strain curves from the corresponding dynamic ones Fig. 3. Only the "loading" portion of the hysteresis loops was considered. For both fibrils the elastic response was found to fit a second-order polynomial appreciably better than a linear function ($R^2 = 0.9989$ and $R^2 = 0.9979$ in the second-order as opposed to $R^2 = 0.9628$ and $R^2 = 0.9722$ in the linear fit for fibril #1 and #2 respectively). This non-linearity is in agreement with single fibril results of van der Rijt et al. (2006) obtained during a dynamic test. However, it is in contrast with the linear response reported for fibrils (Sasaki and Odajima, 1996) and self-assembled fibers (Silver et al., 2002) obtained in previous stress relaxation studies. The disagreement with the previous studies is possibly caused by the shorter relaxation time in our experiments. This could lead to incomplete relaxation and thus an overestimate of stress, which is likely to be greater at higher strains because the total relaxation
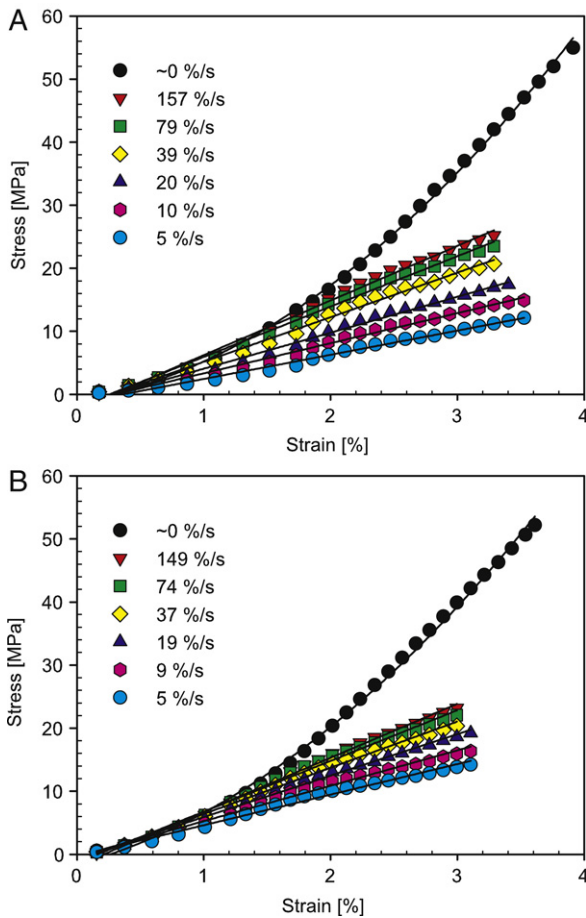
Fig. 3 – Plot of viscous and elastic components of stress as a function of strain. The elastic component is the zero rate stress relaxation data also shown in Fig. 2. **The viscous component is determined by subtracting the elastic part from the dynamic curves also presented in** Fig. 2. **Linear fits are provided for the viscous component and a second-order fit for the elastic (black lines). (A) and (B) are the results on fibril #1 and #2 respectively.**

increases with strain, thus giving rise to the observed non-linearity. If that were the case then the viscous component would be underestimated too. For the viscous component, the strain dependence was found to be approximately linear, which is in agreement with results on self-assembled fibers (Silver et al., 2002). The slope of the linear viscous component increased with the strain rate, and a power-function provided a good fit living up to the requirement of going towards zero at zero strain rate. The fitted powers were 0.242 (R^2 = 0.9798) and 0.168 (R^2 = 0.9749) for fibril #1 and #2. The strain rate dependence is commonly given as the product between viscosity and the strain rate, meaning that a linear dependence implies a constant viscosity while a dependence with power smaller than one implies that the viscosity is a decreasing function of the strain rate. Silver et al. (2002) has proposed that this thixotropy is associated with the interstitial water in the fibril causing hydroplaning of the subfibrillar elements at high strain rates, thus reducing friction between them.

4. Conclusion

Tensile testing was performed on two isolated collagen fibrils from a human patellar tendon, and the elastic stress-strain curve displayed a non-linear shape that was well fitted by a second-order polynomial. The viscous component showed a linear strain dependence with a slope that fitted a power-function of the strain rate with powers of 0.242 and 0.168 for the two fibrils respectively. The strain rate dependence with power <1 and the linearity of the viscous component both agree with previous findings on self-assembled fibers (Silver et al., 2002).

REFERENCES

An, K.N., Sun, Y.L., Luo, Z.P., 2004. Flexibility of type I collagen and mechanical property of connective tissue. Biorheology 41, 239–246.

Eppell, S.J., Smith, B.N., Kahn, H., Ballarini, R., 2006. Nano measurements with micro-devices: Mechanical properties of hydrated collagen fibrils. J. R. Soc. Interface 3, 117–121.

Haraldsson, B.T., Aagaard, P., Krogsgaard, M., et al., 2005. Region-specific mechanical properties of the human patella tendon. J. Appl. Physiol. 98, 1006–1012.

Haut, R.C., 1986. The influence of specimen length on the tensile failure properties of tendon collagen. J. Biomech. 19, 951–955.

Kannus, P., 2000. Structure of the tendon connective tissue. Scand. J. Med. Sci. Sports 10, 312–320.

Rigby, B.J., Hirai, N., Spikes, J.D., Eyring, H., 1959. The mechanical properties of rat tail tendon. J. Gen. Physiol. 43, 265–283.

Sasaki, N., Odajima, S., 1996. Elongation mechanism of collagen fibrils and force-strain relations of tendon at each level of structural hierarchy. J. Biomech. 29, 1131–1136.

Silver, F.H., Christiansen, D.L., Snowhill, P.B., Chen, Y., 2000. Role of storage on changes in the mechanical properties of tendon and self-assembled collagen fibers. Connect. Tissue Res. 41, 155–164.

Silver, F.H., Ebrahimi, A., Snowhill, P.B., 2002. Viscoelastic properties of self-assembled type I collagen fibers: Molecular basis of elastic and viscous behaviors. Connect. Tissue Res. 43, 569–580.

Silver, F.H., Landis, W.J., 2008. Viscoelasticity, energy storage and transmission and dissipation by extracellular matrices in vertebrates. In: Fratzl, P. Collagen (Ed.), Structure and Mechanics. Springer, New York, pp. 133–154.

van der Rijt, J.A.J., van der Werf, K.O., Bennink, M.L., Dijkstra, P.J., Feijen, J., 2006. Micromechanical testing of individual collagen fibrils. Macromol. Biosci. 6, 697–702.

Yang, L., van der Werf, K.O., Koopman, B., et al., 2007. Micromechanical bending of single collagen fibrils using atomic force microscopy. J. Biomed. Mater. Res. Part A 82A, 160–168.

Yang, L., van der Werf, K.O., Fitié, C.F.C., et al., 2008. Mechanical properties of native and cross-linked type I collagen fibrils. Biophys. J. 94, 2204–2211.

Study 2

Tensile Properties of Human Collagen Fibrils and Fascicles Are Insensitive to Environmental Salts

René B. Svensson,[†‡] Tue Hassenkam,[†] Colin A. Grant,[§] and S. Peter Magnusson[‡]*

[†]Nano-Science Center and [‡]Institute of Sports Medicine Copenhagen, Bispebjerg Hospital and Center for Healthy Aging, Faculty of Health Science, University of Copenhagen, Copenhagen, Denmark; and [§]School of Physics and Astronomy, University of Leeds, Leeds, United Kingdom

ABSTRACT   To carry out realistic in vitro mechanical testing on anatomical tissue, a choice has to be made regarding the buffering environment. Therefore, it is important to understand how the environment may influence the measurement to ensure the highest level of accuracy. The most physiologically relevant loading direction of tendon is along its longitudinal axis. Thus, in this study, we focus on the tensile mechanical properties of two hierarchical levels from human patellar tendon, namely: individual collagen fibrils and fascicles. Investigations on collagen fibrils and fascicles were made at pH 7.4 in solutions of phosphate-buffered saline at three different concentrations as well as two HEPES buffered solutions containing NaCl or NaCl + CaCl$_2$. An atomic force microscope technique was used for tensile testing of individual collagen fibrils. Only a slight increase in relative energy dissipation was observed at the highest phosphate-buffered saline concentration for both the fibrils and fascicles, indicating a stabilizing effect of ionic screening, but changes were much less than reported for radial compression. Due to the small magnitude of the effects, the tensile mechanical properties of collagen fibrils and fascicles from the patellar tendon of mature humans are essentially insensitive to environmental salt concentration and composition at physiological pH.

INTRODUCTION

Tendons are a fibrous collagenous connective tissue that is responsible for transmitting forces from muscle to bone to produce joint movement. The importance of tendon in the function of the body is mechanical in nature and investigating the response of tendons under load is essential. When it comes to the examination of tissue mechanical properties, it is often necessary to remove the tissue from its natural environment, thus requiring an adequate substitute. Interstitial fluids contain a complex mixture of a large number of different components including minerals, proteins, sugars, and more.

The most abundant components are Na$^+$ (~140 mM) (1) and Cl$^-$ (~100 mM) (2) making up ~80% of the total osmolarity (~300 mM), and a common substitute is therefore a 150 mM (0.9%) NaCl solution, commonly referred to as physiological saline. Such a simple saline solution does not take into account the physiological pH value of 7.4 (3) and therefore a buffer is often added. A large number of buffers exist with different advantages and disadvantages (4); a common choice is phosphate. However, a number of studies have indicated that such buffered solutions do not correctly mimic the natural environment, but instead yield increased swelling (5,6). Furthermore, it has been reported that buffer solutions have altered the mechanical properties (6–8) compared to freshly harvested tissue tested under ambient conditions. It should be noted that simply testing under ambient conditions is often not realistic, because the tissue will dry quickly, especially if the specimens are small.

Different studies have found that changing the molarity of the buffering solution affects the water content of the tissue (9,10). The hydrating properties of physiological solutions are important, because hydration has been shown to influence mechanical properties (11). Most notably dry tissues are stiffer than hydrated tissues; as hydration increases, so does cyclic relaxation (6), stress relaxation (12,13), and creep (9,10), which are all manifestations of viscous behavior. These studies used sucrose to alter solution molarity; however, this option will be problematic because sucrose solutions are significantly more viscous than water (14).

In a recent study by Grant et al. (15), individual collagen fibrils were investigated by nanoindentation to determine the radial compressive mechanical properties in a number of saline solutions with varying composition, concentration, and pH. It was found that increasing the salt concentration led to a severalfold increase in modulus. However, due to the highly anisotropic structure of collagen fibrils, the mechanical response in the radial direction will be considerably different from that in the axial direction.

A number of recent studies on tensile mechanical properties of individual collagen fibrils report modulus values ranging from 0.2 to 0.86 GPa for hydrated fibrils (16–18). Several studies have looked into the difference between dry and hydrated tissue; however, none have investigated differences in the hydrated environment.

The tendon is known to have a hierarchical structure ranging from the collagen molecule to the whole tendon (Fig. 1). However, the mechanical connection between the levels of the hierarchy is poorly understood. Some studies suggest that fibrils slip significantly during loading (19,20), while the great length of fibrils (21,22) and the inability to
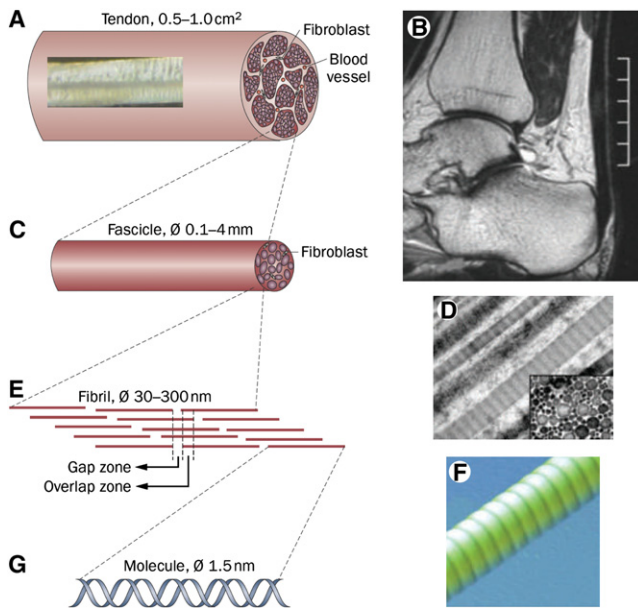
FIGURE 1 (*A*) Schematic of the whole tendon. (*Inset*) Texture of the tendon with crimping. (*B*) Magnetic resonance image of the human Achilles tendon. (*C*) Tendon fascicles which are long separable cylindrical structures. (*D*) Longitudinal transmission electron microscope image of fibrils in a fascicle. (*Inset*) Transmission electron microscope cross section where the fibrils appear as circles. (*E*) Schematic of the highly organized structure of molecules in a collagen fibril giving rise to a characteristic ~68-nm banding pattern of gap and overlap zones. (*F*) Three-dimensional AFM image of a collagen fibril displaying the banding pattern. (*G*) The building blocks of the fibrils are the collagen molecules, a peptide triple helix. (Figure reproduced from Magnusson et al. (45).)

obtain unbroken fibrils from mature tissue (23) indicate that fibrils are mechanically and possibly even physically continuous. It is therefore of great interest to investigate how changes at one hierarchical level relate to the other levels.

In this article, we investigated the axial tensile mechanical properties and swelling of collagen fibrils and fascicles from the human patellar tendon (Fig. 1), to assess the degree to which changes at one hierarchical level would carry over to the other. The environmental factors investigated are osmolarity and presence of calcium. The effect of osmolarity was primarily investigated to determine whether changes to the hydration through osmosis would occur and whether the mechanisms of force transmission would be disrupted or enhanced by salts as indicated by Grant et al. (15). The investigation of calcium was prompted by previous reports showing that energy dissipation in nanoscale pulling and indentation of collagen was significantly increased in $CaCl_2$-containing solutions compared to solutions with only NaCl (24,25).

MATERIALS AND METHODS

Materials

Human patellar tendon tissue was obtained during anterior cruciate ligament replacement surgery (approved by the Danish Council of Ethics).

The tissue had been stored frozen ($-20°C$) in 150 mM phosphate-buffered saline (PBS). Reports on the effect of frozen storage on mechanical properties are inconsistent (26–30), but in our laboratory we have not observed any measurable differences in mechanical properties between fresh and frozen tissue. Individual fascicles were liberated from the tissue, one used for the fibril level experiments and a further six used for experiments at the fascicular level.

Atomic force microscopy (AFM) was performed on a MultiMode microscope with a IIIa controller (Veeco Instruments, Woodbury, NY). Three different cantilevers were used for AFM experimentation (Olympus, Tokyo, Japan):

1. OMCL-AC160TS (k_{spring}~42 N/m),
2. OMCL-TR800PSA long cantilever (k_{spring}~0.15 N/m), and
3. OMCL-TR800PSA short cantilever (k_{spring}~0.57 N/m).

A PicoForce setup was used for mechanical measurements (Veeco Instruments). The exact spring constant of cantilevers were determined by analysis of their thermal spectrum (thermal tune) (31).

PBS solutions were prepared from a $20\times$ concentrated PBS stock solution (4.00 g/L KCl, 160.20 g/L NaCl, 4.00 g/L NaH_2PO_4, 23.00 g/L, Na_2HPO_4) by diluting 3, 20, and 150 times with ultra-pure water (resistivity >18 MΩ·cm) and adjusting to pH 7.4. This yields solutions with concentrations of 1 M, 150 mM, and 20 mM (called PBS1000, PBS150, and PBS20, respectively). Furthermore, two 10-mM HEPES buffers were prepared to investigate the effect of Ca^{2+}, one containing 150 mM NaCl (called HEPES) and another containing 90 mM NaCl, 40 mM $CaCl_2$ (called $CaCl_2$) (pH 7.4). The HEPES solution was used to clear out residual phosphate before the introduction of calcium that would otherwise precipitate as calcium phosphate; it also serves as a control to the effect of HEPES itself.

Experimental overview

Each fascicle and fibril was tested in all five solutions. First, the specimen was tested in each of the three PBS solutions. The order of PBS solutions in this test was varied between experiments in a systematic fashion comprising the six possible permutations of solution order. This allows for the effect of time to be assessed by comparing among the first, second, and third PBS buffers without having the PBS concentration as a confounder (Table 1). Then it was tested in the HEPES solution and finally in the $CaCl_2$ solution. Fascicles and fibrils were tested at two deformation rates of 0.5 and 4 mm/min and 9.81 and 314 μm/s, respectively, to assess viscous effects. To eliminate correlation between rate and time, the order of the testing rates was reversed in every other experiment. The deformation rates for the fascicles

TABLE 1 Results grouped by injection order irrespective of PBS concentration

Time of PBS injection*	No. 1	No. 2	No. 3
Fascicles			
Modulus (GPa)	0.55 ± 14	0.54 ± 14	0.54 ± 15
Relative energy dissipation (%)	24.9 ± 3.8	24.7 ± 2.6	24.5 ± 4.5
Diameter (mm)	0.28 ± 0.16	0.28 ± 0.17	0.28 ± 0.16
Fibrils			
Modulus (GPa)	2.89 ± 0.23	2.88 ± 0.23	2.93 ± 0.21
Relative energy dissipation (%)	14.8 ± 3.4	14.3 ± 4.5	13.9 ± 4.4
Height (nm)	167 ± 50	168 ± 47	171 ± 48

Values are mean ± SD. None of the parameters differ significantly between time-points.
*Time is shown as the injection order (first, second, or third PBS buffer introduced). Each time-point covers two measurements at each PBS concentration.

translate to ~0.1%/s and 1%/s strain rate, and for the fibrils they translate to ~5%/s and 160%/s.

Fascicle testing

Fascicle mechanical testing was performed in a micro tensile tester (200-N tensile stage, petri dish version; Deben, Suffolk, UK) equipped with a 20 N load cell (shown in Fig. 2 A). The middle of the fascicle was kept moist by gauze soaked in the first solution while the ends dried. The dry ends were glued with cyanoacrylate on to the clamps and an aluminum disk was placed on top, which significantly increased the rate of curing. The first solution was introduced after 15 min.

The fascicle was stretched until reaching the force onset (~0.01 N) followed by three preconditioning cycles to 4% strain after which the onset was redetermined (see Fig. 2 B). Using the new onset, six cycles to 4% strain were performed at each deformation rate. Data from the sixth cycle was analyzed. At the end of the test the fascicle was returned to a slack position, and the solution was exchanged while keeping the fascicle moist. The fascicle was incubated in the new solution for 1 h before repeating the test protocol.

In each solution, the fascicle diameter was determined from microscope images taken at the first onset. Cross-sectional area (CSA) was calculated assuming a circular profile (32); subsequently, the CSA in the first solution was used to calculate stress for that specimen in all solutions.

Fibril mechanical testing

Fibril mechanical testing was performed using a previously published method (33) with one improvement to the procedure. The glue used for this study was Araldite 2014 (Huntsman Advanced Materials, Everberg, Belgium), which reduces the initial curing period by 24 h. In brief, tissue was spread and dried on a silicon substrate, then two droplets of glue (~200 μm apart) were placed with an AFM cantilever on a separate fibril. After curing (18 h), the CSA was determined at eight positions along the dry fibril by tapping mode AFM imaging using cantilever 1. Dry CSA was used because it is easier to measure and is not affected by changes in the tapping force. After CSA measurement, one of the glue droplets at

the end of the selected fibril was scraped free using cantilever 1. This free region of the collagen fibril was attached with glue to cantilever 3 in such a way that the fibril was sandwiched between the glue pad and the cantilever. After further curing (18 h), the first buffer solution was introduced and given 30-min equilibration time before mechanical testing. The data acquisition technique requires merging of multiple separate curves and therefore only steady-state measurement can be made (33).

To ensure comparability between fibril and fascicle tests, the fibril testing protocol was kept as identical as technically possible to the one used on fascicles. An initial force onset was determined (~2.5 nN) and preconditioning cycles to 4% strain were performed for 10 min. The final onset was then determined and used throughout the experiment. The test consisted of cycling to 4% strain for 5 min to ensure a steady state before acquiring the force curve in a piecewise manner as previously described (33). When changing deformation rate, the fibril was cycled for 2 min to ensure a steady state at the new rate before acquiring data. The fibril was then relaxed and the buffer solution removed with a syringe, leaving a small amount of solution between the cantilever and the surface to avoid drying out the fibril. The fluid-cell was flushed thoroughly with 10 chamber volumes of the next test solution. The collagen fibril was allowed to equilibrate for 30 min before the testing protocol was repeated.

Fibril height

The effect of solution environment on fibril swelling was investigated by AFM imaging using cantilever 2 for tapping-mode in liquid. AFM samples were prepared as described above. To avoid compression of the fibrils, tapping force was kept low by increasing the amplitude set-point until the tip almost detached from the surface. Even at low tapping force, it is necessary to keep the scan direction parallel to the fibrils to avoid detaching them from the substrate. Due to the low tapping force, tracking was poor along the fibril sides (Fig. 3 B) and therefore only the height was measured. For each fibril, height was measured at the same four points in all solutions.

Data reduction and statistics

Mechanical measurements were made on six fascicles and six fibrils, swelling was assessed on the same six fascicles and 12 other fibrils. Modulus was determined at the lowest common stress in each experiment, by linear regression to the final 20% (stress) of the loading curve. Relative energy dissipation was determined by integrating along the entire hysteresis loop and normalizing to the area under the loading curve. Effect of buffer composition was analyzed by one-way ANOVA with repeated measures. The effect of deformation rate was analyzed by two-way ANOVA with repeated measures. Multiple comparisons were made with Bonferroni corrections. Based on the observed standard deviations, the experiment had a power >98% to detect a 15% change in modulus and relative energy dissipation, at both the fibril and fascicle level. We consider 15% change to be a reasonable requirement in light of the >100% effects of Ca^{2+} and salt concentration reported by others (15,24,25). For the fibril height and fascicle diameter, the relevant magnitude of change is probably somewhat smaller, and the power of these experiments to detect a 5% change was >90%.

RESULTS

Fibrils

Mechanical testing was performed on single collagen fibrils, producing hysteresis loops as shown in Fig. 4 A. The fibrils had a mean dry diameter of 122 ± 22 nm, which belongs in the larger end of the range seen in human patellar tendon (34). The diameter was very uniform along the length of
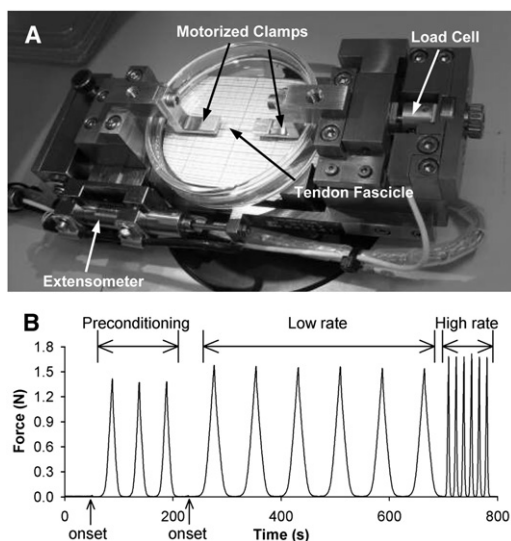

FIGURE 2 Fascicle mechanical test design. (A) Photograph of the mechanical rig showing the most important components. (B) Example of fascicle mechanical data showing onset determinations, preconditioning, and cyclic tests at two deformation rates. The basic scheme is similar to that used for fibrils.
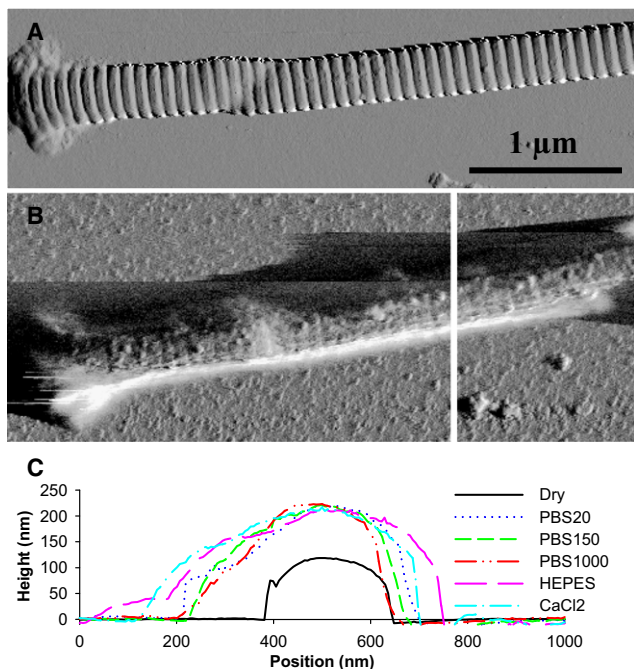
FIGURE 3 AFM images used for measuring fibril heights to assess swelling. (*A*) Dry collagen fibril imaged in air. (*B*) The same fibril imaged in the PBS20 solution. The fibril is casting a shadow to the left due to the low tapping force. (*C*) Line section profiles used to determine fibril height in each solution. The displayed sections were taken at the position shown with a vertical white line in panel *B*. As can be seen, the peak height varies little between the solutions.

fibrils with an average standard deviation of 3.5%. The tested fibrils were usually several hundred micrometers in length, but were entangled in other fibrils, allowing only a shorter part to be tested. The mean testing length of fibrils was 192.8 ± 6.0 μm. We tested the collagen fibrils to a mean strain value of 4.25 ± 0.48% corresponding to a stress of 89 ± 15 MPa using dry CSA. The aim was to reach into a linear response region while keeping stress low
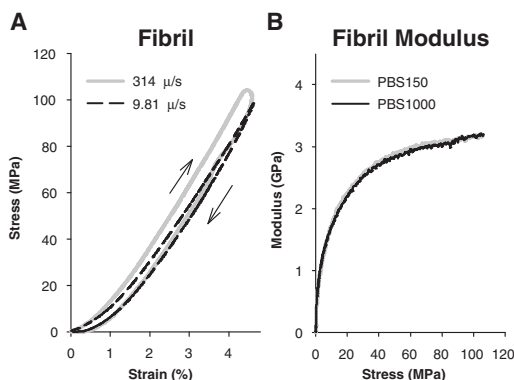

FIGURE 4 (*A*) Representative stress-strain curves obtained on a fibril at two deformation rates. Note that the rounded tip in the high-rate curve is caused by a measuring artifact. (*Arrows*) Loading and unloading direction in the hysteresis loop. (*B*) Plot of modulus as a function of stress for a single fibril. There is a large initial increase followed by a plateau region.

enough to avoid plastic deformation. Fig. 4 *B* shows the modulus (slope) of a representative stress-strain curve as a function of the stress and it can be seen that the modulus reaches a plateau. Although the slope does not become completely constant we still consider it to be in a linear region, and because analysis was performed at a common stress value, the slight nonlinearity would not affect the results. We did not observe any plastic deformation during the tensile tests.

The effect of osmolarity was investigated in the three PBS solutions at concentrations from 20 mM to 1 M. The modulus of collagen fibrils (see Fig. 6 *B*, later) showed no significant difference between any of the solutions. Furthermore, the fibril swelling based on height measurements (Fig. 3) was not affected by the PBS concentration either. However, the relative energy dissipation (see Fig. 6 *C*, later) increased to 17.0 ± 3.8% in PBS1000 from 12.9 ± 3.2% in PBS20 ($P < 0.001$) and 13.2 ± 3.8% in PBS150 ($P < 0.001$).

Replacing the phosphate with a HEPES buffer caused a statistically significant increase in fibril modulus of 2.4 ± 1.6% ($P < 0.05$) compared to the PBS150 solution of equal concentration. Fibril height and relative energy dissipation were not affected by the change from phosphate to HEPES buffer. Investigating the possible effect of calcium on collagen fibril mechanics by including $CaCl_2$ in the HEPES solution did not change any of the measured properties.

The possible viscoelastic effects of the solutions was investigated by increasing the deformation rate from 9.81 μm/s to 314 μm/s. Doing so significantly increased the tensile modulus (see Fig. 6 *B*, later) in all five solutions ($P < 0.01$) with a mean increase across all solutions of 7.6 ± 4.3%. Varying the solution environment did not affect the viscoelastic response because there was no interaction between buffer composition and deformation rate in any of the measurements. We did not analyze the effect of deformation rate on relative energy dissipation because the high rate measurements were affected by a measuring artifact seen as a rounded tip in the unloading part of the hysteresis loop in Fig. 4 *A*.

The initial three PBS solutions were applied in a varied order to eliminate cross talk between composition and time. Analyzing the PBS data by order instead of composition therefore allows us to assess whether changes occurred in the mechanical measurements as the experiment progressed. This was not the case, as there was no significant difference between time points for any of the measured parameters (Table 1).

Fascicles

We performed mechanical tests on fascicles in addition to fibrils to be able to separate intra- and interfibrillar effects (Fig. 5 *A*). The tested fascicles had a mean diameter of
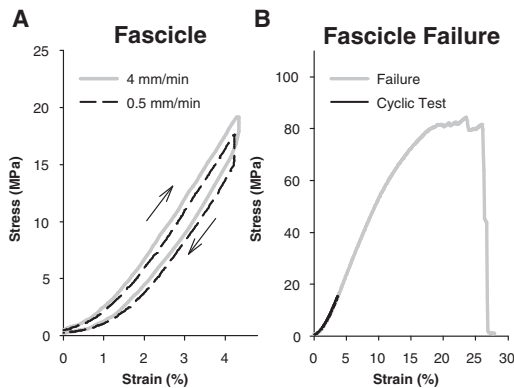
FIGURE 5 (*A*) Stress-strain curves obtained on a fascicle at two deformation rates. (*B*) Comparison between the cyclic test region (~4% strain) used in this study and the failure properties of a representative fascicle.

0.27 ± 0.16 mm and a mean length of 6.93 ± 0.62 mm. The fascicles were tested into the linear region but at sufficiently low stress and strain to avoid plastic deformation. The mean value of the target stress and strain in PBS150 was 12.9 ± 3.9 MPa and 3.87 ± 0.32%, respectively; for comparison, the mean failure stress following the entire experiment was 60 ± 29 MPa and failure strain was 17 ± 7% (see Fig. 5 *B*).

Changing the ionic strength of the environment in the range of 20 mM to 1 M PBS did not have any effect on the modulus of the fascicles which remained constant at ~550 MPa (Fig. 6 *A*). However, the relative energy dissipation (Fig. 6 *C*) showed a statistically significant increase from 23.0 ± 3.7% in PBS150 to 26.3 ± 3.3% in PBS1000 ($P < 0.01$). The swelling of the fascicle as determined by the diameter did not change significantly with solution concentration.

Using a HEPES buffer instead of the phosphate did not significantly affect any of the measured fascicle properties when compared to the PBS150 solution (Fig. 6, *A* and *C*). The presence of Ca^{2+} in the HEPES buffer did not change the mechanical response or swelling either.

Increasing the deformation rate from 0.5 mm/min to 4 mm/min did not significantly affect the modulus (Fig. 6 *A*) or the relative energy dissipation in any of the solutions. In addition, we found no interaction between buffer composition and deformation rate in any of the measurements.

There was no significant difference between time points for any of the measured parameters (Table 1), showing that none of the measured properties changed over the course of the experiment.

DISCUSSION

The main purpose of this study was to investigate the sensitivity of collagen-based materials to changes in the ionic concentration of their environment. Previously, Ca^{2+} has been reported to affect mechanical properties of bone and rat tail tendon (24,25,35). The effect of Ca^{2+} on human
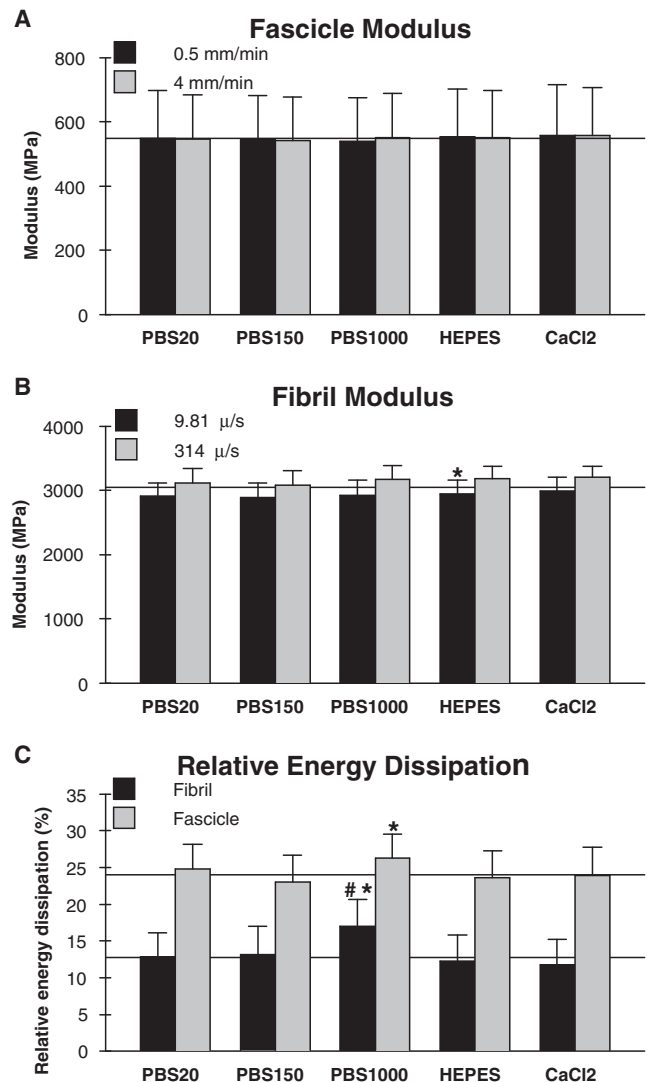
FIGURE 6 Mechanical results for fascicles and fibrils in each of the five solutions. (*A*) Modulus of collagen fascicles measured at two deformation rates (0.5 and 4 mm/min). Difference between deformation rates is not significant in any solution. (*B*) Modulus of collagen fibrils measured at two deformation rates (9.81 and 314 μm/s). Difference between deformation rates is statistically significant in all solutions. (*C*) Relative energy dissipation of collagen fibrils and fascicles at the low rates (9.81 μm/s and 0.5 mm/min). The pound symbol (#) indicates significantly different from PBS20; the asterisk symbol (*) indicates significantly different from PBS150 ($p < 0.05$).) (*Horizontal lines*) Guide to the eye.

tendon at the fibril and fascicle level was therefore also investigated in this study.

Structure

The structural data on fascicle diameter and fibril height did not respond significantly to any of the environmental conditions. At the fascicle level this indicates that the saline solutions utilized in this study had no osmotic effect on the tissue, which is in contrast to previous reports using

solutions with sucrose or polyethylene glycol (5,9). At the fibril level, it has previously been shown by x-ray methods that in cornea the molecular spacing, which is assumed to be proportional to fibril diameter, decreases with increasing environmental ionic strength (36), which is in contrast to the present results. However, the reported decrease going from an ionic strength of 0.03 μm to 1 μm was only ~4%, which is on the order of our measuring uncertainty estimated to be ~3% from trials using only PBS150. This effect may thus have been too small to detect in this study. For the fibril height, this work agrees well with recent findings by Grant et al. (15), who also reported a lack of changes when adding 1 M KCl at either pH 7 or pH 5.

Modulus

For fascicles, the modulus was unaffected by any of the environmental conditions; however, for fibrils, the modulus increased in HEPES compared to PBS150. Although statistically significant, the physiological importance is questionable, because the relative increase was only 2.3% and the effect was not significant compared to PBS20 or PBS1000. It should further be noted that the HEPES solution was always introduced after the PBS150, making time a confounder; but because no significant time correlation was found in the PBS solutions (Table 1) this is unlikely to be an important factor. We therefore conclude that the effect of HEPES on fibrils is so small that the tensile modulus of both collagen fibrils and fascicles must be considered practically insensitive to all of the investigated environmental conditions.

Increasing the deformation rate of tensile testing led to an increased modulus in the fibrils but not in the fascicles. The effect was not modulated by solution composition, which indicates that the investigated solutions had no impact on the viscous response. However, other measures of viscoelasticity such as creep may be more sensitive.

Comparing our results at the fibril and fascicle level, it is clear that the modulus we report is much greater for the fibrils than the fascicles (Table 1). A thorough discussion of this matter is beyond the scope of this work, but in brief, the majority of the difference can be accounted for by adjusting for the hydrated diameter of the fibrils (36–38), the volume fraction of fibrils (39), and artifacts leading to reduced modulus when testing fascicles of short length in vitro (40).

Energy dissipation

The other mechanical parameter investigated was the relative energy dissipation, which showed a statistically significant increase in PBS1000 compared to PBS20 for fibrils and to PBS150 for both fascicles and fibrils. For fibrils, there was an absolute increase of ~4% and a trend to increase with osmolarity, although not significant between PBS20 and PBS150. The increase in relative energy dissipation was caused primarily by a reduction in the energy retention during unloading (data not shown). Therefore, if the increase in relative energy dissipation represents a physical effect, a possible mechanism could be stabilization of the deformed state by electrostatic screening, which would reduce the rate of recovery during unloading.

It seems reasonable for the deformed state to be more strongly stabilized by screening than the undeformed state because existing electrostatic interactions would be disrupted by the deformation. For fascicles, the effect was smaller (3.2%), and there was no trend with respect to osmolarity (Fig. 6 C). The less prominent effect in fascicles is expected because fascicles can dissipate energy by interfibrillar mechanisms such as fibril friction and fluid motion through the matrix in addition to that dissipated within the fibrils. This also explains why the magnitude of relative energy dissipation is greater in fascicles than fibrils (Fig. 6 C).

Ca^{2+} did not significantly affect the relative energy dissipation of fibrils, which indicates that the previously reported increase in energy dissipation during nanoindentation and pulling experiments are related to lateral fibril interactions. The fact that this effect is also present on purified collagen (25) suggests that this interaction is mediated by the collagen itself and not other matrix molecules.

Fibril mechanics

Our finding that the tensile modulus of fibrils is not affected by salt concentration (Fig. 6 B) is in sharp contrast to the radial compressive properties reported by Grant et al. (15). In that work, a twofold increase in modulus was reported when adding 1 M salt to a phosphate buffer at pH 7 regardless of cation (NaCl, KCl or NH_4Cl). This effect was further enhanced at pH 5 where the addition of 1 M KCl led to a sevenfold increase in modulus. A number of important differences between the two experiments can explain the discrepancy, one of which is loading geometry. Because dry collagen fibrils swell markedly upon hydration (11,16,36–38), the mechanical properties in the radial direction on hydrated fibrils probably involves a large extent of water displacement between collagen molecules. This would account for the three-orders-of-magnitude reduction in the reported indentation modulus (11). In contrast, fibrils do not swell significantly along their axial direction, and the difference in tensile mechanical properties between dry and hydrated fibrils also appear to be significantly smaller.

Yang et al. (18) found bending moduli in the range 1–3.9 GPa for dry and 0.07–0.17 GPa for hydrated fibrils suspended across a gap, which is a ~10–20-fold decrease upon hydration. Using a tensile method similar to ours, van der Rijt et al. (16) reported a 10-fold decrease from ~5 GPa to ~0.5 GPa, whereas we have observed an ~2–3-fold decrease in fibril tensile modulus upon hydration in pilot studies. The lesser axial sensitivity to hydration would

imply that modulation of the collagen molecule interactions by salts would also have a lesser impact on the axial properties. The reported effect on the compressive modulus was greatly enhanced at pH 5. We therefore performed a similar measurement on a single fibril, and found that the tensile modulus also appeared to be more sensitive to salts at pH 5 than pH 7 (Fig. S1 in the Supporting Material), which suggests that the same mechanisms are in play. However, the effect was much smaller on our sample under tension (~12%) than reported for compression (~600%), and the effect was reduced at greater stress levels (Fig. S2).

Another major difference is the biochemical integrity of the collagen fibrils under investigation. In this work, we used native collagen fibrils from the patellar tendon of a 28-year-old male human, which likely contains a high concentration of mature cross-links. In contrast, Grant et al. (15) used reconstituted Bovine Achilles tendon, which, due to the reconstitution process, would be expected to contain few-to-no mature cross-links; however, immature cross-links may be present (41). The presence and type of cross-links may significantly affect the tensile properties of the fibril (42) by transmitting force between collagen molecules through covalent bonds rather than the noncovalent interactions responsible for fibril self-assembly. Any disruption or strengthening of the noncovalent interactions would therefore be shielded by the cross-links during tensile testing.

This type of reconstituted bovine collagen has previously been used in single fibril tensile experiments by van der Rijt et al. (16) who were able to attain large moduli (~5 GPa) and stresses (~90 MPa) on dry fibrils. However, upon hydration, plastic deformation was reported already at 15 MPa stress, which appears to be in the toe region (Fig. 4 in (16)). This is far less than the ~90 MPa stress reached in this work, which is limited by technical constraints and not plastic deformation of the fibril. Those results indicate that the lack of cross-links in the reconstituted fibrils may lead to reduced yield strength and possibly reduced moduli, although the low value of 0.5 GPa is likely caused by being in the toe and not the linear region. This is in agreement with recent modeling results showing that the primary effect of cross-linking is on the failure mechanics rather than the modulus (43).

It is possible that performing our experiment on reconstituted fibrils would lead to greater salt sensitivity than observed in this work. A small pilot study on the compressive modulus of a few mature human fibrils (Fig. S3) did not demonstrate any significant effect of salts, indicating that they are indeed less sensitive to their saline environment than the reconstituted fibrils. This suggests that fibril cross-linking is the primary cause of the observed differences in response to salts.

Another concern related to cross-linking is the drying of the fibrils, which is necessary for the glue to cure. Drying the fibrils could very well alter their response; however, in

the work by Grant et al. (15) the fibrils were also dried before being rehydrated and tested, indicating that the drying, per se, does not make the fibril insensitive to the ionic environment. It is possible, though, that increased cross-linking of the fibril when it dries (44) could shield the tensile response as mentioned previously.

CONCLUSIONS

Herein we investigated the tensile mechanical properties of individual collagen fibrils and found that they were largely insensitive to environmental salt concentration (20, 150, and 1000 mM PBS), choice of buffer (phosphate versus HEPES) and the presence of calcium. The only systematic effect was a an increase of ~4% in the relative energy dissipation of collagen fibrils in the 1000 mM PBS solution, indicating a stabilizing effect of the high salt concentration on the deformed state of the fibril. For comparison, equivalent measurements were performed on collagen fascicles, which were also largely insensitive to the environmental conditions. The disagreement of this finding with previous findings on the radial compressive mechanics of fibrils underlines the anisotropic nature of collagen and the need to also investigate fibril mechanics under axial tensile load.

SUPPORTING MATERIAL

REFERENCES

1. Fogh-Andersen, N., B. M. Altura, …, O. Siggaard-Andersen. 1995. Composition of interstitial fluid. *Clin. Chem.* 41:1522–1525.

2. Hodgson, T. H. 1938. The chloride content of blood serum and aqueous humor. Its relation to glaucoma and to the formation of intra-ocular fluid. *J. Physiol.* 94:118–123.

3. Åstrand, P.-O., and K. Rodahl. 1986. Textbook of Work Physiology: Physiological Bases of Exercise, 3rd Ed. McGraw-Hill, Singapore.

4. Good, N. E., G. D. Winget, …, R. M. Singh. 1966. Hydrogen ion buffers for biological research. *Biochemistry.* 5:467–477.

5. Lujan, T. J., C. J. Underwood, …, J. A. Weiss. 2009. Contribution of glycosaminoglycans to viscoelastic tensile behavior of human ligament. *J. Appl. Physiol.* 106:423–431.

6. Chimich, D., N. Shrive, …, R. Bray. 1992. Water content alters viscoelastic behavior of the normal adolescent rabbit medial collateral ligament. *J. Biomech.* 25:831–837.

7. Screen, H. R., J. C. Shelton, …, D. A. Lee. 2005. The influence of non-collagenous matrix components on the micromechanical environment of tendon fascicles. *Ann. Biomed. Eng.* 33:1090–1099.

8. Haut, R. C., and A. C. Powlison. 1990. The effects of test environment and cyclic stretching on the failure properties of human patellar tendons. *J. Orthop. Res.* 8:532–540.

9. Hoffman, A. H., D. R. Robichaud, 2nd, …, P. Grigg. 2005. Determining the effect of hydration upon the properties of ligaments using pseudo Gaussian stress stimuli. *J. Biomech.* 38:1636–1642.

10. Thornton, G. M., N. G. Shrive, and C. B. Frank. 2001. Altering ligament water content affects ligament pre-stress and creep behavior. *J. Orthop. Res.* 19:845–851.

11. Grant, C. A., D. J. Brockwell, …, N. H. Thomson. 2008. Effects of hydration on the mechanical response of individual collagen fibrils. *Appl. Phys. Lett.* 92:3902.

12. Atkinson, T. S., B. J. Ewers, and R. C. Haut. 1999. The tensile and stress relaxation responses of human patellar tendon varies with specimen cross-sectional area. *J. Biomech.* 32:907–914.

13. Haut, T. L., and R. C. Haut. 1997. The state of tissue hydration determines the strain-rate-sensitive stiffness of human patellar tendon. *J. Biomech.* 30:79–81.

14. Först, P., F. Werner, and A. Delgado. 2002. On the pressure dependence of the viscosity of aqueous sugar solutions. *Rheol. Acta.* 41:369–374.

15. Grant, C. A., D. J. Brockwell, …, N. H. Thomson. 2009. Tuning the elastic modulus of hydrated collagen fibrils. *Biophys. J.* 97:2985–2992.

16. van der Rijt, J. A. J., K. O. van der Werf, …, J. Feijen. 2006. Micromechanical testing of individual collagen fibrils. *Macromol. Biosci.* 6:697–702.

17. Shen, Z. L., M. R. Dodge, …, S. J. Eppell. 2008. Stress-strain experiments on individual collagen fibrils. *Biophys. J.* 95:3956–3963.

18. Yang, L., K. O. van der Werf, …, J. Feijen. 2008. Mechanical properties of native and cross-linked type I collagen fibrils. *Biophys. J.* 94:2204–2211.

19. Screen, H. R. C., D. A. Lee, …, J. C. Shelton. 2004. An investigation into the effects of the hierarchical structure of tendon fascicles on micromechanical properties. *Proc. Inst. Mech. Eng. H–J. Eng. Med.* 218:109–119.

20. Screen, H. R. C. 2008. Investigating load relaxation mechanics in tendon. *J. Mech. Behav. Biomed. Mater.* 1:51–58.

21. Craig, A. S., M. J. Birtles, …, D. A. Parry. 1989. An estimate of the mean length of collagen fibrils in rat tail-tendon as a function of age. *Connect. Tissue Res.* 19:51–62.

22. Provenzano, P. P., and R. Vanderby, Jr. 2006. Collagen fibril morphology and organization: implications for force transmission in ligament and tendon. *Matrix Biol.* 25:71–84.

23. Birk, D. E., M. V. Nurminskaya, and E. I. Zycband. 1995. Collagen fibrillogenesis in situ: fibril segments undergo post-depositional modifications resulting in linear and lateral growth during matrix development. *Dev. Dyn.* 202:229–243.

24. Fantner, G. E., T. Hassenkam, …, P. K. Hansma. 2005. Sacrificial bonds and hidden length dissipate energy as mineralized fibrils separate during bone fracture. *Nat. Mater.* 4:612–616.

25. Thompson, J. B., J. H. Kindt, …, P. K. Hansma. 2001. Bone indentation recovery time correlates with bond reforming time. *Nature.* 414:773–776.

26. Matthews, L. S., and D. Ellis. 1968. Viscoelastic properties of cat tendon: effects of time after death and preservation by freezing. *J. Biomech.* 1:65–71.

27. Giannini, S., R. Buda, …, A. Ruggeri. 2008. Effects of freezing on the biomechanical and structural properties of human posterior tibial tendons. *Int. Orthop.* 32:145–151.

28. Moon, D. K., S. L. Y. Woo, …, S. D. Abramowitch. 2006. The effects of refreezing on the viscoelastic and tensile properties of ligaments. *J. Biomech.* 39:1153–1157.

29. Ng, B. H., S. M. Chou, …, A. Chong. 2005. The changes in the tensile properties of tendons after freeze storage in saline solution. *Proc. Inst. Mech. Eng. H–J. Eng. Med.* 219:387–392.

30. Woo, S. L. Y., C. A. Orlando, …, W. H. Akeson. 1986. Effects of post-mortem storage by freezing on ligament tensile behavior. *J. Biomech.* 19:399–404.

31. Hutter, J. L., and J. Bechhoefer. 1993. Calibration of atomic-force microscope tips. *Rev. Sci. Instrum.* 64:1868–1873.

32. Yamamoto, E., K. Hayashi, and N. Yamamoto. 1999. Mechanical properties of collagen fascicles from the rabbit patellar tendon. *J. Biomech. Eng.* 121:124–131.

33. Svensson, R. B., T. Hassenkam, …, S. Peter Magnusson. 2010. Viscoelastic behavior of discrete human collagen fibrils. *J. Mech. Behav. Biomed. Mater.* 3:112–115.

34. Kongsgaard, M., K. Qvortrup, …, S. P. Magnusson. 2010. Fibril morphology and tendon mechanical properties in patellar tendinopathy: effects of heavy slow resistance training. *Am. J. Sports Med.* 38:749–756.

35. Gutsmann, T., T. Hassenkam, …, P. K. Hansma. 2005. Sacrificial bonds in polymer brushes from rat tail tendon functioning as nanoscale Velcro. *Biophys. J.* 89:536–542.

36. Huang, Y. F., and K. M. Meek. 1999. Swelling studies on the cornea and sclera: the effects of pH and ionic strength. *Biophys. J.* 77:1655–1665.

37. Meek, K. M., N. J. Fullwood, …, C. R. Worthington. 1991. Synchrotron x-ray diffraction studies of the cornea, with implications for stromal hydration. *Biophys. J.* 60:467–474.

38. Sasaki, N., S. Shiwa, …, K. Hikichi. 1983. X-ray diffraction studies on the structure of hydrated collagen. *Biopolymers.* 22:2539–2547.

39. Hansen, P., B. T. Haraldsson, …, S. Peter Magnusson. 2010. Lower strength of the human posterior patellar tendon seems unrelated to mature collagen cross-linking and fibril morphology. *J. Appl. Physiol.* 108:47–52.

40. Haut, R. C. 1986. The influence of specimen length on the tensile failure properties of tendon collagen. *J. Biomech.* 19:951–955.

41. Tanzer, M. L. 1968. Intermolecular cross-links in reconstituted collagen fibrils. Evidence for the nature of the covalent bonds. *J. Biol. Chem.* 243:4045–4054.

42. Bailey, A. J., R. G. Paul, and L. Knott. 1998. Mechanisms of maturation and ageing of collagen. *Mech. Ageing Dev.* 106:1–56.

43. Buehler, M. J. 2008. Nanomechanics of collagen fibrils under varying cross-link densities: atomistic and continuum studies. *J. Mech. Behav. Biomed. Mater.* 1:59–67.

44. Silver, F. H., D. L. Christiansen, …, Y. Chen. 2000. Role of storage on changes in the mechanical properties of tendon and self-assembled collagen fibers. *Connect. Tissue Res.* 41:155–164.

45. Magnusson, S. P., H. Langberg, and M. Kjaer. 2010. The pathogenesis of tendinopathy: balancing the response to loading. *Nat. Rev. Rheumatol.* 6:262–268.

"Tensile properties of human collagen fibrils and fascicles are insensitive to environmental salts"
René B. Svensson, Tue Hassenkam, Colin A. Grant, S. Peter Magnusson

Effect of low pH on single fibril tensile modulus
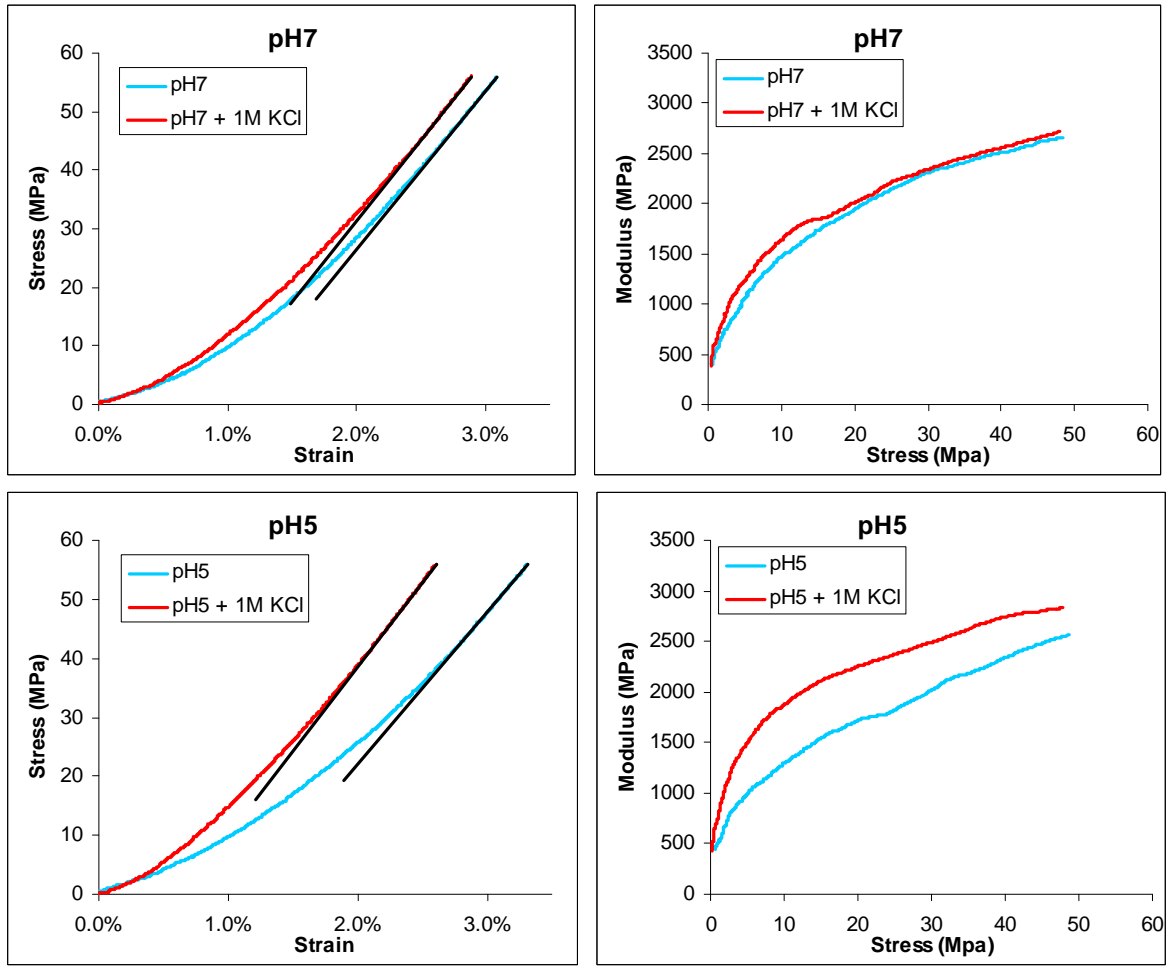
	Modulus (GPa)
pH7	2.69
pH7 + 1M KCl	2.80
pH5	2.57
pH5 + 1M KCl	2.89

FIGURE S1 Tensile tests on a single fibril in pH7 (sodium phosphate) and pH5 (potassium acetate) buffers, showing the effect of 1 M KCl in each of these buffers. The figures in the left column show stress-strain curves, and the figures in the right column display how the modulus increases along the curve. Black lines are linear fits used to determine modulus. The modulus values are shown in the table.

Reduced effect of pH and salt at higher force
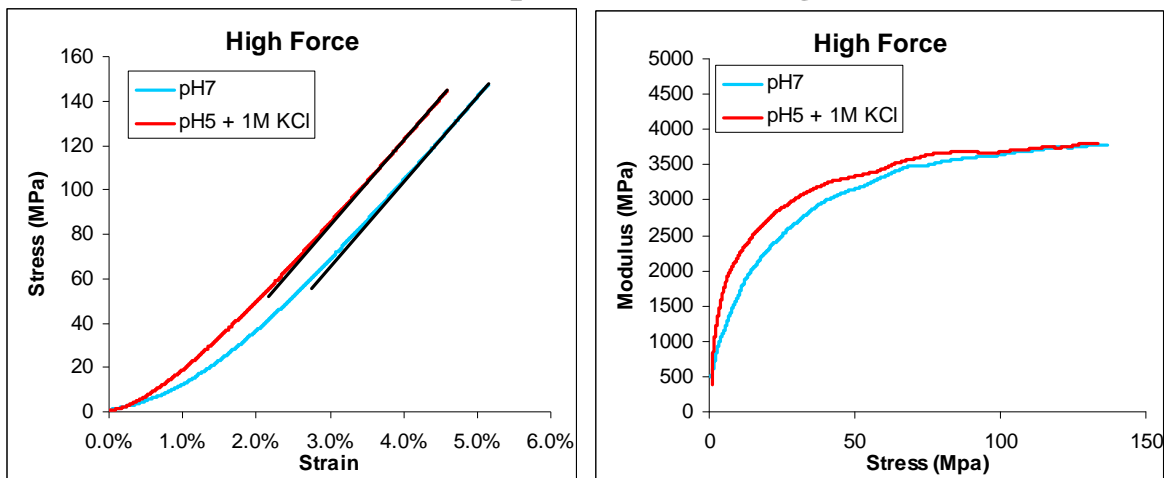
	Modulus (GPa)
pH7 *High Force*	3.82
pH5 + 1M KCl *High Force*	3.81

FIGURE S2 In the same experiment as shown in Fig. S1, measurements were also made to a greater force in the pH7 sodium phosphate buffer and pH5 potassium acetate buffer containing 1M KCl, which were the two conditions differing most in compressive modulus on reconstituted fibrils (1). It can be seen that the difference in modulus is greatest at low stress and drops off at greater stress values. The black lines indicate linear fits used to determine the modulus values in the table.

Compression testing on adult human fibrils
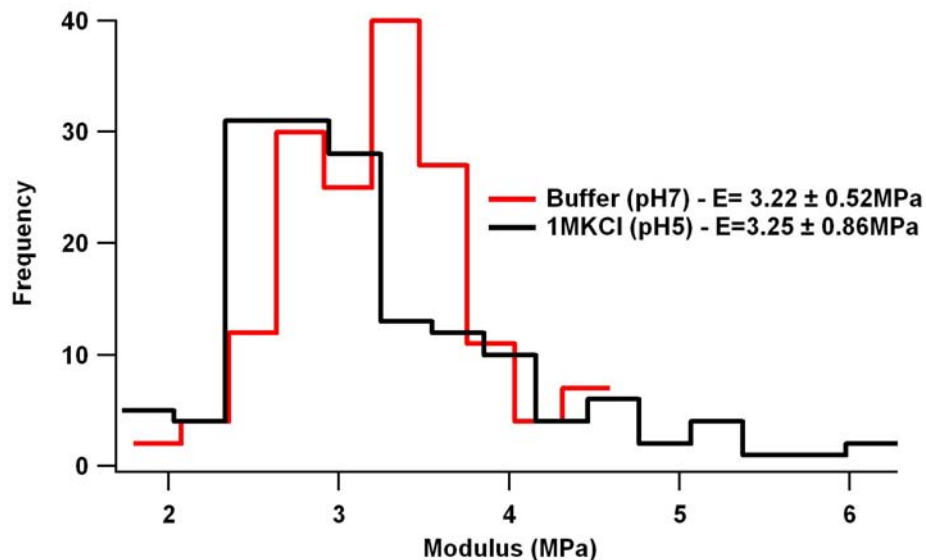
FIGURE S3 Histogram of compressive moduli from a large number of indentations on fibrils from mature human tendon. Measurements were made in pH7 sodium phosphate buffer (red) and pH5 potassium acetate buffer containing 1M KCl (black), which were the two conditions differing most in modulus on reconstituted fibrils (1). As can be seen, the 1M KCl at pH5 did not lead to increased modulus.

SUPPLEMENTARY REFERENCES

1.   Grant, C. A., D. J. Brockwell, S. E. Radford, and N. H. Thomson. 2009. Tuning the elastic modulus of hydrated collagen fibrils. Biophys. J. 97:2985-2992.

Study 3

Mechanical properties of human patellar tendon at the hierarchical levels of tendon and fibril

René B. Svensson,[1,2] Philip Hansen,[1] Tue Hassenkam,[2] Bjarki T. Haraldsson,[1] Per Aagaard,[3] Vuokko Kovanen,[4] Michael Krogsgaard,[5] Michael Kjaer,[1] and S. Peter Magnusson[1]

[1]*Faculty of Health Sciences, Institute of Sports Medicine Copenhagen, Bispebjerg Hospital & Center for Healthy Aging, University of Copenhagen, Copenhagen;* [2]*Nano-Science Center, University of Copenhagen, Copenhagen;* [3]*Institute of Sports Science and Clinical Biomechanics, University of Southern Denmark, Odense;* [5]*Department of Orthopedic Surgery, Bispebjerg Hospital, Copenhagen, Denmark; and* [4]*Biochemistry Laboratory, Department of Health Sciences, University of Jyväskylä, Jyväskylä, Finland*

Svensson RB, Hansen P, Hassenkam T, Haraldsson BT, Aagaard P, Kovanen V, Krogsgaard M, Kjaer M, Magnusson SP. Mechanical properties of human patellar tendon at the hierarchical levels of tendon and fibril. *J Appl Physiol* 112: 419–426, 2012. First published November 23, 2011; doi:10.1152/japplphysiol.01172.2011.—Tendons are strong hierarchical structures, but how tensile forces are transmitted between different levels remains incompletely understood. Collagen fibrils are thought to be primary determinants of whole tendon properties, and therefore we hypothesized that the whole human patellar tendon and its distinct collagen fibrils would display similar mechanical properties. Human patellar tendons ($n = 5$) were mechanically tested in vivo by ultrasonography. Biopsies were obtained from each tendon, and individual collagen fibrils were dissected and tested mechanically by atomic force microscopy. The Young's modulus was 2.0 ± 0.5 GPa, and the toe region reached $3.3 \pm 1.9\%$ strain in whole patellar tendons. Based on dry cross-sectional area, the Young's modulus of isolated collagen fibrils was 2.8 ± 0.3 GPa, and the toe region reached $0.86 \pm 0.08\%$ strain. The measured fibril modulus was insufficient to account for the modulus of the tendon in vivo when fibril content in the tendon was accounted for. Thus, our original hypothesis was not supported, although the in vitro fibril modulus corresponded well with reported in vitro tendon values. This correspondence together with the fibril modulus not being greater than that of tendon supports that fibrillar rather than interfibrillar properties govern the subfailure tendon response, making the fibrillar level a meaningful target of intervention. The lower modulus found in vitro suggests a possible adverse effect of removing the tissue from its natural environment. In addition to the primary work comparing the two hierarchical levels, we also verified the existence of viscoelastic behavior in isolated human collagen fibrils.

atomic force microscopy; collagen; fibril dimensions; modulus; toe region

TENDON TISSUE PLAYS AN ESSENTIAL role in transmitting contractile forces to bone to generate movement and is therefore uniquely designed to resist sizeable loads (up to ~8 times body wt) during human locomotion (16, 22). However, despite this inherent quality, both overuse injuries and complete tendon ruptures occur. The precise mechanism(s) for tendon injuries remains unknown, but it is possible that there are one or more "weak links" in the tendon structure (36).

Tendon is regarded a biological composite with collagen fibrils embedded in a ground substance of primarily proteoglycans and water (45). The collagen fibril is considered the basic force-transmitting unit of tendon, although its specific importance compared with other matrix components is yet to be firmly established (41, 42, 44, 45). Fibrils are made up of tropocollagen molecules arranged in a quarter-staggered manner as described by the Hodge-Petruska model (43) and are held together by intermolecular cross-links. However, exact knowledge of how forces are transferred through the tendon structure remains to be determined. It has been suggested that fibrils are continuous throughout the length of the tendon (13, 44), which would imply similar strains at the fibril and tendon level. On the other hand, other results support a discontinuous fibril model, in which case force transfer must occur between neighboring fibrils (19, 38, 45). Discontinuous fibrils would allow the strain of tendons to exceed that of the lower levels of the hierarchy (19) and enable fibril stiffness to exceed tendon stiffness. If fibrils are much stiffer than tendons then the majority of deformation takes place between fibrils, and fibril quality becomes less important for the overall tendon response than the quality of the interfibrillar matrix. In contrast, if fibrils have similar stiffness to tendons, interfibrillar deformation is small, and the quality of fibrils dominates tendon properties.

Few available studies have attempted to directly compare tendon mechanical properties at different hierarchical levels, and, to the best of our knowledge, none have done so in a human model. Sasaki and Odajima (48) reported the tangent modulus of the collagen molecule > fibril > tendon. In contrast, An et al. (1) summarized mechanical data from the existing literature and showed the modulus of procollagen molecules < collagen fiber < collagen fascicle < tendon. These conflicting observations leave questions regarding the mechanical properties of individual structural levels of tendon and the force transmission between these levels unanswered. Previous attempts to compare different hierarchical levels of tendon may have been hampered due to distinctions between phenotype, species, age, gender, and loading history of the examined tendons (4) in addition to methodological issues of mechanical testing (9).

Ultrasonography-based measurement of tendon properties has proven an attractive noninvasive technique of assessing human whole tendon behavior in vivo (32, 34, 35). This methodology has allowed for characterization of in vivo human patellar tendon mechanical properties (26), and the technique has been widely applied to examine tendon adaptation to aging

Address for reprint requests and other correspondence: R. B. Svensson, Institute of Sports Medicine Copenhagen, Bispebjerg Hospital, Bldg. 8, 1. Floor, Bispebjerg Bakke 23, 2400 Copenhagen NV, Denmark (e-mail: svensson.nano@gmail.com).
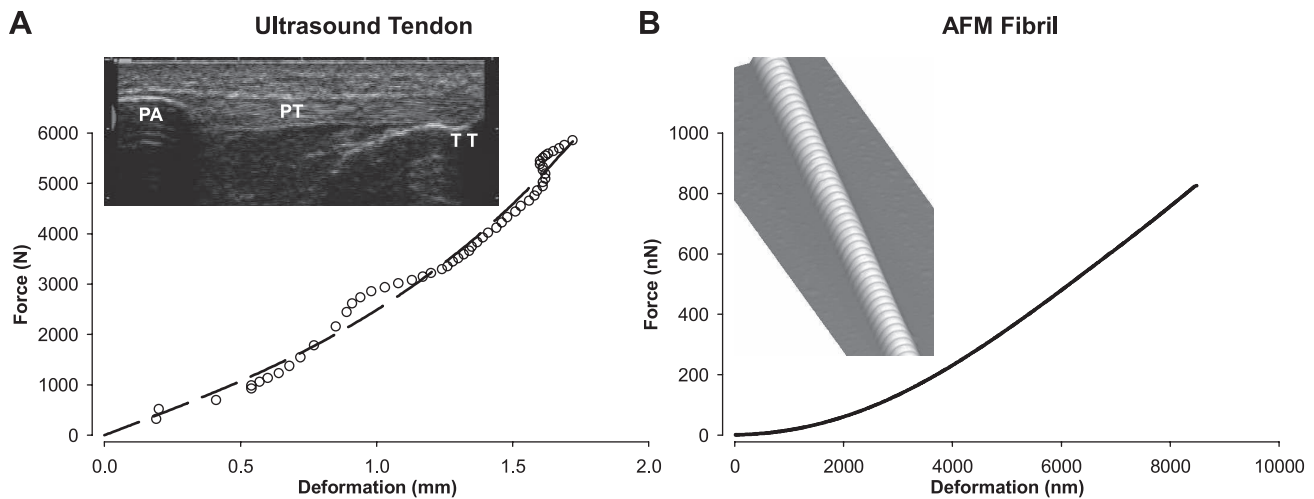
Fig. 1. Representative graphs illustrating force-deformation data for a patellar tendon and fibril. *A*: force-deformation data obtained by ultrasonography on a human patellar tendon (for clarity, only every 3rd point is displayed). *Inset* shows untrasound image used for determining deformation. The following three points of interest are indicated: the patella (PA), patellar tendon (PT), and tibial tuberosity (TT). Data were fitted to a 3rd-order polynomial (black dashed line). *B*: force-deformation data from a patellar tendon fibril obtained by atomic force microscopy (AFM). *Inset* shows a three-dimensional AFM height image of the fibril with the characteristic banding pattern. The graph represents actual data points without a fit.

and habitual loading among others (28, 33, 39, 47). For ex vivo testing of human tendon substructures, microtensile devices have been applied to describe the behavior of tendon fascicles (29, 58). Tests at the fibril level have recently also become possible using, for example, atomic force microscopy (AFM) to measure the mechanical properties of individual collagen fibrils by various experimental approaches (55, 57, 60).

To date, no studies have attempted to compare in vivo whole tendon properties with properties of lower-level hierarchical structures within the same individual. In the present study, we applied the AFM and ultrasonography methodologies to investigate and compare the hierarchical mechanical properties of *1*) whole patellar tendon in vivo and *2*) isolated collagen fibrils in vitro from the same healthy human subjects. We hypothesized that the two distinct structural levels would display similar mechanical properties.

MATERIALS AND METHODS

Subjects

Five males (age: 32 ± 7 yr; weight: 90 ± 11 kg; height: 183 ± 6 cm; body mass index: 26.7 kg/m^2) participated in the study. Subjects were scheduled for elective reconstructive surgery of the anterior cruciate ligament (ACL) and were otherwise healthy. At the time of elective surgery, which was 4–6 mo postinjury, the patients had normal range of knee joint motion, no joint swelling, and were not impaired during normal activities of daily living but were unable to participate in sports activities due to knee instability. Before surgery, they underwent rehabilitation to restore normal thigh strength, and therefore the tendons did not suffer from disuse. All subjects gave their informed consent before inclusion in the study. Approval of the study was obtained from the local Ethics Committee.

In Vivo Tendon Testing

Tendon mechanics. All measurements were performed less than one month before ACL reconstruction. Subjects were seated in a custom-made rigid chair with both hips and knees flexed to an angle of 90°. A load cell (Bofors KRG-4; Bofors) was connected perpendicularly to the lower leg 1–2 cm above the medial malleolus via a leg cuff and a rigid steel rod. An ultrasound probe was fitted into a

custom-made case and secured to the skin above the patellar tendon in the sagittal plane. The ultrasound probe was positioned such that the patella apex, the patellar tendon, and the tibial tuberosity were all visible within the viewing field throughout the ramp contractions (Fig. 1). Synchronous sampling of ultrasound video images and force was obtained by using a custom-built trigger device (7). The subjects performed four to five slow isometric knee extension ramps by applying gradually increasing force up to their maximum over a 10-s period. All measurements were performed on the injured side knee. Ultrasound video was recorded at 50 Hz using frame-by-frame capture software (G400-TV; Matrox Marvel, Dorval, Canada). Force was also sampled at 50 Hz, and the force signal was low pass filtered at a 1.0-Hz cutoff frequency using a fourth-order zero-lag Butterworth filter. Tendon deformation was defined as the change in distance between the patellar apex and the tibia. The deformation was measured by custom tracking software implementing the Lucas-Kanade algorithm, which has been validated previously (26, 35).

Tendon dimensions. Patellar tendon cross-sectional area (CSA) and length were determined by magnetic resonance imaging (MRI) (General Electric, Sigma Horizon LX 1.5 Tesla, T1 weighted SE) (Fig. 2), as previously described (33). In brief, tendon CSA was measured by axial-plane MRI perpendicular to the tendon at the proximal (just
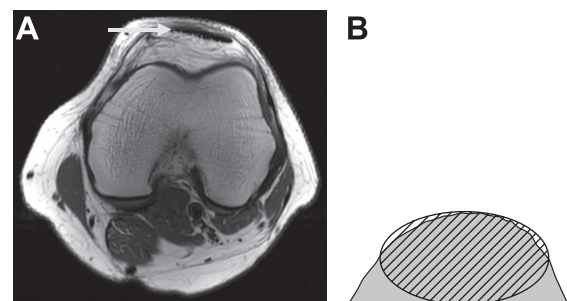
Fig. 2. *A*: axial magnetic resonance imaging of the human patellar tendon (arrow). Patellar tendon cross-sectional area was determined from axial images while tendon length was measured from similar images obtained by sagittal plane scans. *B*: fibril cross section and illustration of the two methods for determining cross-sectional area. The gray area is obtained by integrating the entire cross section, whereas the slashed ellipse is formed with one axis equal to the height and the other equal to the width at half the height.

distal to the patellar bone), mid, and distal (just proximal to the tibial tuberosity) parts of the tendon, and the average value was used for stress calculation. Reproducibility data showed that the typical error percent of repeated measures of tendon CSA was 2.5%. Patellar tendon length was determined from sagittal plane MRI as the distance from the dorsal insertion at the patella apex to the dorsal insertion on the tibia.

Tendon biopsies. During ACL reconstructive surgery, a small tendon sample was taken from the patellar tendon ACL graft of each patient. A thin tendon fiber bundle containing ~10 fascicles was obtained from the anterior aspect and mid one-third of the tendon. The biopsies were then wrapped in sterile gauze moistened by 0.15 M phosphate-buffered saline (PBS) and stored at −20°C. Storage at −20°C in PBS has been reported not to affect mechanical properties (23), which is in agreement with our own unpublished data on fascicles.

Single Collagen Fibril Testing

Sample preparation. Mechanical testing of collagen fibrils (Fig. 1) was performed using a recently described method (55). Two fibrils were tested from each subject. Briefly, small droplets of epoxy glue (DANA LIM Blå Epoxy 335) were deposited ~200 μm apart on a secluded dry collagen fibril (Fig. 3) and cured overnight. The dry fibril was imaged by tapping-mode AFM to determine CSA and ensure structural integrity. One glue droplet was then detached from the substrate using a sharp AFM tip. The detached glue patch was attached with fresh epoxy to another AFM cantilever ($k_{spring} \sim 0.42$ N/m) in such a way that the fibril was sandwiched between the cantilever and the glue patch. The epoxy cured overnight before the fibril was mechanically tested in 0.15 M PBS using a PicoForce AFM scanner (55).

Fibril mechanics. Collagen fibril testing was performed by continuously ramping the sample-cantilever distance. The ramp distance is the sum of fibril deformation and cantilever bending. Fibril deformation was targeted at 4% strain, and cantilever bending was assumed to be 1 μm when selecting the ramp distance. Because actual cantilever bending differed from 1 μm, peak strains also differ from 4%. Data were acquired in a piecewise manner by physically moving the detector as previously described (55). For this method to work, it is necessary that a mechanical equilibrium is reached, which was achieved by continuous ramping for at least 1 min before starting data

Fig. 3. Optical image of a secluded fibril from a human patellar tendon. The fibril has been glued to the surface by two glue droplets placed ~ 200 μm apart.

acquisition. For repeated measurements within an experiment, the modulus had a coefficient of variation below 2%.

Viscoelasticity. To verify the effect of strain rate that we previously reported, mechanical tests were made at different strain rates (9.81, 19.6, 39.2, 78.5, 157, and 314 μm/s), and a stepwise stress relaxation test ("0" μm/s) was also performed as described previously (55). The order in which strain rates were applied varied between experiments. Only the fibril test at 9.81 μm/s was used for comparison with whole tendon properties, since this strain rate (~5%/s) corresponded most closely to that of the in vivo tendon test (~0.6%/s).

Fibril dimensions. The length of fibril between the two initial glue droplets was measured by optical microscopy. In addition, the distance moved with the AFM in the *z* direction to stretch the fibril was determined. The two measures were in good agreement, and the average value was used (mean difference = 3.25 μm). CSA was determined from AFM images. Side angles in AFM cross sections of fibrils were often smaller than expected for tip convolution, and fibril flattening was observed. For this reason, fibril CSA was calculated as the average of *1*) the integrated area under the fibril contour and *2*) the area of an ellipse with one diameter equal to the fibril height and the other equal to the width at half the height (Fig. 2). *Method 1* yielded CSA 20% larger than *method 2*.

Biochemical Analyses

Measurements of collagen and collagen cross-link concentrations were performed as previously reported (27). Briefly, the collagen specific amino acid, hydroxyproline, was measured spectrophotometrically (14) and used for calculating the amount of collagen protein and expressed as a fraction of the dry mass (wt/wt). Hydroxylysylpyridinoline (HP), lysylpyridinoline (LP), and pentosidine (PENT) cross-links of collagen were separated via a single reversed-phase high-performance liquid chromatography (HPLC) run (3) and detected by their natural fluorescence. The HPLC determination of cross-link concentrations in the samples was based on the use of pure HP, LP, and PENT compounds with known concentrations as external standards. The concentrations of the cross-links are expressed as mole per mole of collagen.

Data Reduction and Statistical Analysis

Hierarchy comparison. Ultrasound tendon stress-strain data were analyzed to a greatest common stress for each subject. To reduce noise, each curve was fitted using a third-order polynomial ($r^2 > 0.97$ in all cases) (Fig. 1). No noise was observed for fibrils; therefore, the raw data rather than a fitted curve were used. Dry fibril CSA was used for calculation of fibril stress because it is simpler to measure and is not affected by the tapping force during tapping-mode AFM imaging (see DISCUSSION for further details). Because the stress-strain relation becomes more linear at higher stress, Young's modulus was determined by linear regression to the final 20% stress for both tendons and fibrils.

To evaluate the nonlinear properties of fibrils compared with whole tendon, the length of the toe region was evaluated by extrapolating the linear region onto the strain axis:

$$\text{toe length} = \varepsilon - (\sigma/E)$$

where ϵ and σ are the maximal strain and stress, respectively, and *E* is the modulus. Two-tailed Student's paired *t*-tests were used to examine if fibril and whole tendon mechanical parameters differed. An α level of 0.05 was considered significant. Results are reported as group means ± SD unless otherwise stated.

Fibril viscoelasticity. The effect of strain rate on fibril modulus was analyzed as previously reported (55) by subtracting the stepwise stress-relaxation curve from the dynamic curves to obtain the viscous component of the response. The force onset moved to higher strain with increased strain rate and time. The residual strain responsible for the shift in onset probably represents an increased molecular align-
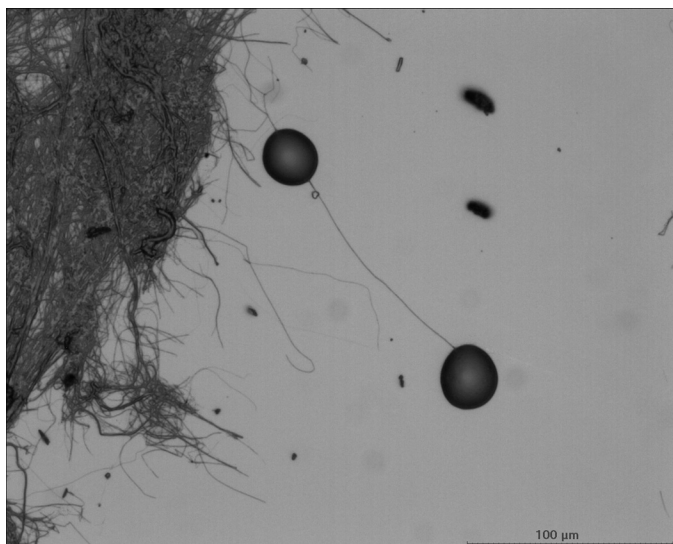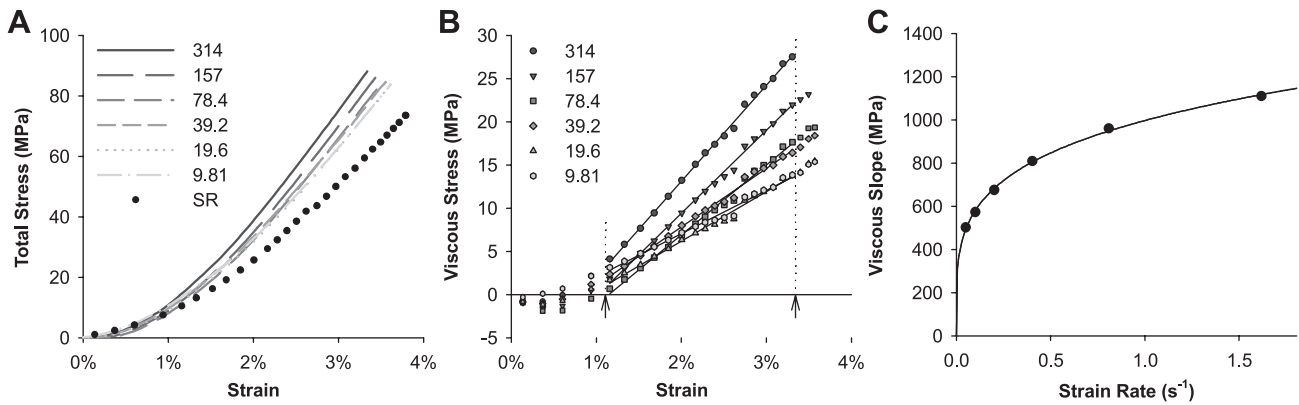
Fig. 4. Example of single fibril viscoelasticity analysis. *A*: stress-strain response of a single fibril loaded dynamically at rates from 9.81 to 314 μm/s and a "zero" rate by stepwise stress relaxation (SR). *B*: viscous stress-strain response obtained by subtracting SR data from the dynamic data. Linear fits made in the range indicated by arrows are shown as black lines. *C*: slope of the linear fits plotted against strain rate. The data are fitted with a power function (black line).

ment. We used the onset of the stepwise stress-relaxation curve for all curves in each experiment and thereby maintained their relative shifts. Because the viscous component becomes negative in the regions of residual strain, we only made linear regression within the strain range where all curves demonstrated positive viscous components (Fig. 4*B*).

RESULTS

Mechanical Characteristics

The main focus of this study was to compare mechanical properties at the fibril and whole tendon hierarchical levels. In Table 1, the sample characteristics at each level of the hierarchy are summarized. The measured values of modulus and toe length are shown in Fig. 5. The mean value of the modulus was 2.0 ± 0.5 GPa for the whole tendon and 2.8 ± 0.3 GPa for the fibril. The mean length of the toe region was 3.3 ± 1.9% for tendons and 0.86 ± 0.08% for fibrils.

Correlating the modulus of fibrils with that of their parent tendons, there was a tendency for increased fibril modulus with increasing tendon modulus albeit the correlation failed to reach significance ($r^2 = 0.59$, $P = 0.13$). There was no correlation between toe region length at the fibril and tendon levels ($r^2 = 0.01$, $P = 0.87$). The absolute modulus at the two hierarchical levels is not directly comparable; see the DISCUSSION for details.

Fibril testing achieved 2.5% lower maximal strain than the whole tendon because of limitations in maximum measurable force with our current AFM setup. However, the toe region at the fibril level was 2.4% shorter than at the tendon level ($P = 0.04$). Subtracting the toe region from the maximum strain, the length of the linear region was similar at the two levels, namely 2.8% for tendons and 2.7% for fibrils.

Table 1. *Structural and mechanical properties*

	Tendon In Vivo	Fibril In Vitro
Length	44 ± 4 mm	200 ± 10 μm
Cross-sectional area	97 ± 10 mm^2	14000 ± 4000 nm^2
Maximum test force	5.6 ± 0.6 kN	1.1 ± 0.3 μN
Maximum test stress	54 ± 9 MPa	76 ± 11 MPa
Maximum test deformation	2.7 ± 0.7 mm	7.0 ± 0.7 μm
Maximum test strain	6.1 ± 1.5%	3.6 ± 0.3%

Values are means ± SD. For fibrils, the length is the tested rather than total length. For fibrils, dry cross-sectional area is reported.

Although the tested fibril length was only ~200 μm, the visible length of fibrils was often >500 μm, and, on occasion, fibrils could be followed for up to 1 mm in the optical microscope. We never observed any split or fused fibrils.

Effect of Strain Rate

The Young's modulus for fibrils increased with rising deformation rate (Fig. 4*A*), and the viscous component shows a linear strain dependency (Fig. 4*B*). We also observe that the slope of the viscous component vs. strain (η) increased with strain rate (ν) following a power function (Fig. 4*C*), in agreement with our previous findings (55).

$$\eta = a \times \nu^b$$

The parameters of the power function were determined by a repeated-measures linear ANOVA on log(η) vs. log(ν) with the testing order as covariate. The effect of order was not significant ($P = 0.90$), but the rate effect was highly significant ($P < 0.001$) with $a = 710$ (600–840) MPa·s^b and $b = 0.23$ (0.22–0.24) [mean (95% confidence interval)]. The *b* value below one is in agreement with the behavior we previously reported indicating shear-thinning properties (55).

Biochemical Results

The mean collagen content was 64 ± 7% of the dry mass. The mean content of cross-links in the tendons were as follows: HP: 0.81 ± 0.23 mol/mol, LP: 0.020 ± 0.006 mol/mol, and PENT: 0.022 ± 0.008 mol/mol. There was a strong positive correlation between PENT and age ($r^2 = 0.91$, $P = 0.01$). Neither HP, LP, nor PENT correlated significantly with Young's modulus or toe length at either the tendon or the fibril level.

DISCUSSION

Young's Modulus

Hierarchical comparison. To compare fibrils and native tendons, it is necessary to determine how much of the tendon is actually made up of fibrils, e.g., identifying the effective CSA (Fig. 6). One way to do this would be to assume that the fraction is equal to the mass fraction of collagen, which is 64% of the total dry mass, which in turn is ~35% of the native
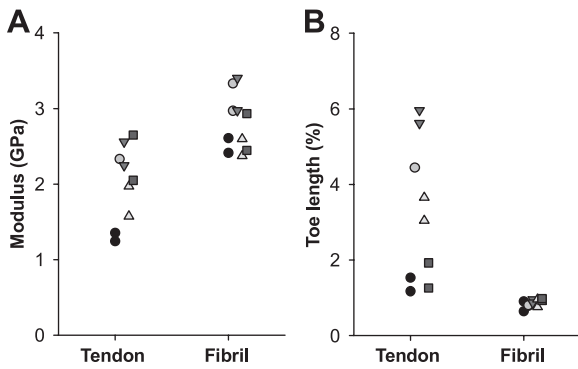
Fig. 5. Measured values of modulus (*A*) and toe region length (*B*) at the tendon and fibril levels. Data points with the same style are from the same subject. Data points are shifted along the *x*-axis for clarity.

hydrated tendon mass (10, 56). This gives a total dry collagen content in native tendon of 22%, and, assuming that fibrils are the only major tensile-bearing units, a fibril Young's modulus of 2.8 GPa using dry CSA would predict a tendon Young's modulus of 0.6 GPa. Another approach would be to account for the volume fraction of hydrated fibrils in the tendon and the fibril swelling upon hydration. Volume fraction assessed by electron microscopy is ~60% (27). Reported values of fibril swelling vary depending on measuring method. AFM measurements have generally found swelling of 50–100% in fibril diameter (24, 30, 57), whereas X-ray methods have found values of 30–40% (37, 49). This approach would predict a tendon Young's modulus in the range 0.4–1.0 GPa depending on the magnitude of swelling.

The cause of the difference in swelling between AFM and X-ray measurements is unknown. It is possible that swelling in AFM is affected by surface proteoglycans; however, in a small pilot study on chondroitinase-ABC-treated fibrils, we saw no significant reduction in swelling. We observed that dry fibrils are flattened onto the substrate surface, and, upon hydration, this flattening may disappear. This would cause an additional increase in fibril height, leading to an overestimated swelling since the height is generally used to measure sizes in AFM due to tip convolution in the sample plane. Although the exact reason for the difference in swelling is unknown, it is our opinion that overestimation of fibril swelling in AFM is more likely than underestimation with the X-ray method, especially when the intention is to measure swelling in the bulk tendon.

Regardless of the method chosen, it is clear that the measured fibril Young's modulus, when adjusted for hydration and volume fraction, predicts much lower tendon Young's modulus than the 2.0 GPa that was measured (Fig. 6). Here the ~40% volume fraction of extrafibrillar matrix was assumed to not contribute to the tendon modulus, which we believe is a reasonable assumption. If the extrafibrillar matrix was to account for the difference in modulus between tendon and fibrils, it should have a modulus of 1.8–4 GPa (by the rule of mixtures), which is unreasonably high.

Methodological considerations. It is interesting to notice that the tendon Young's modulus predicted from the fibril Young's modulus falls in the same range as most in vitro studies of human patellar tendon, which ranges from 0.3 to 1 GPa (2, 9, 11, 29). By comparison, in vivo studies similar to the present work have generally yielded greater modulus val-

ues in the range of 0.8–2.2 GPa (6, 12, 40, 47). For the in vitro moduli, technical issues with gripping can cause an underestimated modulus; however, studies gripping on the natural bone insertions and measuring local deformation in the central part, thus largely precluding the gripping issues, still find moduli far below 2 GPa (2, 9). Gripping is also an issue in the fibril measurements, and preliminary results (data not shown) using fibrils of varying length suggest that the modulus is underestimated by ~15%, which is insufficient to account for the observed difference. For the in vivo measurements, an overestimated modulus could arise from underestimating the CSA, and our preliminary work indicates that this may occur if the surrounding areas have high MRI intensity, but this is not the case for human patellar tendon. Accounting for these technical issues may reduce the gap between in vivo and in vitro results but cannot explain the entire difference. This indicates that removing the tendon from its native environment reduces the modulus, even at the fibril level. The nature of this effect is unknown but could be related to interruption of lateral force transmission between collagen molecules (50). It has been reported that tendon has a lower hydration in vivo than in physiological saline in vitro (10, 56), and this could affect mechanical properties. In a recent study, we did not find any influence of environment ionic composition on fibril modulus, suggesting that it may be the change in hydration per se that is responsible for the reduced modulus in vitro (54). An adverse effect of hydration could have implications for optimal handling of tendon grafts as well as tendon injuries where swelling is present.

Other studies have investigated fibril mechanical properties using a range of techniques and tissues, and their findings are partially summarized in Table 2. The present results are the highest reported modulus values from direct measurements, and, as such, there are no current results that are capable of explaining the large stiffness of human patellar tendon in vivo. In Table 2, only the indirect measurements from Brillouin scattering and molecular modeling are in a range
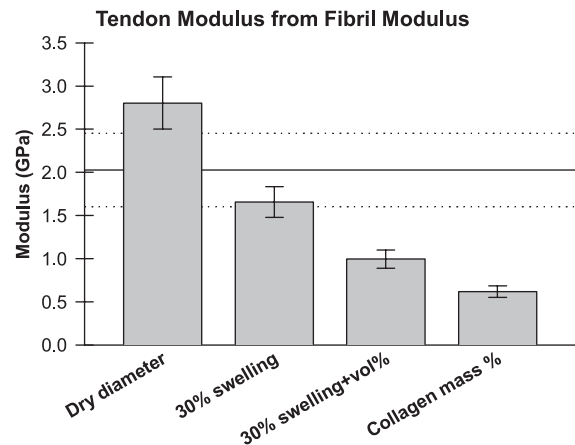
Fig. 6. Comparing modulus at the fibril and tendon level. The bars show the mean modulus of fibrils using the dry diameter, as it would be using a 30% swelled fibril diameter (30% swelling), the predicted tendon modulus using the volume fraction in addition to 30% swelling (30% swelling + vol%), and the predicted tendon modulus using instead the ratio of dry collagen mass to native tendon mass (Collagen mass%). Error bars: 95% confidence intervals. Solid horizontal line is the measured in vivo tendon modulus, and dashed lines are 95% confidence intervals.

Table 2. *Overview of reported fibril Young's moduli*

	Tissue	State	Modulus, GPa	Reference No.
Direct methods				
AFM tensile	Human patellar tendon	PBS immersed	2.8 ± 0.34	Present study
AFM tensile	Bovine achilles	PBS immersed	0.2–0.8	57
MEMS tensile	Sea cucumber dermis	Humid (31–60%)	0.86 ± 0.45 (1.39 ± 0.73)[a]	51
AFM bending	Bovine achilles	PBS immersed	0.07–0.17	59
Indirect methods				
X-ray diffraction	Mineralized turkey tendon	Partially hydrated	0.8–3.4 (0.12–0.52)[b]	25
X-ray diffraction	Bovine achilles	0.15 M NaCl	0.43[c]	48
Brillouin scattering	Rat tail tendon	Partially hydrated	5.1	15
Modeling methods				
Molecular model	None	Fully hydrated	4.36[d]	8
Molecular model	None	Fully hydrated	0.3–1.2[e]	21

AFM, atomic force microscopy; MEMS, micro-electro-mechanical system. [a]Value using a 27% swelling in diameter. In parenthesis is the value using dry diameter. [b]Hydration and volume fraction accounted for. In parenthesis is the "nonmineralized" value. [c]Hydration and volume fraction accounted for. Fibrils from specimen with 0.4 GPa modulus in vitro. [d]Hydration accounted for. A modulus of 38 GPa was predicted beyond ~30% strain. [e]A newer and more advanced model by the same group as the one above.

that could fit the measured tendon modulus, and both techniques evaluate mechanical properties at higher strain rates. Due to viscoelastic behavior of collagen fibrils as shown in the present work and that of indirect (15) and modeling (20) methods, the modulus determined at such high strain rates would be overestimated compared with the fibril and tendon measurements in the present study. In addition, new modeling results using more advanced methods have yielded lower modulus values (Table 2).

Toe Length

It is worth mentioning that, during daily walking activity, the human patellar tendon likely operates in the toe region of the stress-strain curve. Previous studies have described the human knee extensor forces during walking and small-amplitude hopping (5, 17). From these studies, patellar tendon stress during walking would be in the range of 5–15 MPa assuming a tendon CSA of 100 mm^2, which is a reasonable estimate for an average human male (Table 1) (40). During high-intensity jumping, the tendon can reach ~ 40 MPa (16). For comparison, the tendon stress at the end of the toe region was 10 ± 6 MPa in the present work, indicating that tendon operates near the end of the toe region during normal ambulation and operates in the linear region during running and jumping activities. The toe region at the fibril level was significantly shorter than at the tendon level, which is in agreement with X-ray measurements (48) and supports the common belief that the tendon toe region originates in unfolding of macroscopic waviness (crimping) in tendon fiber bundles (31). Crimping can give rise to kinks at the fibril level (18, 46), but we observed no such kinks in the fibrils tested here, possibly because of stretching during sample preparation.

Biochemistry

There was no correlation between any of the measured cross-links and modulus at either the fibril or tendon level. This suggests that even the lower cross-link densities are sufficient to avoid molecular slippage within the tested mechanical range such that additional cross-links have little or no further effect. However, the cross-link density may still affect the maximal stress that can be achieved before fibrils start yielding by molecular slippage (8). To investigate this, testing the fibrils

and tendons to failure would be necessary, which was not possible in the present work. At the fibril level, an additional potential problem is the time requirement of our single fibril technique, which limits the sample size. This is a problem when comparing with a parameter like cross-linking, which is measured in the bulk and likely covers individual fibrils with a range of cross-link concentrations.

Limitations

There are some inherent shortcomings to the present method. First, for technical reasons, the lowest strain rate used in fibril testing was 10-fold higher than for tendons. From the power function for the viscous stress (see RESULTS), we predict that fibrils at a strain rate of 0.5%/s would have 0.15 GPa lower Young's modulus than at 5%/s. This difference is rather small and would only strengthen our conclusions. Second, the lack of statistically significant results for correlation between cross-link concentration and mechanical properties may be explained by the limited sample size due to the unique nature of our material. Third, the period of dehydration required while the epoxy cures could increase the modulus by increased cross-linking (52); however, this does not explain why fibril modulus is too low to account for tendon modulus. Finally, we observed a bias toward large-diameter fibrils because only those visible
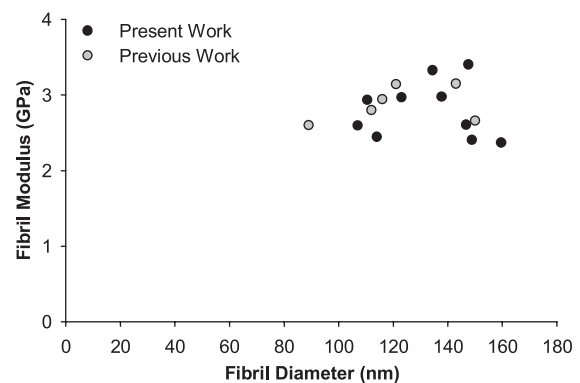

Fig. 7. Relationship between fibril modulus and diameter. Black dots are data from the present work, and gray dots are data from a previous publication (54) also tested in 150 mM PBS at 9.81 μm/s deformation rate. Diameters were backcalculated from cross-sectional areas assuming circularity.

in the optical microscope could be isolated for testing in the AFM. The tested fibrils had a mean dry diameter of 133 nm, equivalent to a hydrated diameter of ~170 nm (assuming 30% swelling), which is much larger than the <100-nm mean diameter observed by electron microscopy on human patellar tendons (27, 53). The tested fibrils may therefore not be fully representative of the fibril population. To our knowledge, there are no reports suggesting a negative correlation between fibril diameter and modulus; in fact, it has been proposed that large-diameter fibrils may demonstrate an increased modulus (41). In addition, we have not observed a relationship between fibril diameter and modulus in any of our works using the present method (Fig. 7). Thus, there is little evidence to suggest that the bias in fibril diameter would explain the low fibril modulus.

In conclusion, in this work, we present the first within-subject study of the mechanical properties of the human tendon hierarchical structure at the fibril and tendon level. Our initial hypothesis that fibril stress-strain properties directly govern overall tendon mechanical properties could not be supported by the present data. Data showed that the modulus of individual fibrils (2.8 GPa), when corrected for hydration and volume fraction (~1 GPa), was insufficient to account for the Young's modulus of their parent tendons in vivo (2.0 GPa). This finding is difficult to reconcile in the absence of other major tendon components of greater stiffness, which suggests a possible loss of stiffness in ex vivo testing. That the loss of stiffness is apparently present in both tissue and fibrils indicates that fibrils govern tissue properties. Finally, our results confirm the presence of viscoelastic and shear thinning behavior at the fibril level.

ACKNOWLEDGMENTS

GRANTS

DISCLOSURES

REFERENCES

1. **An KN, Sun YL, Luo ZP.** Flexibility of type I collagen and mechanical property of connective tissue. *Biorheology* 41: 239–246, 2004.
2. **Atkinson TS, Ewers BJ, Haut RC.** The tensile and stress relaxation responses of human patellar tendon varies with specimen cross-sectional area. *J Biomech* 32: 907–914, 1999.
3. **Bank RA, Beekman B, Verzijl N, de Roos JA, Sakkee AN, TeKoppele JM.** Sensitive fluorimetric quantitation of pyridinium and pentosidine crosslinks in biological samples in a single high-performance liquid chromatographic run. *J Chromatogr B Biomed Sci App* 703: 37–44, 1997.
4. **Bennett MB, Ker RF, Dimery NJ, Alexander RM.** Mechanical properties of various mammalian tendons. *J Zool* 209: 537–548, 1986.
5. **Besier TF, Fredericson M, Gold GE, Beaupre GS, Delp SL.** Knee muscle forces during walking and running in patellofemoral pain patients and pain-free controls. *J Biomech* 42: 898–905, 2009.
6. **Bojsen-Moller J, Brogaard K, Have MJ, Stryger HP, Kjaer M, Aagaard P, Magnusson SP.** Passive knee joint range of motion is unrelated to the mechanical properties of the patellar tendon. *Scand J Med Sci Sports* 17: 415–421, 2007.
7. **Bojsen-Moller J, Hansen P, Aagaard P, Kjaer M, Magnusson SP.** Measuring mechanical properties of the vastus lateralis tendon-aponeurosis complex in vivo by ultrasound imaging. *Scand J Med Sci Sports* 13: 259–265, 2003.
8. **Buehler MJ.** Nanomechanics of collagen fibrils under varying cross-link densities: Atomistic and continuum studies. *J Mech Behav Biomed Mater* 1: 59–67, 2008.
9. **Butler DL, Grood ES, Noyes FR, Zernicke RF, Brackett K.** Effects of structure and strain-measurement technique on the material properties of young human tendons and fascia. *J Biomech* 17: 579–596, 1984.
10. **Chimich D, Shrive N, Frank C, Marchuk L, Bray R.** Water-content alters viscoelastic behavior of the normal adolescent rabbit medial collateral ligament. *J Biomech* 25: 831–837, 1992.
11. **Chun KJ, Butler DL.** Spatial variation in material properties in fascicle-bone units from human patellar tendon. In: *Experimental Mechanics in Nano and Biotechnology*, edited by Lee S, Kim Y. Stafa-Zurich, Switzerland: Trans Tech Publications, 2006, p. 797–802.
12. **Couppe C, Hansen P, Kongsgaard M, Kovanen V, Suetta C, Aagaard P, Kjaer M, Magnusson SP.** Mechanical properties and collagen cross-linking of the patellar tendon in old and young men. *J Appl Physiol* 107: 880–886, 2009.
13. **Craig AS, Birtles MJ, Conway JF, Parry DAD.** An estimate of the mean length of collagen fibrils in rat tail-tendon as a function of age. *Connect Tissue Res* 19: 51–62, 1989.
14. **Creemers LB, Jansen DC, van Veen-Reurings A, van den Bos T, Everts V.** Microassay for the assessment of low levels of hydroxyproline. *Biotechniques* 22: 656–658, 1997.
15. **Cusack S, Miller A.** Determination of the elastic constants of collagen by brillouin light scattering. *J Mol Biol* 135: 39–51, 1979.
16. **Finni T, Komi PV, Lepola V.** In vivo human triceps surae and quadriceps femoris muscle function in a squat jump and counter movement jump. *Eur J Appl Physiol* 83: 416–426, 2000.
17. **Finni T, Komi PV, Lepola V.** In vivo muscle mechanics during locomotion depend on movement amplitude and contraction intensity. *Eur J Appl Physiol* 85: 170–176, 2001.
18. **Franchi M, Fini M, Quaranta M, De Pasquale V, Raspanti M, Giavaresi G, Ottani V, Ruggeri A.** Crimp morphology in relaxed and stretched rat achilles tendon. *J Anat* 210: 1–7, 2007.
19. **Fratzl P, Misof K, Zizak I, Rapp G, Amenitsch H, Bernstorff S.** Fibrillar structure and mechanical properties of collagen. *J Struct Biol* 122: 119–122, 1998.
20. **Gautieri A, Buehler MJ, Redaelli A.** Deformation rate controls elasticity and unfolding pathway of single tropocollagen molecules. *J Mech Behav Biomed Mater* 2: 130–137, 2009.
21. **Gautieri A, Vesentini S, Redaelli A, Buehler MJ.** Hierarchical structure and nanomechanics of collagen microfibrils from the atomistic scale up. *Nano Lett* 11: 757–766, 2011.
22. **Giddings VL, Beaupre GS, Whalen RT, Carter DR.** Calcaneal loading during walking and running. *Med Sci Sports Exerc* 32: 627–634, 2000.
23. **Goh KL, Chen Y, Chou SM, Listrat A, Bechet D, Wess TJ.** Effects of frozen storage temperature on the elasticity of tendons from a small murine model. *Animal* 4: 1613–1617, 2010.
24. **Grant CA, Brockwell DJ, Radford SE, Thomson NH.** Effects of hydration on the mechanical response of individual collagen fibrils (Abstract). *Appl Phys Lett* 92: 3902, 2008.
25. **Gupta HS, Messmer P, Roschger P, Bernstorff S, Klaushofer K, Fratzl P.** Synchrotron diffraction study of deformation mechanisms in mineralized tendon. *Phys Rev Lett* 93: 158101, 2004.
26. **Hansen P, Bojsen-Moller J, Aagaard P, Kjaer M, Magnusson SP.** Mechanical properties of the human patellar tendon, in vivo. *Clin Biomech* 21: 54–58, 2006.
27. **Hansen P, Haraldsson BT, Aagaard P, Kovanen V, Avery NC, Qvortrup K, Larsen JO, Krogsgaard M, Kjaer M, Magnusson SP.** Lower strength of the human posterior patellar tendon seems unrelated to mature collagen cross-linking and fibril morphology. *J Appl Physiol* 108: 47–52, 2010.
28. **Hansen P, Aagaard P, Kjaer M, Larsson B, Magnusson SP.** Effect of habitual running on human achilles tendon load-deformation properties and cross-sectional area. *J Appl Physiol* 95: 2375–2380, 2003.
29. **Haraldsson BT, Aagaard P, Krogsgaard M, Alkjaer T, Kjaer M, Magnusson SP.** Region-specific mechanical properties of the human patella tendon. *J Appl Physiol* 98: 1006–1012, 2005.

30. **Heim AJ, Koob TJ, Matthews WG.** Low strain nanomechanics of collagen fibrils. *Biomacromolecules* 8: 3298–3301, 2007.

31. **Jarvinen TAH, Jarvinen TLN, Kannus BB, Jozsa L, Jarvinen M.** Collagen fibres of the spontaneously ruptured human tendons display decreased thickness and crimp angle. *J Orthop Res* 22: 1303–1309, 2004.

32. **Kjaer M, Langberg H, Bojsen-Moller J, Koskinen SO, Mackey A, Heinemeier K, Holm L, Skovgaard D, Dossing S, Hansen M, Hansen P, Haraldsson B, Caroe I, Magnusson SP.** Novel methods for tendon investigations. *Disabil Rehabil* 30: 1514–1522, 2008.

33. **Kongsgaard M, Reitelseder S, Pedersen TG, Holm L, Aagaard P, Kjaer M, Magnusson SP.** Region specific patellar tendon hypertrophy in humans following resistance training. *Acta Physiol* 191: 111–121, 2007.

34. **Maganaris CN, Paul JP.** In vivo human tendon mechanical properties. *J Physiol (Lond)* 521: 307–313, 1999.

35. **Magnusson SP, Hansen P, Aagaard P, Brond J, Dyhre-Poulsen P, Bojsen-Moller J, Kjaer M.** Differential strain patterns of the human gastrocnemius aponeurosis and free tendon, in vivo. *Acta Physiol Scand* 177: 185–195, 2003.

36. **Magnusson SP, Langberg H, Kjaer M.** The pathogenesis of tendinopathy: balancing the response to loading. *Nat Rev Rheumatol* 6: 262–268, 2010.

37. **Meek KM, Fullwood NJ, Cooke PH, Elliott GF, Maurice DM, Quantock AJ, Wall RS, Worthington CR.** Synchrotron X-ray diffraction studies of the cornea, with implications for stromal hydration. *Biophys J* 60: 467–474, 1991.

38. **Mosler E, Folkhard W, Knorzer E, Nemetschekgansler H, Nemetschek T, Koch MHJ.** Stress-induced molecular rearrangement in tendon collagen. *J Mol Biol* 182: 589–596, 1985.

39. **Narici MV, Maganaris CN.** Adaptability of elderly human muscles and tendons to increased loading. *J Anat* 208: 433–443, 2006.

40. **Onambele GNL, Burgess K, Pearson SJ.** Gender-specific in vivo measurement of the structural and mechanical properties of the human patellar tendon. *J Orthop Res* 25: 1635–1642, 2007.

41. **Parry DAD.** The molecular and fibrillar structure of collagen and its relationship to the mechanical properties of connective tissue. *Biophys Chem* 29: 195–209, 1988.

42. **Parry DAD, Barnes GRG, Craig AS.** A comparison of size distribution of collagen fibrils in connective tissues as a function of age and a possible relation between fibril size distribution and mechanical properties. *Proc R Soc Lond B Biol Sci* 203: 305–321, 1978.

43. **Petruska JA, Hodge AJ.** A subunit model for tropocollagen macromolecule. *Proc Natl Acad Sci USA* 51: 871–876, 1964.

44. **Provenzano PP, Vanderby R.** Collagen fibril morphology and organization: Implications for force transmission in ligament and tendon. *Matrix Biol* 25: 71–84, 2006.

45. **Puxkandl R, Zizak I, Paris O, Keckes J, Tesch W, Bernstorff S, Purslow P, Fratzl P.** Viscoelastic properties of collagen: Synchrotron radiation investigations and structural model. *Philos Trans R Soc Lond B Biol Sci* 357: 191–197, 2002.

46. **Raspanti M, Manelli A, Franchi M, Ruggeri A.** The 3D structure of crimps in the rat achilles tendon. *Matrix Biol* 24: 503–507, 2005.

47. **Reeves ND, Maganaris CN, Narici MV.** Effect of strength training on human patella tendon mechanical properties of older individuals. *J Physiol (Lond)* 548: 971–981, 2003.

48. **Sasaki N, Odajima S.** Elongation mechanism of collagen fibrils and force-strain relations of tendon at each level of structural hierarchy. *J Biomech* 29: 1131–1136, 1996.

49. **Sasaki N, Shiwa S, Yagihara S, Hikichi K.** X-ray-diffraction studies on the structure of hydrated collagen. *Biopolymers* 22: 2539–2547, 1983.

50. **Screen HRC, Chhaya VH, Greenwald SE, Bader DL, Lee DA, Shelton JC.** The influence of swelling and matrix degradation on the microstructural integrity of tendon. *Acta Biomater* 2: 505–513, 2006.

51. **Shen ZL, Dodge MR, Kahn H, Ballarini R, Eppell SJ.** Stress-strain experiments on individual collagen fibrils. *Biophys J* 95: 3956–3963, 2008.

52. **Silver FH, Christiansen DL, Snowhill PB, Chen Y.** Role of storage on changes in the mechanical properties of tendon and self-assembled collagen fibers. *Connect Tissue Res* 41: 155–164, 2000.

53. **Svensson M, Movin T, Rostgard-Christensen L, Blomen E, Hultenby K, Kartus J.** Ultrastructural collagen fibril alterations in the patellar tendon 6 years after harvesting its central third. *Am J Sports Med* 35: 301–306, 2007.

54. **Svensson RB, Hassenkam T, Grant CA, Magnusson SP.** Tensile properties of human collagen fibrils and fascicles are insensitive to environmental salts. *Biophys J* 99: 4020–4027, 2010.

55. **Svensson RB, Hassenkam T, Hansen P, Magnusson SP.** Viscoelastic behavior of discrete human collagen fibrils. *J Mech Behav Biomed Mater* 3: 112–115, 2010.

56. **Thornton GM, Shrive NG, Frank CB.** Altering ligament water content affects ligament pre-stress and creep behaviour. *J Orthop Res* 19: 845–851, 2001.

57. **van der Rijt JAJ, van der Werf KO, Bennink ML, Dijkstra PJ, Feijen J.** Micromechanical testing of individual collagen fibrils. *Macromol Biosci* 6: 697–702, 2006.

58. **Yamamoto E, Hayashi K, Yamamoto N.** Mechanical properties of collagen fascicles from stress-shielded patellar tendons in the rabbit. *Clin Biomech* 14: 418–425, 1999.

59. **Yang L, van der Werf KO, Fitié CFC, Bennink ML, Dijkstra PJ, Feijen J.** Mechanical properties of native and cross-linked type I collagen fibrils. *Biophys J* 94: 2204–2211, 2008.

60. **Yang L, van der Werf KO, Koopman B, Subramaniam V, Bennink ML, Dijkstra PJ, Feijen J.** Micromechanical bending of single collagen fibrils using atomic force microscopy. *J Biomed Mater Res A* 82A: 160–168, 2007.

Study 4

informa
healthcare

Tensile Force Transmission in Human Patellar Tendon Fascicles Is Not Mediated by Glycosaminoglycans

René B. Svensson,[1] Tue Hassenkam,[2] Philip Hansen,[1] Michael Kjaer,[1] Stig P. Magnusson[1]

[1]*Institute of Sports Medicine Copenhagen, Bispebjerg Hospital and Center for Healthy Aging, University of Copenhagen, Copenhagen, Denmark,* [2]*Nano-Science Center, University of Copenhagen, Copenhagen, Denmark*

Abstract

Correct mechanical function of tendons is essential to human physiology and therefore the mechanical properties of tendon have been a subject of research for many decades now. However, one of the most fundamental questions remains unanswered: How is load transmitted through the tendon? It has been suggested that the proteoglycan-associated glycosaminoglycans (GAGs) found on the surface of the collagen fibrils may be an important transmitter of load, but existing results are ambiguous and have not investigated human tendons. We have used a small-scale mechanical testing system to measure the mechanical properties of fascicles from human patellar tendon at two different deformation rates before and after removal of GAGs by treatment with chondroitinase ABC. Efficiency of enzyme treatment was quantified using dimethylmethylene blue assay. Removal of at least 79% of the GAGs did not significantly change the tendon modulus, relative energy dissipation, peak stress, or peak strain. The effect of deformation rate was not modulated by the treatment either, indicating no effect on viscosity. These results suggest that GAGs cannot be considered mediators of tensile force transmission in the human patellar tendon, and as such, force transmission must either take place through other matrix components or the fibrils must be mechanically continuous at least to the tested length of 7 mm.

Keywords: chondroitinase, force transmission, glycosaminoglycan, human patellar tendon, mechanical properties

INTRODUCTION

Force transmission is a fundamental function of tendon tissue. Yet, the mechanisms of force transmission at the microscopic level remain unclear. Tendon consists of collagen fibrils [1] with a diameter range of 10–500 nm [2–4], which are embedded in a matrix (the ground substance) consisting of a large number of different molecules, including water, proteoglycans, glycosaminoglycans (GAGs), elastin, and glycoproteins such as fibronectin among others [5]. This structural composition is similar to that of a fiber-reinforced composite where fibers transmit force laterally to adjacent fibers through the matrix. Such a tendon model in which strain is shared between fibrils and matrix is quite well supported in the literature by findings of fiber slippage at the microscopic level [6–8] and by X-ray diffraction studies showing that the constituent fibrils are stretched less than the whole structure [9–11]. Despite these convincing evidence, the apparently great length of fibrils in mature tendon [12,13] has led to the proposition that fibrils are mechanically continuous and transfer force directly between fibrils without major modulation by the matrix.

Among the components of the tendon ground substance, the proteoglycan decorin and its associated GAG, either chondroitin sulfate (CS) or dermatan sulfate (DS), have attracted special interest as possible force-transmitting structures (Figure 1). The idea that CS and DS serve as force transmitters originates in structural studies showing that the decorin core-protein binds specifically along the banding pattern at the surface of collagen fibrils [14] and that the GAGs assume an extended linear conformation bridging between neighboring fibrils [15,16]. Recently it was also shown that the GAGs become skewed during loading [17], further supporting the possibility of force transfer. Computer modeling has also been reported [18], which was able to predict mechanical properties in the correct order of magnitude, however, only when tuning the parameters to optimal values. Using more realistic values, the predicted GAG stress exceeded the strength of the GAG bridges even when assuming covalent bonding. These findings have prompted investigators to
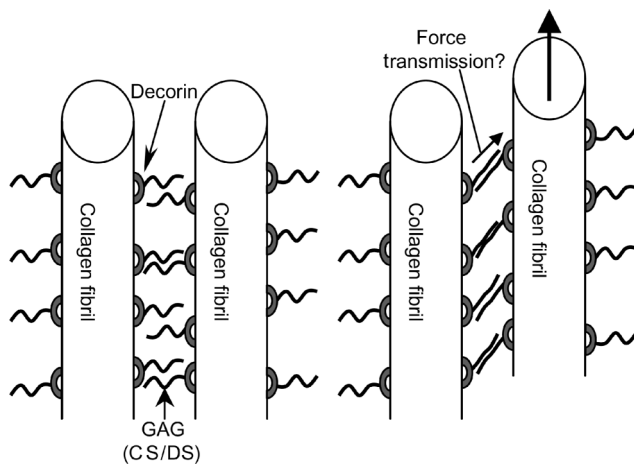
RIGHTSLINK

Figure 1. Schematic illustration of the hypothetical mechanism for tensile force transmission. Left: Unloaded collagen fibril interface with decorin and attached glycosaminoglycans (GAGs). Right: Illustration of force transmission through GAGs. A force is applied to one fibril (large arrow); bridging GAGs transmit this force (small arrow) to the neighboring fibril through non-covalent interactions.

determine how the mechanical properties of different tissues are affected by removing CS and DS, albeit with inconclusive results. Changes in mechanical properties have been reported in human lung tissue [19] and rat-tail tendon [20], whereas others have shown that the modulus and viscoelastic properties were unaffected in rat-tail tendon fascicles [21] and human ligament [22,23].

The purpose of the present work was to investigate the influence of CS and DS on force transmission in fascicles from the human patellar tendon. Fascicles from the human patellar tendon were chosen for several reasons: First, human tendon has not been investigated previously and the use of fascicles ensures a more parallel fibril arrangement than larger specimens such as the human ligament strips previously reported [22,23]. We believe that using fascicle subunits also alleviates reported issues of regional variations [24]. Second, the human patellar tendon is subjected to high loads unlike lung tissue, and although reported in vitro modulus of rat-tail tendon is in the same range as in vitro human patellar tendon [25–27], it is likely subject to relatively little stress-in-life if it follows the same pattern as wallaby tendons [28]. In addition, rat-tail tendon is often obtained at an age of ∼15 weeks when the fibril diameter distribution [29] reaches much larger values than in mature human patellar tendon [30,31]. Lastly, the patellar tendon frequently sustains injury by repetitive loading, and increased GAG levels have been reported in the tendinopathic tendon [32] pointing at a function of GAGs in overloaded tendon. For these reasons, fascicles of human patellar tendon are in our opinion a highly suitable choice for assessing the importance of GAG-mediated tensile force transfer between parallel collagen fibrils in humans.

MATERIALS AND METHODS

The study consisted of one group treated with a buffered solution of chondroitinase ABC (Ch-ABC) for 2 hr (treated group) and one group treated only with buffer (control group). Mechanical properties were measured in both groups before and after treatment. GAG content was determined by dimethylmethylene blue (DMMB) assay after mechanical testing, and the content in the control group was assumed equal to the starting content in both the control and the treated groups.

Materials

Tissue from the anterior portion of the human patellar tendon was obtained from five males during routine anterior cruciate ligament reconstruction. Procedures were approved by the Danish Council of Ethics in agreement with the Declaration of Helsinki, and informed consent was obtained from all subjects involved. Two experiments were performed on fresh tissue, and the remaining samples were wrapped in gauze soaked with phosphate buffered saline (PBS) and stored frozen at –20°C for 5 weeks prior to testing. Individual fascicles were dissected out for mechanical testing, and larger pieces of fascicular material were dissected to assess sulfated GAG content (∼1.5 mg). In total, 18 fascicles from 5 subjects were tested: 9 Ch-ABC-treated and 9 controls. Two control and two treated fascicles were taken from each tendon except one where the material was only sufficient for one in each group. Fascicles from the same tendon were tested in pairs of one control and one treated to ensure complete homogeneity of the procedure.

Several solutions were used. *Buffer1*: 20 mM Tris, 150 mM NaCl, and 5 mM CaCl$_2$ (pH 7.4). *Stop-buffer*: 20 mM Tris, 150 mM NaCl, and 10 mM EDTA (pH 7.4) [23]. *Papain-Digest*: 5 mg/mL papain (25 mg/mL suspension in 50 mM sodium acetate, pH 4.5), 30 mM NaOH, 5 mM EDTA, and 10 mM L-cysteine. *DMMB-reagent*: 16 g/L 1,9-dimethylmethylene blue, 3.04 g/L glycine, 2.37 g/L NaCl, and 9.5 mM HCl [33]. Papain, L-cysteine, and 1,9-dimethylmethylene blue were obtained from Sigma-Aldrich (St. Louis, MO, USA).

Chondroitinase ABC Treatment

The larger tissue pieces used for DMMB analysis were paired with each of the fascicles used for mechanical testing and they were moved between the different solution baths together (Figure 2A). Mechanical testing was performed in *buffer1* for all specimens. Following the pre-treatment mechanical test, fascicles were moved in a slack state to the incubation bath by moving the entire clamp–fascicle–clamp complex. Moving the entire clamp complex ensures continuity of the loading conditions. The tissue was incubated for 2 hr in *buffer1* (control) or *buffer1* with 0.1 U/mL Ch-ABC (Sigma-Aldrich) (treated). After incubation, the fascicles received the post-treatment mechanical test
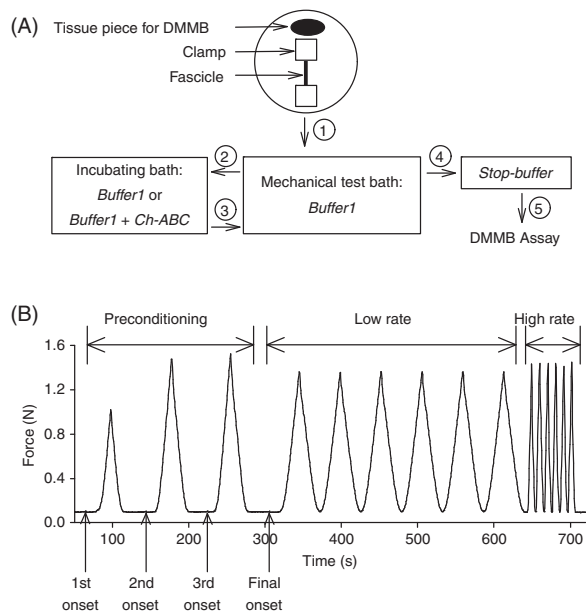
Figure 2. Schematic of treatment and testing protocols. (A) Flow diagram of the treatment procedure: (1) pre-treatment mechanical test, (2) treatment for 2 hr in either control or Ch-ABC solution, (3) post-treatment mechanical test, (4) incubation in stop-buffer, (5) dimethylmethylene blue assay. (B) Experimental data showing the testing protocol. Onset was determined before each preconditioning cycle and right before the actual test. The test consisted of six loading/unloading cycles at a low (0.5 mm/min) and a high (4 mm/min) rate.
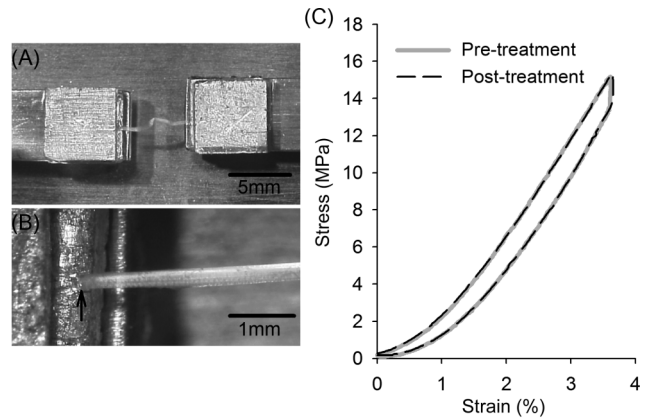

Figure 3. (A) Microscopic image of a mechanical test specimen. (B) Close-up of the clamping site. The glue–fascicle interface is marked with a black arrow. The fascicle inside the glue to the left of the interface is transparent because it is dry. (C) Example hysteresis loops at 0.5 mm/min of a fascicle in the Ch-ABC-treated group before and after treatment.

and were then moved to a *stop-buffer* bath for 15 min before being dried in an oven at 55°C overnight.

Mechanical Testing

Mechanical tests were made in a micro-tensile tester (200 N tensile stage, petri dish version, Deben, Suffolk, UK) equipped with a 20 N load cell. The central part of the fascicles was kept moist with *buffer1*-soaked gauze while the ends were dried and glued onto the end clamps with cyanoacrylate glue. An aluminum disk was placed on top, which greatly increased the curing rate of the glue (Figure 3A and B). After the glue had cured for at least 15 min, the clamp complex was placed in the *buffer1* bath for 30 min before mechanical testing and remained fully hydrated throughout the experiment. Strain was based on clamp–clamp distance.

A preconditioning protocol was performed as follows (Figure 2B): An onset force of 0.01 N was used. Three preconditioning cycles to 4% strain from the onset point were made. The stretch at the onset point increased, presumably due to increased fiber alignment in the fascicle, causing the increase in peak force seen in Figure 2B. After preconditioning, the fascicle was stretched to the final onset point and the length at this point was used throughout the experiment. Mean fascicle diameter at four positions was measured by microscopy and used for calculating cross-sectional area (CSA) assuming a circular shape [34].

Due to the low slope in the toe region, it is difficult to determine the onset consistently; therefore a target force rather than a target strain was used to ensure equal loading before and after treatment. The force target was set at ~90% of the peak force in the final preconditioning cycle. The actual testing protocol consisted of six cycles to the target force at 0.5 mm/min, followed by six cycles at 4 mm/min. The sixth cycle at each rate was used for mechanical analysis.

Following the treatment protocol (see previous section), a single preconditioning cycle was made before performing the post-treatment test, and finally the fascicle was loaded to failure at a rate of 2 mm/min.

Dimethylmethylene Blue Assay

Sulfated GAG content was determined using the DMMB assay [33]. Standards of DS in water were used. Twenty-five microliters of *papain-digest* solution was added to both the samples and 5 µL of each standard, and they were incubated at 65°C until the sample collagen was digested (20–60 min). The volume was increased to 100 µL by adding 50 mM Tris (pH 8.0) and 10 µL was transferred to wells of a 96-well plate. To each well, 250 µL of *DMMB-reagent* was added simultaneously, and absorbance was read at 520 nm after ~15 s (Opsys MR, Dynex Technologies, Chantilly, VA, USA). Measurements were made in triplicate.

Data Reduction and Statistics

For all tested fascicles, the modulus was determined by a linear fit to the final 20% (by stress) of the stress–strain curve. Dissipated energy in the hysteresis loop was determined by integrating along the entire stress–strain curve (Figure 3C), and the relative energy dissipation was determined by dividing by the integral of only the loading part of the curve up to the maximum strain.

The response to Ch-ABC treatment did not correlate within subjects, thus each fascicle was considered an independent sample. At each rate, two-way mixed-effects ANOVA was used to examine the effect of Ch-ABC treatment on modulus and relative energy dissipation. Within each treatment group, two-way repeated measures ANOVA was used to analyze the effect of deformation rate. Failure properties were analyzed by two-tailed, unpaired t-test. Results are reported as mean $\pm$ SD and for the effect of treatment, 95% confidence intervals (CIs) are also reported.

RESULTS

Structure and Mechanics

The specimens used for the Ch-ABC and the control groups were chosen randomly; the mean properties of each group before and after treatment can be seen in Table 1. Two experiments were made on fresh tissue and the remaining seven on tissue that had been frozen. No difference in mechanical properties and effect of Ch-ABC treatment was observed between the fresh and the frozen samples. Failure of fascicles tended to occur closer to the clamps than the center but never at the actual interface, and the broken ends contained fibers with a large variety of lengths indicating failure over a larger region of the fascicle.

The effect of treatment on the modulus did not differ significantly between the Ch-ABC and the control group either at 0.5 mm/min ($p = 0.64$, CI $= -28$ to 16 MPa) or at 4 mm/min ($p = 0.21$, CI $= -52$ to 7.7 MPa) (Figure 4A). The same was the case for the relative energy dissipation at both 0.5 mm/min ($p = 0.45$, CI $= -0.52$ to 1.3%) and 4 mm/min ($p = 0.94$, CI $= -1.0$ to 0.95%) (Figure 4B). Ch-ABC treatment did not have any effect on the failure properties when comparing the treated with the control group for the peak stress ($p = 0.82$, CI $= -34$ to 45 MPa) (Figure 4C) and peak strain ($p = 0.83$, CI $= -3.0$ to 3.7%) (Figure 4D).

Viscoelasticity was observed as a significant increase in the modulus when increasing the deformation rate from 0.5 to 4 mm/min in both the Ch-ABC ($p = 0.03$) and control ($p = 0.001$) groups (Table 1). However, this
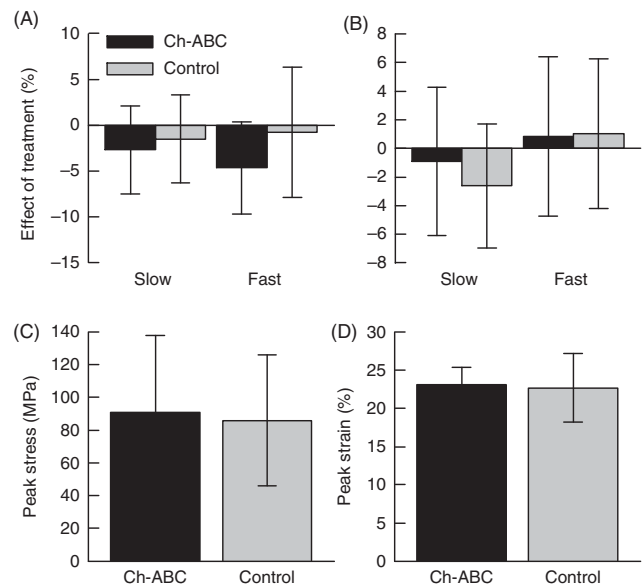

Figure 4. (A, B) Percentage change from pre- to post-treatment in (A) modulus and (B) relative energy dissipation at 0.5 mm/min (slow) and 4 mm/min (fast). (C, D) Failure mechanics at 2 mm/min. (C) Peak stress; (D) peak strain (strain at peak stress). Error bars are $\pm$SD.

viscoelastic response was unaffected by the treatment in both the Ch-ABC ($p = 0.21$) and control ($p = 0.67$) groups. Increasing the deformation rate also resulted in decreased relative energy dissipation in the Ch-ABC ($p = 0.004$) but not the control ($p = 0.08$) group. Again the rate effect was not correlated to the treatment for the Ch-ABC ($p = 0.20$) or control ($p = 0.09$) group.

Chondroitinase Efficacy

We found that papain incubation reduced the GAG content of DS standards, seen as a downward shift of the standard curve in Figure 5. This effect was not observed when incubating at 60°C in the absence of papain, nor when papain was added without incubation at 60°C. Approximately 125 µg of papain per milligram of tissue (containing ~3 µg GAGs) was used, which is similar to previous studies [19,33]; however, the specific activity (31 U/mg) was relatively high and could possibly explain the observed GAG loss. This loss of

Table 1. Measured mechanical and structural parameters (mean $\pm$ SD)

	Ch-ABC		Control	
Deformation rate (mm/min)	0.5	4	0.5	4
Modulus: pre-treatment (MPa)	540 ± 230	570 ± 220	570 ± 270	590 ± 280
Modulus: post-treatment (MPa)	530 ± 240	540 ± 230	560 ± 280	590 ± 280
Relative energy dissipation: pre-treatment (%)	23.6 ± 4.7	22.0 ± 3.8	23.9 ± 2.3	22.8 ± 2.7
Relative energy dissipation: post-treatment (%)	23.4 ± 4.0	22.2 ± 3.6	23.2 ± 2.5	23.0 ± 3.3
Tested fascicle length (mm)	6.74 ± 0.56		6.89 ± 0.48	
Fascicle diameter (mm)	0.29 ± 0.11		0.33 ± 0.16	

None of the treatment effects were significant and none of the differences between the treated and control groups were significant. The effect of deformation rate was significant for the modulus in both groups and for the relative energy dissipation in the Ch-ABC but not in the control group.
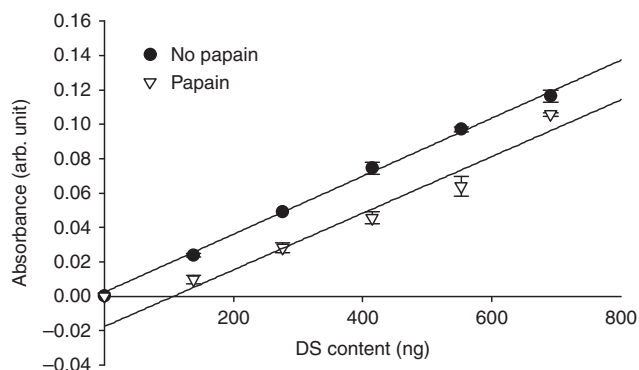
Figure 5.   Dimethylmethylene blue assay results on DS standards incubated with and without papain for 90 min at 60°C. Error bars are ±SD from duplicate measures. A downward shift is seen following papain treatment. The first data point (0,0) has been omitted in both fits.

GAGs makes it difficult to precisely assess samples with low GAG content. None of the controls but most of the treated samples had such a low GAG content. Therefore, we report a maximal concentration assuming that zero absorbance originated from a GAG content equal to that lost in the papain incubation, and a minimal concentration assuming zero content at zero absorbance.

The minimal and maximal GAG contents for the treated samples were $0.04 \pm 0.05\%$ and $0.08 \pm 0.07\%$, respectively. The GAG content of the control samples was $0.37 \pm 0.07\%$, and thus the Ch-ABC treatment removed 79–89% of the GAG content.

DISCUSSION

In the present work, we investigated the changes in modulus and energy dissipation following Ch-ABC digestion, for the first time at the fascicular level in human tissue (Figure 4). As GAGs are not expected to form covalent bonds between fibrils, viscosity could be important in force transmission mediated by the GAGs. To assess possible viscous effects as previously reported [19], measurements at two deformation rates were performed. With the present equipment, only low rates of 0.5 and 4 mm/min corresponding to approximately 0.15 and 1%/s strain rate were available, and at neither rate was there a significant effect of Ch-ABC treatment (Figure 4). Increasing the deformation rate did increase the modulus as expected for a viscoelastic material (Table 1), which has also previously been reported [35,36], but the effect was not significantly modulated by Ch-ABC treatment. Although the limited maximal strain rate reduces our ability to detect changes in viscoelastic behavior, Lujan et al. [22] did not observe any significant viscous effects on ligaments even at 10 times greater strain rate. Tissue viscous behavior leads to dissipation of energy, sometimes represented by the loss modulus. The fact that we found no effect of Ch-ABC treatment on the

relative energy dissipation or on the strain rate response of the relative energy dissipation (Figure 4B) further supports that CS and DS have no significant effect on viscoelasticity of the human patellar tendon under tensile load.

The failure mechanics did not show any effect of Ch-ABC treatment either, as both the peak strain and stress were essentially equal in the treated and control groups (Figure 4C and D). It has to be noted that the variation in the peak stress and modulus between specimens was large, which has also been observed in other studies [26,37]. We suspect that part of the large variation in modulus and peak stress is related to the variation in fascicle diameter, because a negative correlation between the logarithm of CSA and modulus has previously been reported [38], the cause of which is unclear but not likely related to clamping as bone–tendon–bone specimens were used. In the present study, correlating the logarithm of CSA to the modulus at 0.5 mm/min and to failure stress yields coefficients of determination of $R^2 = 0.44$ and $R^2 = 0.39$, respectively, indicating that ~40% of the variation in the mechanics originates in the CSA variation. Due to the repeated measures design, the large inter-specimen variation does not affect the comparison between pre- and post-treatment properties, but affects the failure mechanics where the specimen could not serve as its own control. This can be seen from the large CI of the effect on failure stress, which is equivalent to approximately ±45%.

The present results show that CS and DS are not involved in force transmission between fibrils in fully mature human tendon fascicles where collagen fibrils are long and highly aligned and where the GAG content is low. This suggests that either a different linker molecule exists or that collagen fibrils are continuous at least up to the length tested in the present work (~7 mm). Our finding is in agreement with a thorough study on human medial collateral ligament strips by Lujan et al. [22], where both stress relaxation and cyclic tests were recorded in the toe and linear regions and also in a dehydrating solution of polyethylene glycol to more closely mimic the in vivo situation. Under none of these conditions was any effect of GAG removal reported. In the present work, stress relaxation was also attempted, but we observed a marked change in mechanical response following the relaxation test, which persisted after a period of rest. For this reason, stress relaxation was omitted from our testing protocol. The findings in human ligament and the present results on human tendon are also in agreement with recent work on tendon fascicles from rat tail [21], which is further interesting because the GAG content in those rat-tail fascicles was approximately 10 times greater (3.2%) than in the human tendon and ligament.

Taken together, these works provide evidence that regardless of species (human or rat), tissue type (tendon or ligament), and level of hierarchy (fascicle

or larger tissue strips), decorin-associated GAGs are not important transmitters of force nor do they affect viscosity in tissues under tensile load. A reduction in modulus following GAG digestion has been reported in mouse Achilles tendon [24], but only close to the bone insertion, suggesting that the effect may be related to the greater compressive stress in that region [39]. Increased stiffness has been observed in rat-tail fascicles after GAG removal [20], which could indicate a lubricating effect of GAGs. The increase in stiffness was related to a reduction in the swelling caused by the buffer, which brought the stiffness up to the level observed under ambient conditions. This can explain why the effect was not observed by Fessel and Snedeker[21] because the swelling in that study was controlled with polyethylene glycol. However, it is difficult to reconcile the finding with those of the present work and that of Lujan et al. [22] in which the swelling was not controlled for. The choice of buffer—Tris in the works that find no effect of GAG removal and PBS in the one that does—could have an influence; however, experiments in our lab using PBS yielded the same values for modulus and relative energy dissipation as the Tris buffer, indicating that this buffer choice would not change the mechanical response.

If CS and DS do not transmit force between fibrils, a number of roles not related to tensile mechanics can be proposed. One alternative role for the molecules could be as spacers to control the separation of collagen fibrils, which could be important during fibrillogenesis to avoid lateral fibril fusion [40] and to provide resistance against radial compression. It should be noted that even though the role of decorin in fibrillogenesis is well established, the influence of the GAG chain remains less clear. Another possibility is that the GAGs could act as sensory molecules relaying information about matrix deformation. For such a purpose, the bridging structure would seem ideal in sensing shear or sliding between neighboring fibrils and both CS and DS have been shown to interact with a number of other matrix proteins implicated in cell signaling [41]. More studies in a range of different fields are therefore needed to fully elucidate the importance of the CS and DS GAGs in tendon, but the present data do not support a role in tensile load transmission.

CONCLUSION

In the present work, human patellar tendon fascicles were chosen for their great linearity and high loading in vivo, to investigate the importance of GAGs in tensile force transmission. Our findings show that neither modulus nor energy dissipation was affected by the removal of at least 79% of the sulfated GAGs, indicating that decorin-associated GAGs have no influence on either elastic or viscous behavior under tensile load. This is in agreement with results on other types of tissue and leaves the question of how force is transmitted between fibrils, if not through GAGs, unanswered.

REFERENCES

[1]   Kannus, P. (2000). Structure of the tendon connective tissue. *Scand. J. Med. Sci. Sports* 10:312–320.

[2]   Lavagnino, M., Arnoczky, S.P., Frank, K., and Tian, T. (2005). Collagen fibril diameter distribution does not reflect changes in the mechanical properties of in vitro stress-deprived tendons. *J. Biomech.* 38:69–75.

[3]   Magnusson, S.P., Qvortrup, K., Larsen, J.O., Rosager, S., Hanson, P., Aagaard, P., Krogsgaard, M., and Kjaer, M. (2002). Collagen fibril size and crimp morphology in ruptured and intact Achilles tendons. *Matrix Biol.* 21:369–377.

[4]   Williams, I.F., Craig, A.S., Parry, D.A.D., Goodship, A.E., Shah, J., and Silver, I.A. (1985). Development of collagen fibril organization and collagen crimp patterns during tendon healing. *Int. J. Biol. Macromol.* 7:275–282.

[5]   Wang, J.H.C. (2006). Mechanobiology of tendon. *J. Biomech.* 39:1563–1582.

[6]   Screen, H.R.C. (2008). Investigating load relaxation mechanics in tendon. *J. Mech. Behav. Biomed. Mater.* 1: 51–58.

[7]   Screen, H.R.C., Lee, D.A., Bader, D.L., and Shelton, J.C. (2004). An investigation into the effects of the hierarchical structure of tendon fascicles on micromechanical properties. *Proc. Inst. Mech. Eng. Part H–J. Eng. Med.* 218:109–119.

[8]   Screen, H.R.C., Bader, D.L., Lee, D.A., and Shelton, J.C. (2004). Local strain measurement within tendon. *Strain* 40:157–163.

[9]   Puxkandl, R., Zizak, I., Paris, O., Keckes, J., Tesch, W., Bernstorff, S., Purslow, P., and Fratzl, P. (2002). Viscoelastic properties of collagen: Synchrotron radiation investigations and structural model. *Philos. Trans. R. Soc. Lond. B. Biol. Sci.* 357:191–197.

[10] Fratzl, P., Misof, K., Zizak, I., Rapp, G., Amenitsch, H., and Bernstorff, S. (1998). Fibrillar structure and mechanical properties of collagen. *J. Struct. Biol.* 122:119–122.

[11] Krauss, S., Fratzl, P., Seto, J., Currey, J.D., Estevez, J.A., Funari, S.S., and Gupta, H.S. (2009). Inhomogeneous fibril stretching in antler starts after macroscopic yielding: Indication for a nanoscale toughening mechanism. *Bone* 44: 1105–1110.

[12] Craig, A.S., Birtles, M.J., Conway, J.F., and Parry, D.A.D. (1989). An estimate of the mean length of collagen fibrils in rat tail-tendon as a function of age. *Connect. Tissue Res.* 19: 51–62.

[13] Provenzano, P.P., and Vanderby, R. (2006). Collagen fibril morphology and organization: Implications for force transmission in ligament and tendon. *Matrix Biol.* 25:71–84.

[14] Scott, J.E., and Orford, C.R. (1981). Dermatan sulphate-rich proteoglycan associates with rat tail-tendon collagen at the d band in the gap region. *Biochem. J.* 197:213–216.

[15] Scott, J.E. (1992). Supramolecular organization of extracellular matrix glycosaminoglycans, in vitro and in the tissues. *FASEB J.* 6:2639–2645.

[16] Cribb, A.M., and Scott, J.E. (1995). Tendon response to tensile stress: An ultrastructural investigation of collagen:proteoglycan interactions in stressed tendon. *J. Anat.* 187:423–428.

[17] Liao, J., and Vesely, I. (2007). Skewness angle of interfibrillar proteoglycans increases with applied load on mitral valve chordae tendineae. *J. Biomech.* 40:390–398.

[18] Redaelli, A., Vesentini, S., Soncini, M., Vena, P., Mantero, S., and Montevecchi, F.M. (2003). Possible role of decorin glycosaminoglycans in fibril to fibril force transfer in relative mature tendons – a computational study from molecular to microstructural level. *J. Biomech.* 36:1555–1569.

[19] Al Jamal, R., Roughley, P.J., and Ludwig, M.S. (2001). Effect of glycosaminoglycan degradation on lung tissue viscoelasticity. *Am. J. Physiol. Lung Cell. Mol. Physiol.* 280:L306–L315.

[20] Screen, H.R.C., Chhaya, V.H., Greenwald, S.E., Bader, D.L., Lee, D.A., and Shelton, J.C. (2006). The influence of swelling and matrix degradation on the microstructural integrity of tendon. *Acta Biomater.* 2:505–513.

[21] Fessel, G., and Snedeker, J.G. (2009). Evidence against proteoglycan mediated collagen fibril load transmission and dynamic viscoelasticity in tendon. *Matrix Biol.* 28:503–510.

[22] Lujan, T.J., Underwood, C.J., Jacobs, N.T., and Weiss, J.A. (2009). Contribution of glycosaminoglycans to viscoelastic tensile behavior of human ligament. *J. Appl. Physiol.* 106:423–431.

[23] Lujan, T.J., Underwood, C.J., Henninger, H.B., Thompson, B.M., and Weiss, J.A. (2007). Effect of dermatan sulfate glycosaminoglycans on the quasi-static material properties of the human medial collateral ligament. *J. Orthop. Res.* 25:894–903.

[24] Rigozzi, S., Muller, R., and Snedeker, J.G. (2009). Local strain measurement reveals a varied regional dependence of tensile tendon mechanics on glycosaminoglycan content. *J. Biomech.* 42:1547–1552.

[25] An, K.N., Sun, Y.L., and Luo, Z.P. (2004). Flexibility of type I collagen and mechanical property of connective tissue. *Biorheology* 41:239–246.

[26] Johnson, G.A., Tramaglini, D.M., Levine, R.E., Ohno, K., Choi, N.Y., and Woo, S.L.Y. (1994). Tensile and viscoelastic properties of human patellar tendon. *J. Orthop. Res.* 12:796–803.

[27] Kato, Y.P., Christiansen, D.L., Hahn, R.A., Shieh, S.J., Goldstein, J.D., and Silver, F.H. (1989). Mechanical-properties of collagen-fibers – a comparison of reconstituted and rat tail tendon fibers. *Biomaterials* 10:38–41.

[28] Ker, R.F., Wang, X.T., and Pike, A.V.L. (2000). Fatigue quality of mammalian tendons. *J. Exp. Biol.* 203:1317–1327.

[29] Parry, D.A.D., Barnes, G.R.G., and Craig, A.S. (1978). A comparison of size distribution of collagen fibrils in connective tissues as a function of age and a possible relation between fibril size distribution and mechanical properties. *Proc. R. Soc. Lond., B, Biol. Sci.* 203:305–321.

[30] Hansen, M., Kongsgaard, M., Holm, L., Skovgaard, D., Magnusson, S.P., Qvortrup, K., Larsen, J.O., Aagaard, P., Dahl, M., Serup, A., Frystyk, J., Flyvbjerg, A., Langberg, H., and Kjaer, M. (2009). Effect of estrogen on tendon collagen synthesis, tendon structural characteristics, and biomechanical properties in postmenopausal women. *J. Appl. Physiol.* 106:1385–1393.

[31] Kongsgaard, M., Qvortrup, K., Larsen, J., Aagaard, P., Doessing, S., Hansen, P., Kjaer, M., and Magnusson, S.P. (2010). Fibril morphology and tendon mechanical properties in patellar tendinopathy effects of heavy slow resistance training. *Am. J. Sports Med.* 38:749–756.

[32] Samiric, T., Parkinson, J., Ilic, M.Z., Cook, J., Feller, J.A., and Handley, C.J. (2009). Changes in the composition of the extracellular matrix in patellar tendinopathy. *Matrix Biol.* 28:230–236.

[33] Farndale, R.W., Buttle, D.J., and Barrett, A.J. (1986). Improved quantitation and discrimination of sulphated glycosaminoglycans by use of dimethylmethylene blue. *Biochim. Biophys. Acta* 883:173–177.

[34] Yamamoto, E., Hayashi, K., and Yamamoto, N. (1999). Mechanical properties of collagen fascicles from the rabbit patellar tendon. *J. Biomech. Eng.* 121:124–131.

[35] Haut, R.C., and Little, R.W. (1972). A constitutive equation for collagen fibers. *J. Biomech.* 5:423–430.

[36] Sanjeevi, R. (1982). A viscoelastic model for the mechanical-properties of biological-materials. *J. Biomech.* 15:107–109.

[37] Hansen, P., Haraldsson, B.T., Aagaard, P., Kovanen, V., Avery, N.C., Qvortrup, K., Larsen, J.O., Krogsgaard, M., Kjaer, M., and Magnusson, S.P. (2010). Lower strength of the human posterior patellar tendon seems unrelated to mature collagen cross-linking and fibril morphology. *J. Appl. Physiol.* 108:47–52.

[38] Atkinson, T.S., Ewers, B.J., and Haut, R.C. (1999). The tensile and stress relaxation responses of human patellar tendon varies with specimen cross-sectional area. *J. Biomech.* 32:907–914.

[39] Vogel, K.G. (2004). What happens when tendons bend and twist? Proteoglycans. *J. Musculoskelet. Neuronal Interact.* 4:202–203.

[40] Raspanti, M., Viola, M., Sonaggere, M., Tira, M.E., and Tenni, R. (2007). Collagen fibril structure is affected by collagen concentration and decorin. *Biomacromolecules* 8:2087–2091.

[41] Rühland, C., Schönherr, E., Robenek, H., Hansen, U., Iozzo, R.V., Bruckner, P., and Seidler, D.G. (2007). The glycosaminoglycan chain of decorin plays an important role in collagen fibril formation at the early stages of fibrillogenesis. *FEBS J.* 274:4246–4255.

Study 5

Fracture mechanics of collagen fibrils: Influence of natural cross-links

René B. Svensson[1,2], Hindrik Mulder[3], S. Peter Magnusson[1]

[1]Institute of Sports Medicine Copenhagen, Department of Orthopedic Surgery M, Bispebjerg Hospital and Center for Healthy Aging, Faculty of Health Sciences, University of Copenhagen, Copenhagen, Denmark.
[2]Nano-Science Center, Faculty of Science, University of Copenhagen, Copenhagen, Denmark.
[3]Unit of Molecular Metabolism, Scania University Hospital, Malmö, Sweden.

Abstract

Tendons are important load-bearing structures in the body, which often suffer injury in relation to sports and work. Type I collagen fibrils are the primary components of tendon and carry the majority of the mechanical loads experienced by the tissue, however, knowledge of how load is transmitted between and within fibrils is limited. One of the aspects that have been shown to influence tendon mechanical behavior is the presence of covalent enzymatic cross-links between collagen molecules. To improve our understanding of how molecular bonds translate into tendon mechanics we utilized an atomic force microscopy technique to measure the mechanical behavior of individual collagen fibrils loaded to failure.

Fibrils from human patellar tendons, rat-tail tendons, $NaBH_4$ reduced rat-tail tendons and tail tendons of Zucker diabetic fat (ZDF) rats were tested. We found a characteristic three-phase stress-strain behavior in the human collagen fibrils with an initial rise in stress and modulus followed by a short plateau with reduced modulus, which was finally followed by an even greater increase in stress and modulus leading up to failure. In comparison the rat-tail tendons also had the initial increase and plateau phase, but the third region was almost absent and the plateau continued all the way to failure. The importance of cross-link lability was investigated by $NaBH_4$ reduction of the rat-tail fibrils, which did not alter their behavior. In addition a potential influence of advanced glycation caused by hyperglycemia was assessed in fibrils from Zucker diabetic fat (ZDF) rats, which also did not alter the behavior compared to native rat-tail fibrils.

Based on these results we propose that force transmission within collagen fibrils involve initially non-covalent interactions laterally along molecules, followed by slippage of molecules or small filaments at higher loads. In human fibrils this slippage can be stopped by trivalent mature cross-links while divalent cross-links in rat-tail fibrils are not able to do so.

Introduction

Mechanical stability and function of humans and other higher organisms is made possible by connective tissues that carry both tensile and compressive loads. Despite differences in structures and loading conditions, connective tissues are to a large extent all based on the same protein, namely collagen [1-2]. One of the most collagen rich connective tissues are tendons, which connect muscles to bones across joints, and thereby enable muscle-generated forces to create movement [3]. Some tendons can experience large loads, up to ~400 kg during jumping, because they insert close to the joint while the external load is applied further away creating a large difference in moment arms [4]. In-vitro studies have found the failure stress of human tendon to be on the order of 30-75MPa [5-7], which is equivalent to 300-750 kg on a 1 cm^2 tendon Since damage occurs even before ultimate failure this yields a relatively low safety margin and makes tendons a common site of both sports and work related injuries [8-10].

The central part of tendon consists mainly of fibrillar type I collagen [11-12]. The type I collagen molecule is a 300 nm long triple helix consisting of two α1 and one α2 chain and is able to assemble by staggered lateral aggregation into thin (20-500nm), long (possibly > 1mm) fibrils [13-16]. In tendon all fibrils are parallel to transmit unidirectional tension, while other tissues have different organizations depending on shape and mechanical loading. The non-helical ends (telopeptides) of collagen molecules are involved in the formation of intermolecular covalent cross-links within the fibril [17].

There are two basic types of natural cross-links; enzymatic and advanced glycation end-products (AGEs). Enzymatic cross-links are essential in the formation of functional collagen fibrils, while AGEs accumulate with age and diabetes and may impair normal function [18-19]. Cross-linking directly affect the mechanical function of connective tissues [17, 20-21] and also affect the biochemistry by making the collagen less susceptible to proteolytic degradation [22-23]. This makes cross-links an important parameter in connective tissue behavior especially as it relates to ageing and diabetes.

Enzymatic cross-link formation is initiated by the enzyme lysyl oxidase (LOX) acting on specific lysines in the telopeptides [17]. The resulting allysine reacts rapidly with a specific lysine in the helical region of a neighboring molecule to form an 'immature' divalent intermolecular bond [24-25]. Over time immature cross-links can react with an additional telopeptide allysine to form a trivalent 'mature' bond [17, 26]. Whether the additional bond is intra- or intermolecular is still unknown, however, the latter is expected to enhance mechanical strength to a greater extent than the former. Hydroxylation of lysines is common in collagen and can affect the nature of cross-links. Generally, cross-links derived from hydroxylated allysines are more stable than their non-hydroxylated counterparts because they undergo amadori rearrangement [17]. Significant variations in cross-link types have been reported on different tissues and for example in rat-tail tendon (RTT) the majority of cross-links are of an immature type that is acid labile and consequently RTT collagen is highly soluble in weak acids [27-28]. The cause of this difference is likely the low mechanical load on tails since mechanically loaded rat tendons like achilles do contain mature cross-links [29].

AGE cross-links are formed by reaction of reducing sugars, such as glucose [30]. This type of reaction is largely unspecific producing both cross-linking and non-cross-linking compounds all over the protein. The amount of AGEs formed on a protein increases with time until the molecule is degraded, and due to the extensive half-life of collagen this allows large amounts to accumulate [31-32]. AGEs have also been implicated in the development of the late complications of diabetes, where plasma glucose levels are elevated. The complications mainly arise in the microvasculature in kidneys, retina and perhaps neural vasculature [33].

Natural cross-linking occurs at the fibril level yet measurements of their mechanical influence at this level have not previously been described. In this paper we investigate the ultimate tensile properties of collagen fibrils from human patellar tendons (containing mature enzymatic cross-links) and rat-tail tendons (dominated by immature enzymatic cross-links), relating our findings to cross-link type and stability. To our knowledge the failure properties of human collagen fibrils have not been reported before.

Materials and Methods
Materials
Human patellar tendon tissue was obtained during anterior cruciate ligament (ACL) autograft surgery on three otherwise healthy males. Surgery took place 4-6 months post injury and the subjects underwent rehabilitation prior to the surgery ensuring that the patellar tendon did not suffer from disuse. All subjects gave their informed consent. Samples were wrapped in PBS soaked gauze and stored frozen at –20ºC.

Tails of three healthy 12-week old female Wistar rats and two 16-week old Zucker Diabetic Fat (ZDF) rats were stored frozen at –20ºC. After thawing, several fascicles were extracted from the distal end. The fascicles were wrapped in PBS soaked gauze and stored at –20ºC until use. All procedures were approved by the local ethics committee.

NaBH$_4$ reduction
Some RTT fascicles were treated with NaBH$_4$ (Sigma-Aldrich) to reduce acid labile immature cross-links thereby making them stable. Nine mg NaBH$_4$ was dissolved in 2 mL of 0.15 mM NaOH. Fascicles were placed in 10mL of 150mM phosphate buffer (pH = 7.4) and 0.5 mL of the NaBH$_4$ solution was added every 15 min for 1 hour while stirring . Following treatment the fascicles were washed twice by placing them in 5 mL of 150 mM phosphate buffer and stirring for 5 min. Fascicles were then stored on 150mM PBS soaked gauze at –20ºC until use.

Efficacy of the reduction was determined by measuring solubility in acetic acid. Collagen fascicles (~10mm segments) were dissolved in 3.5 mL of 0.05 M acetic acid for 20 hours at ~5 ºC. The resulting solution was ultracentrifuged at 100,000g for 1 hour at 4 ºC after which 3 mL of the supernatant was separated from the gel-like pellet with the remaining 0.5 mL of solvent [27]. Collagen content in the two fractions was determined by a colorimetric hydroxyproline assay using chloramine-T oxidation and reading color reaction with 4-dimethylaminobenzaldehyde at 570nm [34]. Solubility is expressed as the supernatant hydroxyproline fraction of the total content, the content of 0.5 mL of supernatant was subtracted from the pellet value and added to the total supernatant content to account for solvent left with the pellet.

Mechanical Testing
Mechanical testing of collagen fibrils was performed similarly to our previously published method [35] with modifications that allow testing to failure. The system is limited to 20 µm deformation, which only allowed failure testing of short fibril segments <40 µm. A stiffer AFM cantilever (OMCL-AC160TS, spring constant ~ 42 N/m) was used, which enabled measurement of the entire force range up to failure. The long tip (10µm) on this cantilever type hindered glue deposition at the cantilever end. To overcome this issue the tip was removed by mechanically breaking it against a sharp silicon edge.
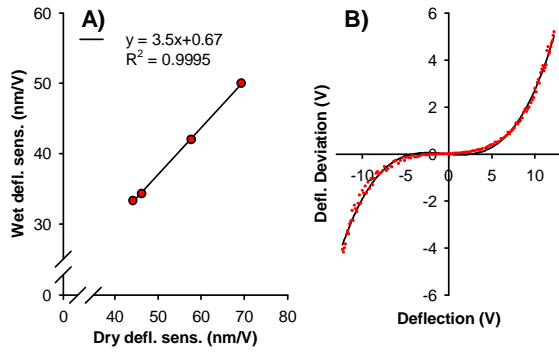
Figure 1: A) There was a linear relation between AFM deflection sensitivity in the dry and the wet state. B) Deviation from linearity of the detector as a function of the measured deflection voltage. Red dots are data from three separate measurements (down sampled 40x for clarity) and the black line is a 3rd order polynomial fit.
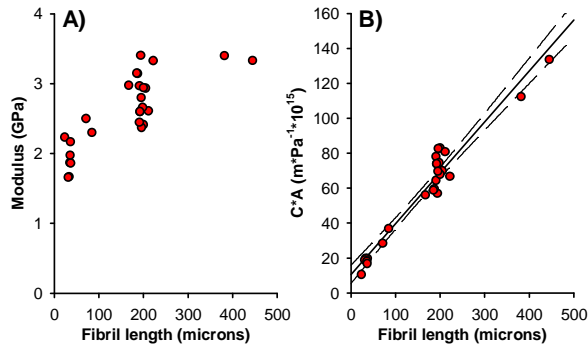
Figure 2: A) Across our present and previous measurements we observe an increase in collagen fibril modulus with the length of the tested specimen. B) Plot of the fibril compliance multiplied with fibril CSA (C*A) as a function of fibril length. A good linear correlation is observed (see text for details).

Despite the stiff cantilever, deflection often exceeded the linear range of the detector (±3 V), and therefore the detector non-linearity was determined by engaging on a hard silicon substrate to produce a linear deflection vs. distance response. Deviation of the detector signal from linearity was well described by a 3rd order polynomial, and the fit to three such measurements made on three separate days and cantilevers was used to correct all measured deflection values (Figure 1B). The cantilever deflection sensitivity was determined in the dry state before glue was deposited on the cantilever. To determine the corresponding wet deflection sensitivity an experiment was performed to measure sensitivity both dry and wet at various laser positions along the cantilever. A linear relation between dry and wet sensitivity was found and used to calculate wet values in all experiments (Figure 1A).

Collagen fibrils were tested at various strain rates in the low strain range (~5%) (results not reported here), which functioned as preconditioning. The failure test consisted of a single pull to failure at a speed of 20 µm/s (~60 %/s strain rate).

Due to equipment failure, ZDF rats were tested on a different AFM (MFP-3D, Asylum Research, Santa Barbara, CA). The described method was used except that wet deflection sensitivity was measured directly in mQ water before each experiment.

Fibril imaging
Tapping mode AFM imaging in air was performed before mechanical testing to determine the dry CSA and ensure structural integrity of collagen fibrils. When possible the remaining piece of fibril following mechanical test was also imaged to investigate the structure.

Data analysis and statistics
Mechanical data were analyzed using one-way ANOVA and post-tests employed Tukey's correction for multiple comparisons. Breakage site and fibril disruption were analyzed by table analysis using a Fishers exact binomial test for significance. A significance level of 0.05 was used. Measured values are reported as mean ± standard deviation and group differences are reported as mean difference with 95% confidence intervals. For human patellar tendon (Human) N = 7 fibrils from three different persons. For native rat-tail tendon (N-RTT) N = 8 fibrils from three different rats. For reduced rat-tail tendon (R-RTT) N = 6 fibrils from the same three rats as N-RTT. For ZDF rat-tail tendon (ZDF-RTT) N = 4 fibrils from two different rats.

End-effects
Material properties can usually be assumed independent of specimen dimensions. By pooling the present data obtained on short fibrils with data from our previous works on longer fibrils [35-36] we observe a clear increase in low strain (~4%) modulus with increasing length (Figure 2A). The most likely explanation for this is the presence of so called end-effects related to deformation in the gripping regions at the ends of the specimen. With the present method part of the end-effects are likely related to fibril bending due to the geometry of the setup. As a simple model the end-effects can be incorporated as an added spring element in series with the specimen. The specimen may change length and CSA, while the end-spring does not change length but possibly follows the CSA of the specimen. The compliance of two serially connected springs is:

$$C = \frac{1}{k} = \frac{1}{k_{end}} + \frac{1}{k_{fib}} = \frac{l_{end}}{A_{end} \cdot E_{end}} + \frac{l_{fib}}{A_{fib} \cdot E_{fib}}$$

$$\Rightarrow C \cdot A_{fib} = \frac{l_{end}}{A_{end} \cdot E_{end}} \cdot A_{fib} + \frac{1}{E_{fib}} \cdot l_{fib}$$

Here C is the compliance, k is the spring constant, l is the length, A is the CSA and E is the elastic modulus. Subscripts *end* and *fib* designate the end-effect element and the fibril respectively. From this it is seen that a 3D

plot of $C \cdot A_{fib}$ versus the fibril length and CSA should give a plane, however, we found that the CSA dependence was small suggesting that A_{end} is proportional to A_{fib}, which simplifies the relation to give:

$$C \cdot A_{fib} = \frac{l_{end}}{E_{end}} + \frac{1}{E_{fib}} \cdot l_{fib}$$

Plotting $C \cdot A_{fib}$ versus fibril length thus yields a straight line with the slope given by the inverse of fibril modulus and the intersect defining the magnitude of the end-effects (Figure 2B). From this a fibril modulus of 3.4 GPa is predicted and given the mean modulus of short human collagen fibrils in the present study (1.9 GPa) we estimate that ~45% of the measured strains are due to end-effects.

To present data as close to the 'true' value as possible we have included this correction to the strains. It should be noted that this is a simple multiplicative factor and the original measured values can be obtained by dividing reported strains and multiplying reported modulus values by 0.55.

Results

Human collagen fibrils

Human collagen fibrils displayed three distinct phases in the mechanical response up to failure (Figure 3). In region I (~0-7% strain) the modulus increased with strain reaching a peak value (Mod1) around which the stress-strain response was fairly linear. In region II (~7-15% strain) the modulus dropped leading to a flattening of the stress-strain curve. Finally, in region III (~15-25%
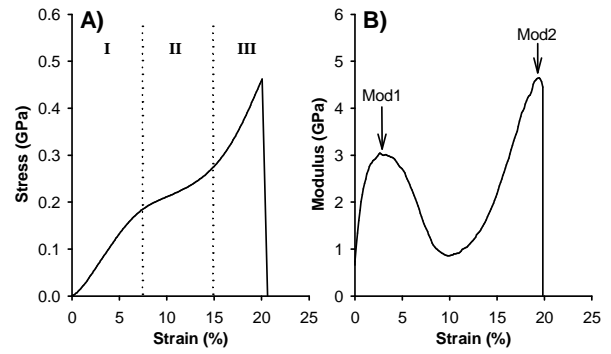
Figure 3: A) Stress-strain response of a representative human collagen fibril. Three distinct regions (denoted I, II and III) are observed. B) The local modulus of the same curve as a function of strain. The three regions give rise to two distinct peak modulus values, Mod1 and Mod2.

strain) the modulus started increasing again and continued to do so until ultimate failure at which point the peak modulus (Mod2) was often greater than it was in region I. The mechanical parameters are summarized in Table 1.

Rat tail collagen fibrils

The mechanical behavior of collagen fibrils from RTT was different from that observed in human patellar tendon fibrils (Figure 4). Like the human fibrils, modulus increased with strain in region I leading up to a peak value after which the modulus decreased in region II. However, unlike human fibrils, the increasing modulus in region III was either absent or less distinct, reaching a lower value than in region I. Mechanical parameters are summarized in Table 1. Both the reduced and the ZDF rat-tail fibrils behaved similarly to the

| **Table 1**: Structural and mechanical test parameters.				
	Human	N-RTT	R-RTT	ZDF-RTT	RTT-all
Test length (µm)	33±5	34±4	37±5	32±2	35±4
CSA (µm^2)	0.021±0.004	0.033±0.018	0.031±0.011	0.025±0.006	0.036±0.014
Mod1 (GPa)	3.5±0.4	2.2±0.9	2.9±0.4	2.9±0.5	2.6±0.7
Mod1 strain (%)	3.3±1.1	4.6±2.8	4.0±0.9	5.7±2.5	4.6±2.2
Mod2 (GPa) [#]	4.3±1.4	1.4±0.7	1.5±0.5	1.9±0.5	1.6±0.6
Ultimate stress (MPa)	540±140	200±110	290±80	270±60	250±100
Ultimate strain (%)	20±1	16±4	19±4	16.5±2	17±4
Mod2/Mod1 [#]	1.24±0.35	0.60±0.30	0.51±0.18	0.73±0.34	0.59±0.26

[#] Not all RTT fibrils showed the 2nd modulus increase, presented data is for 5 N-RTT, 5 R-RTT and 3 ZDF-RTT fibrils that did. Mean±SD.

Table 2: Mechanical differences between groups.				
	Effect of reduction: R-RTT – N-RTT	Effect of diabetes: ZDF-RTT – N-RTT	Effect of Human: Human – N-RTT	Pooled RTT: Human – RTT-all
Mod1 (GPa)	+0.67 (-0.27 – 1.61)	+0.71 (-0.35 – 1.78)	+1.29 (0.38 – 2.19)*	+0.90 (0.29 – 1.52)*
Mod1 strain (%)	-0.5 (-3.5 – 2.5)	+1.1 (-2.4 – 4.5)	-1.3 (-3.8 – 2.4)	-1.3 (-3.2 – 0.5)
Mod2 (GPa)	+0.11 (-1.64 – 1.85)	+0.55 (-1.47 – 2.57)	+2.93 (1.31 – 4.54)*	+2.76 (1.84 – 3.67)*
Ultimate stress (MPa)	+90 (-70 – 260)	+70 (-110 – 250)	+340 (190 – 500)*	+300 (200 – 400)*
Ultimate strain (%)	+2.6 (-2.6 – 7.7)	+0.4 (-5.4 – 6.3)	+4.3 (-0.6 – 9.3)	+3.4 (0.2 – 6.5)*
Mod2/Mod1	-0.09 (-0.64 – 0.46)	+0.13 (-0.50 – 0.76)	+0.64 (0.13 – 1.15)*	+0.64 (0.35 – 0.93)*

* Statistically significant ($p < 0.05$). Mean difference (95% confidence interval)
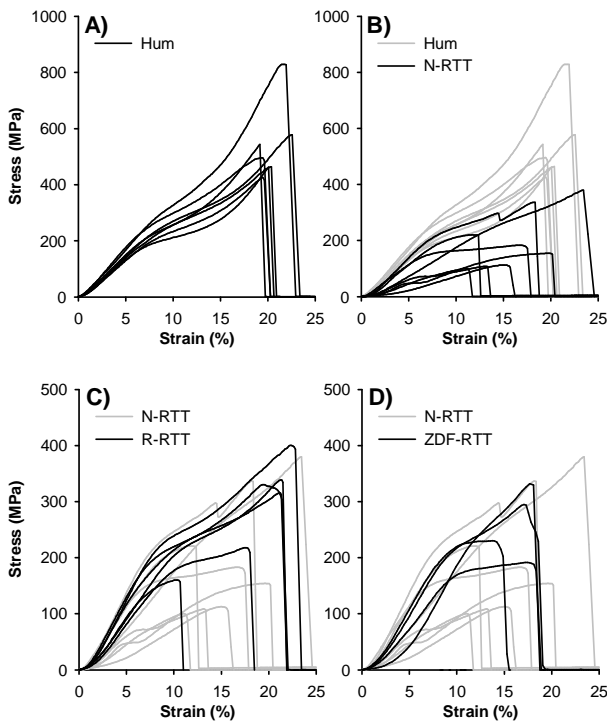
Figure 4: Mechanical response of A) All human collagen fibrils. B) All native RTT fibrils (black) compared to the human fibrils (gray). C) Reduced RTT (black) compared to native RTT (gray). D) Zucker Diabetic Fat RTT (black) compared to native RTT (gray).

native fibrils, and thus differently from human patellar tendon fibrils (Figure 4C+D).

Efficacy of NaBH₄ treatment
NaBH$_4$ efficacy was evaluated by solubility in dilute acetic acid. Control fascicles had a solubility of $86 \pm 9\%$ and solubility of NaBH$_4$ treated fascicles was below the detection limit ($< 1\%$). For comparison the human fascicles had a solubility of $4.8 \pm 0.8\%$.

Mechanical effects
Mechanical differences between the groups in region I (linear) and region III (failure) are reported in Table 2. Differences in region II (middle plateau) are not included because it was poorly defined in RTT, which displayed plateau all the way to failure. Neither the reduced nor the ZDF RTT differed significantly from native RTT in any of the mechanical parameters. Human fibrils had a significantly higher modulus (Mod1) in region I than the native RTT fibrils and in region III both modulus (Mod2) and failure stress were significantly higher (Table 2). Mod2 was on average greater than Mod1 for human fibrils, in contrast to native RTT fibrils, which had a lower Mod2 than Mod1, the difference between the two ratios was statistically significant (Table 2).
Since all the RTT groups behaved similarly they were also pooled (RTT-all) and significant differences to the human fibrils were seen in the same parameters as for
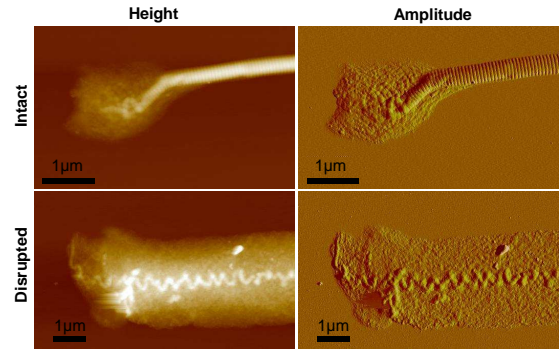
Figure 5: Height and amplitude AFM images of collagen fibril breakage sites after failure testing. A failure mode with a largely intact fibril and one with a heavily disrupted fibril was observed (the structure present towards the right of the images continues throughout the rest of the fibril).

Table 3: Fibril breakage site and structure after failure. (Number of fibrils)

	Disrupted	Intact
End	0	6
Mid	9	4

	Disrupted	Intact
Hum	1	4
RTT	9	6

	End	Mid
Hum	4	2
RTT	5	12

the native RTT, with the addition of failure strain also reaching significance (Table 2).

Structural effects
Two different structures were observed on the broken fibrils. Some were relatively intact and retained D-banding along the entire fibril up to the breakage site, while others displayed gross disruption of fibril structure throughout the length (Figure 5). Twenty fibrils could be imaged of which ten had intact structure and ten were disrupted. Breakage site (mid or end) was assessed from the length of the broken fibril compared to the original length in twenty-three fibrils. Failure in the mid-substance occurred in fourteen fibrils and nine had ruptured at the end.

Using Fishers exact test a significant (p=0.008) relationship between breakage site and structure of the broken fibril was found. Of the end-failures 100% were intact and 69% of the mid-substance failures were disrupted (Table 3). Tissue origin also tended to relate to failure site and structure such that human fibrils had predominantly intact end failures and rat fibrils had disrupted mid-substance failures, these relationships were not significant however. None of the mechanical parameters were significantly related to breakage site or structure when the confounding factor of tissue origin was accounted for.

Discussion

Cross-linking in collagen is believed to be a major source of mechanical strength in connective tissues, and improved mechanical properties during development is likely related to maturation of enzymatic cross-links [17]. We believe that the three distinct regions observed in the mechanical response of human patellar tendon fibrils can be explained by the organized structure of collagen in the fibril. We propose that in region I, molecules are held together by non-covalent interactions along their length, and the increase in modulus is caused by increasing alignment and stretching of the molecules. In region II, molecules start slipping as non-covalent interactions break, causing the modulus to decrease. Finally in region III the slippage is stopped by covalent cross-links causing the modulus to rise again as the molecular backbone is stretched. A recently reported modeling study found a similar behavior for two molecules connected by a single cross-link at the $\alpha 1(I)$ C-telopeptide [37]. We suggest that the highly ordered molecular packing and cross-link specificity allow these features to be observed even when up-scaled to a fibril with hundreds of thousands of molecules. The plateau may have a physiological function to increase the toughness (energy to break) of the fibril and reducing the risk of brittle failure.

Native RTT collagen contains mostly immature cross-links, as evidenced by the high acid solubility, while adult human patellar tendon collagen contains significant amounts of mature cross-links [28, 38]. Our results show that these two tissues also differ markedly in their mechanical response at the fibril level. The differences in mechanical behavior occur predominantly at the high strain level in region III in agreement with the idea of cross-links governing the behavior in this region. RTT fibrils display a longer plateau while in contrast human fibrils have a significant rise in stress and modulus (Figure 4), suggesting that molecular slippage is not stopped by cross-links in RTT. The relation between cross-linking and the occurrence of a plateau in the stress-strain response has been reported at the fascicle level in rats treated with β-APN, which suppresses lysyl oxidase activity and thereby enzymatic cross-link formation [20]. A plateau in the mechanical response leading up to failure was also recently reported by molecular modeling [39]. The difference in behavior of human and RTT fibrils is similar to the difference between two molecules with or without a cross-link reported in a computer model [37]. If failure in RTT involves molecular slippage it can also explain the tendency for greater disruption observed following failure, since slippage is likely to occur throughout the fibril. In contrast, failure related to molecular breakage will be more brittle and concentrated at a single site as was more common in the human fibrils.

Immature cross-links differ from mature by having a labile imine bond. We speculated that molecular slippage in RTT fibrils was caused by breakage of the labile bonds and to test this hypothesis we treated RTT fascicles with $NaBH_4$ to stabilize the bond [40-42]. The treatment was efficient in stabilizing the immature cross-links as seen from the lack of acid solubility, but while there was a tendency for increased modulus in region I and higher failure stress, there was no effect on the curve shape in region III (Figure 4C). This result suggests that the imine bond is fairly stable against mechanical load at neutral pH. We propose that rather than lability, it is the divalent nature of the immature, in contrast to the trivalent mature cross-link, that is responsible for the mechanical difference. Further proof of this hypothesis would require manipulation of cross-link valence, which has not been possible in the present work.

Another possible difference in cross-linking between the human and RTT tissue is a greater extent of AGE cross-linking due to the much greater age of the human tissue. To elucidate this we tested fibrils from ZDF rats that are expected to have increased AGE formation due to hyperglycemia, but they did not behave similar to the human fibrils. It should be noted that while we did not find significant differences between the RTT groups, the confidence intervals were fairly wide (Table 2) and as such there may be some relevant effects that we did not have the power to detect. However, it is quite clear both from the numerical results and the observed stress-strain curves that none of the RTT groups behaved like the human fibrils.

To our knowledge, only one previous study by Yang et al. has investigated failure properties of mammalian collagen fibrils [43]. In that study, native collagen fibrils from bovine achilles tendons were reported to fail at a strain of 13% and a stress of 60 MPa (~135 MPa using dry CSA, assuming ~50% swelling as reported [43]). We suspect that the lower values of failure stress and strain compared to the present findings were caused by a limited breakage of cross-links in the preparation by Yang et al., which involves swelling in 0.01M HCl overnight [44]. In the same paper cross-linking agents were found to improve mechanical properties, with glutaraldehyde treatment increasing failure strain to 22% and stress to 290 (~650 MPa using dry CSA). These values are well in line with our findings, however, Yang et al. did not find the three distinct regions that we observe for mature human collagen. We believe this difference is due to the lesser specificity of synthetic cross-linking compared to that of natural enzymatic cross-links. Randomly dispersed cross-links would not act in unison and thus not produce the synchronous slippage that we propose takes place in the human fibrils.

There is also a previous report of collagen fibril failure using fibrils from sea cucumber, however, these behave significantly different from the present work, failing at a much higher strain of 80% and a stress of 230 MPa (~1.1 GPa using dry CSA) and also displaying quite different stress-strain behavior [45]. This difference is likely due to the echinoderm origin of the

collagen, which for example manifests in spindle shaped rather than cylindrical fibrils.

Relation to tendon failure

In order to compare the present failure properties of fibrils to those of tendons it is necessary to account for the fibril content in the tendon. Using a fibril swelling of 30% at physiological hydration and a fibril volume fraction in tendon of 60% the stress and modulus of fibrils must be divided by 2.8 to compare with tendon values (see [36] for details). For the RTT fibrils this normalization yields a failure stress of 90 MPa with a corresponding strain of 17%, by comparison native RTT has been reported to fail at ~50-110 MPa stress and 12-20% strain [46-48]. These values correspond reasonably suggesting that tendon failure may occur through fibril breakage rather than slippage, although the range of values makes the conclusion uncertain. For the human fibrils the failure stress and strain normalized to the tendon level becomes 190 MPa and 20% respectively. For the strain this is within the ~10-25% that has been reported for human patellar tendons but the fibril stress is quite a bit greater than the ~30-75 MPa found at the tendon level [5-7]. This could suggest that human patellar tendons fail by fibril slippage rather than breakage, but this is again inconclusive. There may also be other explanations for example local defects may occur along a fibril such that natural full-length fibrils of up to several mm would be weaker than the 40μm long segments tested in the present work [49]. In addition the strength of tendons may be underestimated due to stress-concentrations [50].

Conclusions

There was a clear difference in mechanical behavior between collagen fibrils from mature human patellar tendons and from rat-tail tendons. The human fibrils displayed a region of increasing modulus at high strains before abrupt failure. In contrast rat-tail tendons had a plateau leading up to failure. Because of these different curve shapes, human fibrils failed at significantly higher stress than rat-tail fibrils. We propose that these mechanical observations relate to the prominent differences in cross-link maturity of the tissues. By $NaBH_4$ reduction we determined that cross-link lability was not involved in mechanical behavior, which suggests that cross-link valence may instead cause the difference. Rat-tails are a common tendon model in research but it is important to appreciate the differences in both cross-linking and fibril mechanics as reported here when comparing to load-bearing tendons.

Acknowledgments

References

[1] van der Rest M, Garrone R. Collagen family of proteins. FASEB J 1991;5(13):2814-23.
[2] Exposito JY, Valcourt U, Cluzel C, Lethias C. The fibrillar collagen family. Int J Mol Sci 2010;11(2):407-26.
[3] Kannus P. Structure of the tendon connective tissue. Scand J Med Sci Sports 2000;10(6):312-20.
[4] Finni T, Komi PV, Lepola V. In vivo human triceps surae and quadriceps femoris muscle function in a squat jump and counter movement jump. Eur J Appl Physiol 2000;83(4-5):416-26.
[5] Chun KJ, Butler DL. Spatial variation in material properties in fascicle-bone units from human patellar tendon. In: Lee S, Kim Y, editors. Experimental mechanics in nano and biotechnology. Stafa-Zurich: Trans Tech Publications Ltd, 2006. p. 797-802.
[6] Haraldsson BT, Aagaard P, Krogsgaard M, Alkjaer T, Kjaer M, Magnusson SP. Region-specific mechanical properties of the human patella tendon. J Appl Physiol 2005;98(3):1006-12.
[7] Johnson GA, Tramaglini DM, Levine RE, Ohno K, Choi NY, Woo SLY. Tensile and viscoelastic properties of human patellar tendon. J Orthop Res 1994;12(6):796-803.
[8] Nainzadeh N, Malantic-Lin A, Alvarez M, Loeser AC. Repetitive strain injury (cumulative trauma disorder): Causes and treatment. Mt Sinai J Med 1999;66(3):192-6.
[9] Lian OB, Engebretsen L, Bahr R. Prevalence of jumper's knee among elite athletes from different sports - a cross-sectional study. Am J Sports Med 2005;33(4):561-7.
[10] Ker RF, Alexander RM, Bennett MB. Why are mammalian tendons so thick. J Zool 1988;216:309-24.
[11] Epstein EH. [α1(III)]₃ human skin collagen - release by pepsin digestion and preponderance in fetal life. J Biol Chem 1974;249(10):3225-31.
[12] Gelse K, Poschl E, Aigner T. Collagens - structure, function, and biosynthesis. Adv Drug Deliv Rev 2003;55(12):1531-46.
[13] Parry DAD, Craig AS. Quantitative electron microscope observations of collagen fibrils in rat-tail tendon. Biopolymers 1977;16(5):1015-31.
[14] Hodge AJ, Petruska JA. Recent studies with the electronmicroscope on ordered aggregates of the tropocollagen macromolecule. In: Ramachandran GN, editor. Aspects of protein structure. New York: Academic Press, 1963. p. 299-300.
[15] Kadler KE, Holmes DF, Trotter JA, Chapman JA. Collagen fibril formation. Biochem J 1996;316:1-11.
[16] Provenzano PP, Vanderby R. Collagen fibril morphology and organization: Implications for force transmission in ligament and tendon. Matrix Biol 2006;25(2):71-84.
[17] Bailey AJ, Paul RG, Knott L. Mechanisms of maturation and ageing of collagen. Mech Ageing Dev 1998;106(1-2):1-56.
[18] Corman B, Duriez M, Poitevin P, Heudes D, Bruneval P, Tedgui A, et al. Aminoguanidine prevents age-related arterial stiffening and cardiac hypertrophy. Proc Natl Acad Sci USA 1998;95(3):1301-6.
[19] Hammes HP, Martin S, Federlin K, Geisen K, Brownlee M. Aminoguanidine treatment inhibits the development of experimental diabetic-retinopathy. Proc Natl Acad Sci USA 1991;88(24):11555-8.
[20] Puxkandl R, Zizak I, Paris O, Keckes J, Tesch W, Bernstorff S, et al. Viscoelastic properties of collagen: Synchrotron radiation

investigations and structural model. Philos Trans R Soc Lond, B, Biol Sci 2002;357(1418):191-7.

[21] Wagner DR, Reiser KM, Lotz JC. Glycation increases human annulus fibrosus stiffness in both experimental measurements and theoretical predictions. J Biomech 2006;39(6):1021-9.

[22] Vater CA, Harris ED, Siegel RC. Native cross-links in collagen fibrils induce resistance to human synovial collagenase. Biochem J 1979;181(3):639-45.

[23] Mott JD, Khalifah RG, Nagase H, Shield CF, Hudson JK, Hudson BG. Nonenzymatic glycation of type IV collagen and matrix metalloproteinase susceptibility. Kidney Int 1997;52(5):1302-12.

[24] Cannon DJ, Davison PF. Crosslinking and aging in rat tendon collagen. Exp Gerontol 1973;8(1):51-62.

[25] Tanzer ML. Intermolecular cross-links in reconstituted collagen fibrils - evidence for nature of covalent bonds. J Biol Chem 1968;243(15):4045-54.

[26] Eyre DR, Wu JJ. Collagen cross-links. Top Curr Chem 2005;247:207-29.

[27] Yang S, Litchfield JE, Baynes JW. Age-breakers cleave model compounds, but do not break maillard crosslinks in skin and tail collagen from diabetic rats. Arch Biochem Biophys 2003;412(1):42-6.

[28] Eyre DR, Paz MA, Gallop PM. Cross-linking in collagen and elastin. Annu Rev Biochem 1984;53:717-48.

[29] Carroll CC, Whitt JA, Peterson A, Gump BS, Tedeschi J, Broderick TL. Influence of acetaminophen consumption and exercise on achilles tendon structural properties in male wistar rats. Am J Physiol Regul Integr Comp Physiol 2012;302(8):R990-R5.

[30] Monnier VM, Sell DR. Prevention and repair of protein damage by the maillard reaction in vivo. Rejuv Res 2006;9(2):264-73.

[31] Thorpe CT, Streeter I, Pinchbeck GL, Goodship AE, Clegg PD, Birch HL. Aspartic acid racemization and collagen degradation markers reveal an accumulation of damage in tendon collagen that is enhanced with aging. J Biol Chem 2010;285(21):15674-81.

[32] Verzijl N, DeGroot J, Thorpe SR, Bank RA, Shaw JN, Lyons TJ, et al. Effect of collagen turnover on the accumulation of advanced glycation end products. J Biol Chem 2000;275(50):39027-31.

[33] Brownlee M. Negative consequences of glycation. Metab Clin Exp 2000;49(2):9-13.

[34] Syk I, Agren MS, Adawi D, Jeppsson B. Inhibition of matrix metalloproteinases enhances breaking strength of colonic anastomoses in an experimental model. Br J Surg 2001;88(2):228-34.

[35] Svensson RB, Hassenkam T, Grant CA, Magnusson SP. Tensile properties of human collagen fibrils and fascicles are insensitive to environmental salts. Biophys J 2010;99(12):4020-7.

[36] Svensson RB, Hansen P, Hassenkam T, Haraldsson BT, Aagaard P, Kovanen V, et al. Mechanical properties of human patellar tendon at the hierarchical levels of tendon and fibril. J Appl Physiol 2012;112(3):419-26.

[37] Uzel SGM, Buehler MJ. Molecular structure, mechanical behavior and failure mechanism of the C-terminal cross-link domain in type I collagen. J Mech Behav Biomed Mater 2011;4(2):153-61.

[38] Hansen P, Haraldsson BT, Aagaard P, Kovanen V, Avery NC, Qvortrup K, et al. Lower strength of the human posterior patellar tendon seems unrelated to mature collagen cross-linking and fibril morphology. J Appl Physiol 2010;108(1):47-52.

[39] Buehler MJ. Nanomechanics of collagen fibrils under varying cross-link densities: Atomistic and continuum studies. J Mech Behav Biomed Mater 2008;1(1):59-67.

[40] Davison PF. The contribution of labile crosslinks to the tensile behavior of tendons. Connect Tissue Res 1989;18(4):293-305.

[41] Eyre DR, Weis MA, Wu JJ. Advances in collagen cross-link analysis. Methods 2008;45(1):65-74.

[42] Bailey AJ. Intermediate labile intermolecular crosslinks in collagen fibres. Biochim Biophys Acta 1968;160(3):447-53.

[43] Yang L, van der Werf KO, Dijkstra PJ, Feijen J, Bennink ML. Micromechanical analysis of native and cross-linked collagen

type I fibrils supports the existence of microfibrils. J Mech Behav Biomed Mater 2012;6:148-58.

[44] Yang L, van der Werf KO, Fitié CFC, Bennink ML, Dijkstra PJ, Feijen J. Mechanical properties of native and cross-linked type I collagen fibrils. Biophys J 2008;94(6):2204-11.

[45] Shen ZL, Dodge MR, Kahn H, Ballarini R, Eppell SJ. In vitro fracture testing of submicron diameter collagen fibril specimens. Biophys J 2010;99(6):1986-95.

[46] Haut RC. Age-dependent influence of strain rate on the tensile failure of rat-tail tendon. J Biomech Eng-T Asme 1983;105(3):296-9.

[47] Silver FH, Christiansen DL, Snowhill PB, Chen Y. Role of storage on changes in the mechanical properties of tendon and self-assembled collagen fibers. Connect Tissue Res 2000;41(2):155-64.

[48] Gentleman E, Lay AN, Dickerson DA, Nauman EA, Livesay GA, Dee KC. Mechanical characterization of collagen fibers and scaffolds for tissue engineering. Biomaterials 2003;24(21):3805-13.

[49] Bazant ZP. Scaling theory for quasibrittle structural failure. Proc Natl Acad Sci USA 2004;101(37):13400-7.

[50] Bennett MB, Ker RF, Dimery NJ, Alexander RM. Mechanical properties of various mammalian tendons. J Zool 1986;209:537-48.